**TECHNISCHE
UNIVERSITÄT
WIEN**

**VIENNA
UNIVERSITY OF
TECHNOLOGY**

DISSERTATION

Large Scale Applications of Airborne Laser Scanning for a Complex Mountainous Environment

ausgeführt zum Zwecke der Erlangung des akademischen Grades eines Doktors der technischen Wissenschaften unter der Leitung von

Univ.Prof. Dipl.-Ing. Dr.techn. Wolfgang Wagner
Institut für Photogrammetrie und Fernerkundung (E122),
Technische Universität Wien

eingereicht an der Technischen Universität Wien
Fakultät für Mathematik und Geoinformation

von
Dipl.-Ing. Markus Hollaus
Matr.Nr.: 9340616
Distelberg 9, A-6274 Aschau

Wien, am 25. Oktober 2006 ....

Acknowledgements

Kurzfassung

Im Laufe des letzten Jahrzehnts hat sich das flugzeuggetragene Laserscanning (ALS) als Standardverfahren zur Erfassung topographischer Daten etabliert. Es liefert aber nicht nur wertvolle Informationen zur Erstellung von Geländemodellen, sondern ermöglicht eine detaillierte dreidimensionale Beschreibung von Objekten. Derartige Informationen über Objekthöhen stellen in Kombination mit herkömmlichen zweidimensionalen Fernerkundungsdaten (z.B. Luftbilder oder Satellitenbilder) eine ausgezeichnete Datenquelle für eine detaillierte Ableitung der Landbedeckung dar. Speziell für wasserwirtschaftliche Anwendungen (z.B. hydraulische Abflussmodellierungen) sind Landbedeckungsklassen, welche die Rauhigkeit der Geländeoberfläche widerspiegeln, von besonderem Interesse. Ein weiteres viel versprechendes Anwendungsgebiet von ALS Daten liegt in der quantitativen Ableitung von Forstparametern, da mittels ALS sowohl Boden- als auch Vegetationspunkte gemessen werden können und somit die Abschätzung der Baumhöhen ermöglicht wird. Dies führte dazu, dass in skandinavischen Ländern ALS Daten für die Erstellung von operationellen Waldinventuren herangezogen werden. Im alpinen Raum ist der Einsatz von ALS Daten in der Forstwirtschaft derzeit noch auf kleine Pilotprojekte beschränkt.

Ziel dieser Dissertation war es, anhand zweier Anwendungsgebiete (Abfluss relevante Landbedeckungsklassifizierung, Ableitung von quantitativen Forstparametern) die Möglichkeiten einer großflächigen Anwendung unter Verwendung von State-of-the-Art ALS Daten sowie Prozessierungsmethoden zu evaluieren und zu diskutieren. Die durchgeführten Untersuchungen wurden anhand eines 128 km^2 großen, alpinen Testgebietes im südlichen Vorarlberg durchgeführt, von welchem sowohl ALS Daten aus einer kommerziellen Laserscannbefliegung sowie detaillierte Waldinventurdaten einer lokalen Forstverwaltung zur Verfügung stehen.

Im Zuge einer objektorientierten Landbedeckungsklassifizierung konnte der komplementäre Informationsgehalt von ALS Daten (Höheninformationen) und Farb-Infrarot Orthophotos (Spektralinformationen) aufgezeigt werden. Weiters ergaben die Untersuchungen, dass die Einbeziehung der Höheninformation zur Generierung Abfluss relevanter Landbedeckungsklassen zu einer deutlichen Qualitätssteigerung führt.

Für die Abschätzung von Waldparametern aus ALS Daten stellt die Höhendifferenz zwischen dem ersten vom Flugzeug aus sichtbaren reflektierenden Objekt und der Geländeoberfläche eine fundamentale Eingangsgröße dar. Aus diesen Höhendifferenzen können beispielsweise Baumhöhen sowie stammflächengewichtete Mittelhöhen (Loreyhöhen) abgeleitetet werden. Um eine qualitative Abschätzung dieser Parameter zu erhalten, wurde zunächst mit Hilfe von ca. 22000 Boden-

Kontrollpunkten die Genauigkeit des Geländemodells überprüft. Die Untersuchungen haben gezeigt, dass die erzielten Genauigkeiten (root mean square error) mit zunehmender Geländeneigung sinken. So wurden für schwach geneigte Geländebereiche (Geländeneigung <10°) Genauigkeiten von ca. 10 cm und für Geländebereiche mit einer Geländeneigung von mehr als 60° Fehler von mehr als 50 cm festgestellt. Die Genauigkeiten der abgeleiteten Baumhöhen sowie Loreyhöhen wurden mit Hilfe der terrestrischen Waldinventurdaten überprüft, wobei die Höhen sowohl aus den 3D Punktwolken als auch aus dem interpolierten Differenzmodell (Oberflächenmodell minus Geländemodell) extrahiert wurden. Die aus der 3D Punktwolke beziehungsweise aus dem Differenzenmodell extrahierten Baumhöhen weisen Genauigkeiten von $R^2 = 0.89$ und $R^2 = 0.79$ auf. Die Loreyhöhen konnten aus der 3D Punktwolke mit einem Bestimmtheitsmaß von $R^2 = 0.87$ und aus dem interpolierten Differenzemodell mit $R^2 = 0.70$ abgeschätzt werden. Untersuchungen über die Auswirkung unterschiedlicher ALS Punktdichten auf die abgeleiteten Höhen haben gezeigt, dass sich die flächenbezogenen Loreyhöhen für unterschiedlichste Punktdichten mit vergleichbarer Genauigkeit ermitteln lassen, wohingegen es bei den Baumhöhen mit einer abnehmenden Punktdichte zu einer deutlichen Unterschätzung kommt.

Für die Ermittlung des Holzvorrates wurde einerseits ein in Norwegen weit verbreitetes multiplikatives Regressionsmodell getestet und andererseits ein physikalisch basiertes lineares Schätzmodell entwickelt. Unter Verwendung der Waldinventurstichprobendaten als Referenzdaten konnte gezeigt werden, dass sowohl mittels multiplikativen Regressionsmodell als auch mittels linearem Schätzmodell der Holzvorrat mit einem Bestimmtheitsmaß von $R^2 = 0.84$ bzw. $R^2 = 0.87$ sehr genau ermittelt werden konnte. Untersuchungen hinsichtlich variierender ALS Eigenschaften haben gezeigt, dass sowohl die ALS Punktdichte als auch die Phänologie während der ALS Befliegung auf die erzielbaren Genauigkeiten beider Modelle einen sehr geringen Einfluss haben.

Zusammenfassend kann gesagt werden, dass basierend auf den vorliegenden ALS Daten und State-of-the-Art Algorithmen quantitative Waldparameter operationell abgeschätzt werden können. Da in Österreich ALS Daten bereits für große Gebiete vorliegen bzw. gegenwärtig beflogen werden, können zukünftig die daraus abgeleiteten flächenhaften Waldparameter eine wertvolle Ergänzung zu operationellen terrestrischen Aufnahmeverfahren darstellen.

Abstract

Today, airborne laser scanning (ALS) is the standard method for detailed topographic data acquisition. Due to the technological advances of laser scanners, differential global positioning systems (dGPS) and inertial measurement units (IMU), ALS has achieved high economic performance and has reached a status which is interesting not only for topographic mapping activities but also for several other applications. As already mentioned in Wehr and Lohr (1999) ALS can complement, or partly replace other existing geo-data acquisition technologies and open up new exciting areas of applications. With hydrology as the main driving force in Austria, extensive ALS flight campaigns have been carried out since the disastrous floods 2002 and therefore, ALS data are available for large areas today. The aim of this thesis was to investigate and to discuss the large area use of ALS for applied sciences namely for hydrologic and hydraulic applications as well as for forestry.

For distributed hydrologic models and for two-dimensional hydraulic river flood models high precision digital terrain models (DTM) form the basis. In addition to the DTM roughness relevant information such as the height and the spatial distribution of vegetation and buildings is required for these applications. Airborne laser scanner data offer these object heights and provide in conjunction with the complementary information of high-resolution colour-infrared orthophotos an excellent data source for land cover mapping relevant for hydrologic / hydraulic applications. Several studies demonstrate the high potential to use ALS data for these applications but these studies are mostly constraint to small test sites. To overcome this spatial limitation, the current thesis discusses and summarises the experiences to process ALS data for a large mountainous region and demonstrates the applicability of this technique in real-world applications.

Airborne laser scanning is currently one of the most promising remote sensing techniques for quantitative retrieval of forest parameters. While ALS has reached an operational status for mapping of boreal forests, its large area application over mountainous environments is lacking behind. This is because alpine forests often have high horizontal and vertical structural diversity and are situated in steep terrain. Also, ALS data acquisition and processing is more demanding over mountainous areas than over relatively flat regions. In this thesis state-of-the-art ALS technology and software packages were used to map canopy heights and to estimate stem volume for a 128 km^2 region in the western part of the Austrian Alps. Spruce and fir were the dominant tree species. Rather than employing data and methods tuned for a particular task and for a small study area, data and methods which already serve other operational applications were used. Thus, it was ensured that the results obtained in this study are of practical relevance. For the estimation of stem volume a multiplicative regression model mostly used in Scandinavia was used. Their

transferability to the alpine environment was analysed and their performance evaluated. This statistical approach requires a multitude of quantities derived from first- and last-echo ALS data. Since the physical understanding is lost in such a multi-parameter regression analysis approach, the next objective of this thesis was to develop a more physically-based linear model to estimate stem volume by combining forest inventory data and ALS data. The proposed linear model only used the canopy volumes as independent variables, which were calculated for sample plot sub-areas. The canopy volume represents the volume between the terrain surface and the top most surface of the tree tops. The divisions of the plot areas depend on predefined, fixed canopy height ranges. For the validation of the ALS derived forest parameters 22 000 ground control points and field-measured forest inventory data from 103 sample plots were available, which are operationally used by the local forest administration. As the used forest inventory data were based on variable sample plot sizes (so-called Bitterlich plots) a further objective of this thesis was to test the usability of such available forest inventories as reference data.

The analyses within this thesis showed that for large area applications the applied georeferencing algorithm (e.g. simultaneously hybrid block adjustment of laser scanner strips) and the hierarchic robust filtering technique were adequate methods to derive high accurate topographic models like DTMs, digital surface models (DSMs) and other subsequent products such as canopy height models (CHMs). However, some inaccuracies of the CHM arose in areas covered by homogeneous meadows with high grass or scrubs due to the technical limitations of current ALS systems. New ALS systems, which provide calibrated intensities of the laser echoes or which record the full echo-waveform, may provide crucial information to overcome these problems (Wagner et al., 2004a). The investigations concerning the use of ALS for hydrologic / hydraulic relevant land cover classifications showed that the complementary informational content of ALS data and colour infrared orthophotos was an excellent data source for object-oriented land cover classifications. As the defined land cover classes can be assigned to surface roughness classes, the derived land cover maps can be used as input data for two dimensional hydraulic river flood models. The high quality of topographic and thematic input information leads to a reduction of uncertainties of the model outputs. Furthermore, the derived land cover maps can be used to support the preparation of the necessary information needed for integrated river basins to comply with the EU Water Framework Directive.

The validation of the DTM with the ground control points showed that over non-forested terrain DTM errors increased from 10 cm for relatively flat terrain (local slope $< 10°$) to over 50 cm for local slopes greater than about 60°. The validations of the ALS derived single-tree heights and Lorey's mean heights showed good correlations using both, three dimensional first-echo points ($R^2 = 0.89 - 0.79$) and a grid-based canopy height model ($R^2 = 0.87 - 0.70$).

Furthermore, it could be shown that the influence of different ALS point densities on the achievable accuracies of the calculated Lorey's mean heights was negligible.

Concerning the stem volume estimation it could be shown that the multiplicative regression model could successfully be used also for the highly structured alpine forests. The achieved coefficient of determination (R^2) was 0.84 and the standard deviation of the residuals derived from a cross-validation was 100.0 m^3ha^{-1}. Unfortunately, for this pure statistical approach the multiple regression analyses led to different sets of independent variables if ALS data with different acquisition times or point densities were used for the calculations. Therefore, it is recommended that for ALS data sets with different properties (e.g. point densities, acquisition times) separate regression models should be used. This has the disadvantage that for each regression model an adequate reference data set is needed. For ALS data with varying properties, robust and reliable results of high accuracies (e.g. $R^2 = 0.87$, standard deviation of the residuals derived from a cross-validation is 90.0 m^3ha^{-1}) could be achieved with the proposed linear approach. Due to the simplicity of this linear model, a physically explicit connection between the stem– and the canopy volume is available.

Concluding it can be stated that ALS has now reached the maturity not only for topographic data acquisition but also for operational hydrology and forestry applications within complex alpine environments. Due to the multiple-shift usage of ALS data their manifold operational applications can be realised within acceptable costs in the near future.

Keywords: LiDAR; DTM; canopy height; stem volume; forest inventory; land cover; surface roughness;

Contents

List of Figures

List of Tables

1. Introduction

An Airborne Laser Scanner (ALS) system, often referred to as LiDAR (Light Detection and Ranging) or laser altimetry, is based on emitting short laser pulses towards the Earth's surface and on measuring round-trip times of return signals after diffusions and reflections on objects. In addition to recorded round-trip times, which are directly related to distances of the sensor to the objects, the direction of each laser beam is measured by the system. These polar coordinates of object points are transformed into a national ground survey coordinate system using the flight path positions measured with a differential Global Positioning System (dGPS) and an Inertial Measurement Unit (IMU).

Airborne Laser Scanner systems were developed for measuring the topography of the Earth's surface. One of the most crucial reasons for using ALS is the capability of laser beams to penetrate the forest canopy through small openings, and to measure the forest ground surface. As summarised in Ackermann (1999), in European type coniferous and deciduous forests common penetration rates of 20-40% can be expected and up to 70% in deciduous forests in winter time, if the ALS data have near vertical incident angles. Kraus and Pfeifer (1998) demonstrated that the calculation of Digital Terrain Models (DTMs) in wooded areas can be done successfully with a mean distance between points of 3.1 m and a penetration rate of about 25%, assumed that the vegetation and terrain points are mixed randomly. As an active remote sensing technique ALS systems are not dependent on the sun as a source of illumination as it is the case for passive sensors operating in the optical domain. Consequently, the recorded signal is not influenced by shadows caused by clouds or neighbouring objects. The measurement geometry of ALS systems is rather simple, that means that a three-dimensional (3D) point on the surface can be measured from one position. Furthermore, the small footprint sizes of laser beams, ranging between 0.2 and 2.0 m, allow data acquisition for the generation of DTMs even for highly urbanised areas and forests with very dense canopies. Finally, the mapping of surfaces with poor texture like coastal areas, wetlands, snow- and ice-covered areas is feasible with ALS.

During the last decade rapid technical developments (sampling density, multiple echoes, positional accuracy, data storage, etc.), which were mainly technology driven (Ackermann, 1999), pushed up the initially measuring rates of 2 kHz to 150 kHz (Leica, 2006). Currently, typical point densities vary between 1 to 4 points per square meter (p/m²) from 1,000 m flying height depending on the flying speed of the aircraft and the maximum scanning angle. For helicopter-based systems point densities of more than 20 p/m² can be achieved. Today, ALS is a well established technology for the highly automated generation of DTMs with high-quality (Ackermann, 1999; Axelsson, 1999; Kraus, 2003b; Wehr and Lohr, 1999). Additionally to these high technical advances, ALS

has achieved high economic performance and has reached a status which is interesting also for other applications. As mentioned in Wehr and Lohr (1999) ALS can complement, or partly replace, other existing geo-data acquisition technologies, and open up new exciting areas of application.

1.1. *Applications of airborne laser scanner data*

The multifaceted fields of ALS research and application include for instance traditional DTM generations (e.g. roads, railway tracks, pipelines, waterway landscapes, costal areas, whole countries), surveying and reconstruction of city areas (e.g. 3D city models, 3D building models), mapping of electrical transmissions infrastructure (e.g. power lines), derivation of vegetation parameters (e.g. forest stand- and single tree based parameters) and land cover classification purposes.

1.1.1. *Topographic mapping*

The main application of ALS is the determination of high accurate DTMs, which have a wide range of potential applications. Precise DTMs, including fine topographic features like small ditches and gullies, are mainly used for hydrologic and hydraulic applications. As reported in Marks and Bates (2000) two-dimensional (2D) hydraulic surface flow models are mostly constrained by inadequate parameterisation of topography and roughness coefficients, primarily due to insufficient or inaccurate data. Today, DTMs and their derived products such as slope, aspect and drainage network derived from ALS measurements compensate this lack of data and represent the natural topographic conditions in an appropriate form. Thus the uncertainties of the simulation results derived from hydrologic and hydraulic models can be minimised. Furthermore, ALS-DTMs are in use for modelling flood risk areas (Kraus, 2003c) or for the production of orthophotos or the orthorectifaction of high spatial resolution satellite imagery like IKONOS or QUICKBIRD data. Finally, ALS-DTMs are excellent data sources for engineering purposes (e.g. street construction) as well as for the increasing visualisation applications.

1.1.2. *Digital city models*

In addition to the DTM generation ALS data are an attractive data source for deriving digital city models. The large variety of applications using such models, ranges from environmental

planning and monitoring to location based services, navigation, modelling of the propagation of waves for telecommunications and many more. In the past digital city models were mainly derived by semiautomatic stereoscopic analysis of aerial images. During the last years the major technical developments in the ALS sector led to the fact that for the generation of city models primarily ALS data are in use today. The set up of a digital city model requires - apart from the generation of a DTM - first the detection and second the reconstruction of buildings. The majority of the available building detection algorithms is based on the extraction of geometric regular surfaces (roofs) from ALS data making use of surface properties such as local co-planarity (Rottensteiner et al., 2005a). The approaches for the reconstruction of buildings are oriented to the required level of detail ranging from simple vertical prisms to single roof planes. The achievable qualities of digital city models derived from ALS data are restricted by the measured point densities. For improving the accuracies and the reliability Rottensteiner and Briese (2003) suggested the integration of aerial images into the process of building extraction mainly due to the higher spatial resolution of aerial images. Thus, several approaches (Haala and Walter, 1999; Huber et al., 2003; Rottensteiner and Briese, 2003; Rottensteiner et al., 2005b; Sohn and Dowman, 2003) concentrated on using laser scanner data and optical imagery simultaneously for the generation of digital city models.

1.1.3. Power lines

A further area of application using ALS data is the extraction and reconstruction of 3D power lines from ALS point clouds. For energy providers the 3D reconstruction of power lines is important in order to control if the physical parameters of the cables are still within safe margins and to quickly detect anomalies or defects. Traditionally, tachymetric techniques have been used for the exact 3D measurements, which is very time consuming and costly. The use of photogrammetric approaches is near impossible due to the small diameter objects. In contrast to phogrammetric methods the technology of ALS is able to provide dense, fast and accurate measurements on such complex structures at reasonable cost. A semiautomatic software tool to detect and to reconstruct power lines is implemented into the Terrasolid software (Terrasolid, 2006). Furthermore, Melzer and Briese (2004) developed a fully automated method for the 3D reconstruction of power lines based on ALS data. After common preprocessing steps, they use a 2D Hough transformation for locating groups of parallel power lines (corridors) in the projection of the point cloud onto the x-y-plane. In a final step a 3D fit is computed locally within its corresponding corridor for each power line.

1.1.4. *Vegetation mapping*

In addition to the detection and reconstruction of man-made objects ALS data have a great potential for forestry applications. Although small footprint laser scanning systems were not developed for purposes of geometric description of vegetation, these laser systems have proven to be more suitable for estimating of important forest variables than several passive optical sensors. As summarised in Holmgren (2003) such forest parameters are necessary for forest management planning, to support decisions at different administrative levels, for strategic forest planning for long term timber supply for small private forest owners or for companies, tactical planning concerning allocation of forest operations in time and space and operational planning of forest treatments, such as clear felling. As an active remote sensing system a small footprint ALS system enables receiving data also for objects shadowed by neighbouring ones. The count of received backscattered echoes is depending on the objects within the travel path of the laser pulse. Therefore, state-of-the-art laser scanner systems measure the round-trip time of multiple echoes from one laser pulse, e.g. first- and last-echo, or up to five echoes. Laser scanner systems recording the full waveform of the backscattered signal have become commercially available recently (Wagner et al., 2006b; Wagner et al., 2004b). Due to small openings in the forest canopy the ground surface but also the vertical and horizontal distribution of the vegetation (forest) structure can be described with ALS data in an efficient and accurate way. In general, ALS provides an irregular distributed 3D point cloud including points from ground surface, branches, leaves, needles and man made objects. Therefore, ALS does not allow determining forest parameters directly. A common way to derive forest parameters (e.g. stem volume, basal area, tree height, crown closure, etc.) from ALS data is to build up relationships to field data using regression models. The field data are normally measured on a plot level and include the traditional forest parameters like tree height, diameter at breast height and tree species. A comprehensive survey of using ALS in forestry is given by Lim et al. (2003), Hyyppä et al. (2004) and Næsset et al. (2004) who summarise the application of ALS in operational forest inventories in Norway, Sweden and Finland respectively. Even though, ALS is in use for operational forest inventories in these countries, the use of ALS for forestry applications in alpine environments is reduced to small study areas. The reasons for that can be the complex topography, the relatively low point density achievable with former ALS systems and finally the lack of appropriate algorithms. Furthermore, forests in alpine environments are more complex (multilayered) than most of the Scandinavian forests.

1.1.5. Land cover classification

Today, ALS data are available for whole countries (Switzerland, Netherland), for large districts (South Tyrol / Italy, Vorarlberg / Austria, Saxon-Bohemian Switzerland / Germany, Baden-Württemberg / Germany) and for corridors along several rivers. All these data sets have been gathered for the generation of high precision DTMs, for the extraction of buildings and/or for the derivation of forest parameters. Until now, the object height information derived from the subtraction of the DTM from the digital surface model (DSM) has not been widely used for the purpose of conventional land cover classifications.

The research area of land cover classification has a long history and is one of the major applications of remotely sensed data. Especially for low or medium spatial resolution satellite imagery the spectral signature of each pixel is used for assigning them a land cover class. Such pixel based methods are still in use but are very limited for land cover classifications based on very high spatial resolution images such as aerial orthophotos or satellite imagery like IKONOS or QUICKBIRD. For the analyses of such data sources object-oriented approaches have been established and were already implemented into commercial software packages (e.g. eCognition). In addition to averaged spectral signatures the shapes of objects are important for these object-oriented classification techniques. The two-dimensional description of object shapes is possible by calculating geometric parameters (e.g. area, length, width, compactness, asymmetry, etc.) for each object (segment). The accuracies of the derived results are quite good but particularly for shadowed areas several problems occur. First of all, the generated object borders do not correspond with the reality and therefore, the calculated shape parameters are not representative for the objects. Secondly, the spectral information is of low significance in areas which are shadowed. Further restrictions are evident if land cover classes have to be differentiated regarding to object heights (e.g. building height classes, surface roughness classes, etc.). To overcome these limitations several authors (Flood, 2001; Haala and Walter, 1999; Hodgson et al., 2003; Hoffmann and Van der Vegt, 2001; Hollaus et al., 2005; Rottensteiner et al., 2005b) recommended the integration of the object height information derived from ALS data with multi-spectral image data. Therefore, a higher degree of automatisation in the land cover classification workflow as well as an enhancement of the derived results can be reached using the complementary informational content of these two data sources.

1.2. Objectives

Nowadays, small footprint airborne laser scanner (ALS) data are the standard data source for the generation of high precision digital elevation models as mentioned above and have reached a technical status, which allows to use these data for a multitude of applications. Kraus (2003a) summarised that especially for applied sciences ALS becomes a relevant branch of gathering geo-data. Also Maas and Vosselman (2004) mentioned the high potential of ALS for the fast acquisition of 3D geo-data with high accuracy. From an economic point of view 3D geo-data acquisition via ALS will develop into a cost efficient method. The reasons are the rapid technical developments (e.g. measurement frequency, position accuracy), the minimisation of the field-operation costs, the decrease of data costs due to the multiple usage of the data and the possible high degree of automatisation which reduces post-processing time and costs.

As summarised in the introduction, the field of using ALS data in applied sciences is wide and the data are already available for large regions, but especially for complex mountainous environments the available algorithms to derive the needed information are often not satisfactory for practical applications. Therefore, this thesis concentrated on large area applications of ALS data for a complex alpine environment. The operational use of ALS data for forestry and hydrology was the main objective of this work. For the presented work ALS data of a 128 km² test site in Vorarlberg, Austria were used, which had been acquired within the framework of an operational DTM mapping activity. In addition to the available ALS data the choice of this study region was driven by the accessibility of operationally used forest inventory data, which serve as reference data for the analyses. In order to achieve the above objectives the following specific aims of this thesis can be formulated:

- To investigate the capability of state-of-the-art ALS technology for generating topographic models (e.g. DTMs, DSMs) for a large mountainous area. Due to the difficult topography of the study area (altitudes ranging between 800 m and 2,900 m) the whole region had been gathered by two flight-campaigns at different acquisition times. The point density on the surface and the flying altitudes vary, which made the generation of homogenous models difficult. Thus, the derived accuracies of the generated topographic models for different acquisition times (summer, winter) and point densities were analysed.

- To examine the usefulness of ALS data for conventional land cover classification purposes. The focus for using the derived land cover products lied in hydrologic and hydraulic applications.

- To assess the potential of using ALS data in combination with colour-infrared (CIR) orthophotos for the generation of high spatial resolution land cover maps using an object-oriented classification approach.

- To identify the possibilities for using the complementary information content of CIR orthophotos and ALS data for the parameterisation of hydraulic / hydrologic models.

- To demonstrate the potential of ALS data for mapping canopy heights of mountainous forests. The influence of different ALS point densities and acquisition times on the derived canopy height accuracies was investigated.

- To evaluate the transferability of the statistical model for estimating stem volume developed by Næsset (1997b; 2002; 2004b) to the alpine study area in Austria. This multiplicative model is widely used for Scandinavian forests which are characterised by a rather homogenous forest structure. In contrast to Scandinavian forests, Austrians forests show high variability and complex structure due to varying ecological conditions (Koukal, 2004).

- To develop a physical based model for estimating stem volume, which consider the high variability and complex structure of Austrian's forests. A simple linear model including only a low number of parameters was used.

- To study the usability of forest inventory data, which are in use for the forest administration "Stand Montafon Forstfonds", for calibrating the regression models and for validating the derived forest parameters (canopy height, stem volume). The design of the forest inventory data is based on permanent sample plots distributed in a regularly grid of 350 m. The tree specific parameters were gathered based on so-called Bitterlich plots, which are characterised with variable sample plot sizes. This forest inventory data have the advantage of being available but the disadvantage that they are not optimised to serve as reference data.

- To study the influence of varying ALS point densities and acquisitions times on the estimated stem volume. For large mountainous areas the ALS data are normally gathered with varying system parameters (e.g. varying point densities).

Finally, this thesis should contribute to an increased knowledge about the usability and potential of airborne laser scanner data for forestry and for hydrologic applications.

1.3. Structure of the work

Chapter 1 gives a brief introduction into the methodology of small footprint airborne laser scanning. The remaining part of chapter 1 concerns an overview of the most common areas of applications for ALS data with emphasis on applied sciences. Chapter 2 gives a short overview of the historical development of laser technology and of available LiDAR systems. Furthermore, an overview of state-of-the-art ALS data processing (e.g. georeferencing, derivation of topographic models) is given in chapter 2. A literature review of using ALS data for applied sciences (hydrology and forestry) concludes this chapter. In chapter 3 the study area and the used data (e.g. ALS data, aerial photography and forest inventory data) are described. The methods for deriving forest parameters from small footprint ALS data as well as the approach for using ALS data for land cover classification purposes is outlined in chapter 4. The results are presented in chapter 5 and the findings are discussed in chapter 6 focusing on the aspects of what can be reached with the available ALS data, and what can be expected from future ALS systems. Chapter 7 draws an overall conclusion of the presented studies and provides perspectives for future investigations, concerning unsolved problems and potential application areas.

2. Status of research

This chapter gives a short historical introduction into the developments of laser technologies for three-dimensional mapping of the Earth surface and presents an overview of available airborne laser scanner (ALS) systems. A detailed literature review of currently available systems as well as their physical background is given in the following sections. In addition to the descriptions of ALS systems the status of research regarding to the georeferencing of ALS data and the derivation of surface models is delineated. Furthermore, this chapter deals with the state-of-the-art concerning the use of ALS for hydrologic applications as well as for forestry. A general comparison between airborne laser scanning and aerial photography concludes this chapter.

2.1. LiDAR background

The use of laser technology for remote sensing purposes goes back more than 40 years. In the year 1960 Theodore Maiman demonstrated the first successful laser (light amplification by simulated emission of radiation) in the infrared and optical part of the electromagnetic spectrum. Lillesand et al. (2004) pointed out that the use of LiDAR for precise determination of the Earth topography began in the late 1970s. The initial systems were laser profiler, which measured the elevation data only along a single track defined by the flight line of the aircraft. Such systems were also called laser altimeter and were originally designed to measure the range to the first surface intercepted by the laser beam.

One of the first systems was the Atmospheric Oceanographic LiDAR (AOL), which was developed by the NASA and the National Oceanic and Atmospheric Administration (NOAA) in 1975. The purpose of this program was to investigate the potential of an airborne LiDAR system in the areas of altimetry, hydrograhpy and fluorosensing. In the year 1994 a separate airborne LiDAR system for topographic mapping purposes was developed by NASA. This sensor, referred to as the Airborne Topograhic Mapper (ATM), was primarily dedicated to map the surface elevation of polar ice sheets (e.g. Greenland Ice Sheet and other Arctic glaciers) and to measure the topography of the sea ice in the central Arctic Basin, ocean beaches and drainage systems. For the ATM a conical scanning mirror is used to direct the laser beam along an elliptical sampling pattern beneath the aircraft, whereas only the first-return signal is recorded.

In addition to these airborne systems, Flood (2001) summarised that laser altimetry was successfully applied also from near-Earth orbit during the Shuttle Laser Altimeter (SLA) mission and from satellite platforms. Currently an operational satellite mission that deploy laser altimeter is

operated by NASA, namely the Geosciences Laser Altimeter (GLAS) on board the ICESat satellite (Zwally et al., 2002). The proposed satellite mission Vegetation Canopy LiDAR (VCL) was suspended by the NASA. The primary purpose of ICESat is to measure the changes in the size of Earth's polar ice sheets, the heights of global clouds and aerosols and global land topography. Space borne laser altimetry was also applied to measure the topography of the Mars using the Mars Observer Laser Altimeter (MOLA).

Most of these mentioned systems are used for surveying non-vegetated areas, where it is sufficient to record only the time between the laser shot and the first returned signal. In vegetated environments it is useful to record not only the first but also the last or even intermediate returns. For some applications, the recording of the full backscattered waveform for each emitted pulse may be desired. This kind of waveform digitisation can provide vertical information within the vegetation canopy.

One of the first systems, which were capable to record the full waveform, was the Scanning LiDAR Imager of Canopies by Echo Recovery (SLICER). This system evolved from profiling LiDAR altimeter by the addition of a scanning mechanism and allowed the acquisition of both cross- and along-track information. During the last decade several studies (Drake et al., 2002; Dubayah and Drake, 2000; Harding et al., 2001; Lefsky et al., 1999a; Lefsky et al., 2002; Means et al., 1999; Parker et al., 2001) were investigated, which showed the high potential for using SLICER data to derive forestry information. The principles and algorithms developed for SLICER data can also be applied to canopy LiDAR data, which are acquired by the airborne LiDAR Vegetation Imaging System (LVIS) and the spaceborne VCL. As summarised in Blair et al. (1999) LVIS has provided the test-bed and data sets for algorithm development, instrument design, calibration and validation of the VCL mission. The high power laser employed for SLICER and LVIS enables significantly higher flight altitudes (e.g. 8 to 10 km AGL) than are typically used by airborne laser altimeter, yielding in footprint sizes of 10 to 25 m in diameter. Also the space based VCL with an orbital altitude of 400 km is characterised through individual laser footprints of 25 m in diameter. Thus, over forested areas such large footprints typically contain in addition to canopy areas some openings to the ground. The capability of SLICER, LVIS and VCL to record the complete time-varying distribution of the laser return echo energy with very high temporal resolution has confirmed the ability of these large footprint LiDAR systems to estimate important structural forest attributes. For example, the vegetation height can be extracted from the waveform data based on the time difference between the first and the last returns within one footprint.

However, these above mentioned systems are commonly experimental and are designed to push technological envelopes rather than to be cost-effective (Nelson et al., 2003). On the other hand small footprint airborne laser scanner systems (ALS) are available commercially today, and

the new sensors meet the requirements of high sampling intensity and multiple return recording. The sophisticated ALS systems have established itself as a robust and cost-effective operational tool (Flood, 2001) and have revolutionised the area of topographic surveying. Therefore, ALS are currently the primarily data acquisition method for generating high accurate digital terrain models (DTMs). In addition to the classical DTM generation ALS data are already in use for a multitude of applications as summarised in the section 1.1.

The developments of ALS systems were associated with the advances in position and orientation systems, realised by differential global positioning systems (dGPS) and inertial navigation systems (INS), also referred to as inertial measurement units (IMU). Thus, in the 1990s, profiling LiDAR systems were gradually replaced by ALS systems, which have been successfully established itself within few years to an independent technology for the highly automated generation of topographic data.

An extensive overview of commercial available resources (e.g. existing systems and firms) on ALS is given by Baltsavias (1999b). As ALS is a rapidly growing technology several technical improvements occur since Baltsavias came out with his overview paper. Especially the sampling frequency, the positioning accuracy and the number of recorded echoes have been improved during the last seven years. One of the first small footprint ALS systems optimised for capturing the full waveform is the Riegl LMS-Q560, which was introduced into the market in 2004. Also the companies Leica, Optech and Topeye have been starting offering small footprint full waveform systems.

As summarised in this section, there are currently many types of LiDAR instrumentations available. However, the focus of this thesis was confined to small footprint ALS systems, whose components and physical background are described in more detail in the following sections.

2.2. Airborne Laser Scanner systems

As already mentioned in the introduction, ALS has achieved high economic performance for topographic data acquisition and are in use for a multitude of practical applications. Today, the ALS market is a prospering business and several companies offer topographic data for relatively low costs. However, ALS has not been reached their technical limits until now, and still several improvements and extensions of the entire processing chain including data recording systems as well as post processing algorithms are available within short update rates.

2.2.1. System components

Nowadays, a large variety of different ALS instruments is used in different platforms (e.g. plane, helicopter), which are operating at different altitudes above ground. The flying altitude (e.g. 100 to 6,000 m) depends on the specifications of the used laser and the required footprint size and point density on the ground. Baltsavias (1999b) and Wehr and Lohr (1999) give a detailed overview of ALS specifications and sensors available in the 1990's. In the following a short description of the main ALS components and their functions is given. A typical ALS system consists of (1) a laser ranging unit, (2) an opto-mechanical scanner, (3) a position and orientation unit and (4) a control, processing and storage unit (Figure 2.1).
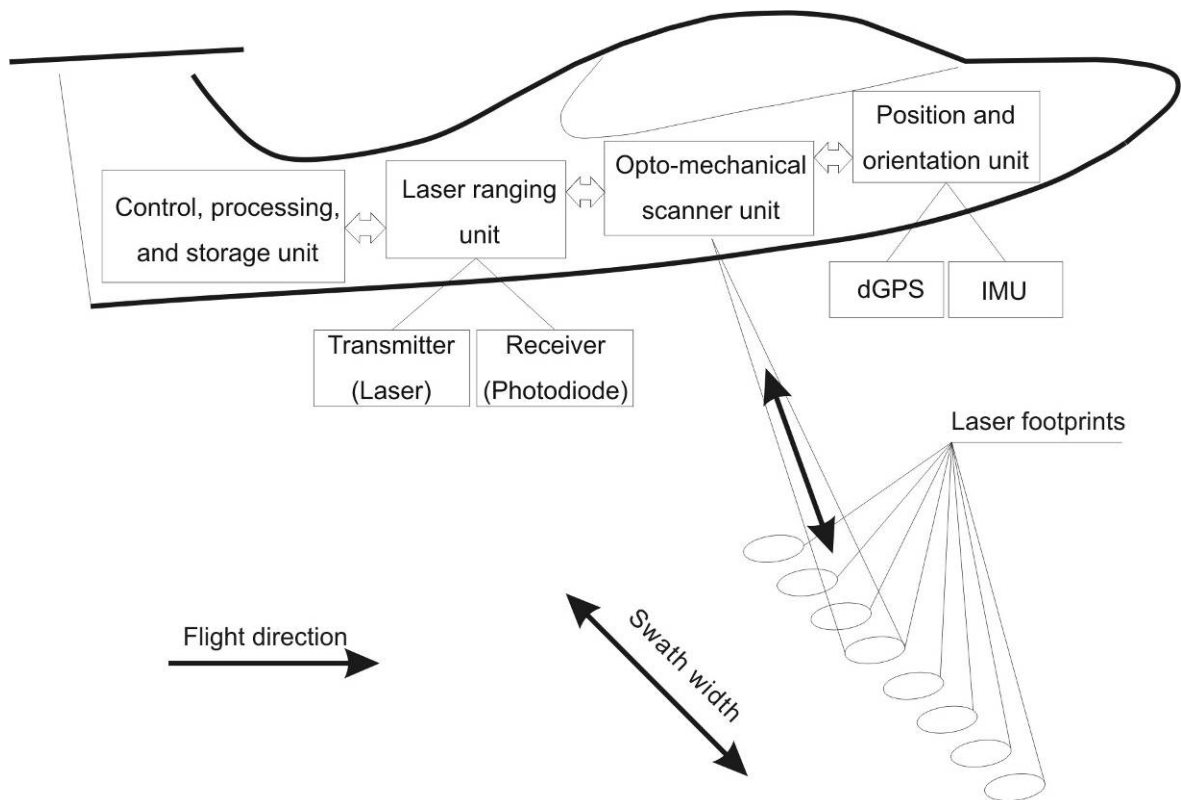
Figure 2.1: Components of a typical airborne laser scanner system.

2.2.2. Laser ranging unit

The laser ranging unit can be subdivided in a transmitter, a receiver and the optics for both units. The transmitter typically consists of a semiconductor diode laser or an Nd:YAG

(neodymium:yttrium-aluminium-garnet) solid-state laser pumped by semiconductor lasers, which generates the laser light (Wehr and Lohr, 1999). As summarised by Weitkamp (2005) the transmitter optics of an ALS systems serves the dual purpose of expanding the laser-beam diameter in order to reduce the area density of the laser pulse energy and of reducing the divergence of the laser beam. The receiver optics collects the backscattered light and focuses it onto the detector, which converts the photons to electrical impulses. An associated processing unit extracts the relevant information, which are collected from a high-speed data recorder. The whole laser ranging unit is monostatic, which means that the transmitting and receiving apertures are mounted on the aircraft so that the transmitting and receiving paths share the same optical path (Wehr and Lohr, 1999). For practical realisation the transmitter and the receiver are mounted coaxial, with the axes of the transmitted beam and receiver field of view (FOV) coinciding, or side by side or biaxial, with the two axes parallel or near-parallel, but not identical (Weitkamp, 2005). Therefore, it is ensured that an illuminated surface point is in the FOV of the optical receiver. For the range measurements two different principles are applied, namely the pulse ranging and the phase difference measurement. The pulse ranging principle measures the travelling time of short pulses which are transmitted from the laser, backscattered from an object and detected from a receiver. This measurement principle is commonly used for airborne systems and is described in more detail in section 2.3. The phase difference measurement is applied for so-called continuous wave (CW) lasers, which continuously emit laser light. Currently, these laser systems are seldom in use (Wehr and Lohr, 1999) and are therefore not further described in this thesis.

2.2.3. Opto-mechanical scanning unit

The opto-mechanical scanning unit is responsible for the deflection of the transmitted laser beams across the flight path. As pointed out by Wehr and Lohr (1999) the design of the deflection unit (e.g. oscillating mirror, rotating polygon, multifaceted mirror, fiber scanner, nutating mirrors) defines the scan pattern on the ground. Oscillating mirrors produce zigzag-lines or with two-axis galvanometers a bidirectional meander-type scans of parallel lines. Rotating polygons, multifaceted mirrors and fiber scanners produce parallel lines, whereas nutating mirrors produce elliptical scan pattern. The motion of the aircraft in combination with the deflection of the laser beam across the flight path generates strip-wise measurements of the illuminated surface. If pulse laser scanners are used, the achievable point density on the ground mainly depends on the survey altitude, the speed of the aircraft, the deflection unit, the scanning angle and the pulse repetition frequency. For continuous wave laser scanners the most important factor influencing the point density is the measurement rate instead of the pulse repetition frequency.

2.2.4. Position and orientation unit

In addition to the distances between the laser ranging unit and the measured objects on the ground the positions and the orientations of the ALS system must be measured. A differential global positioning systems (dGPS) consisting of an onboard GPS receiver and one or more ground stations provides the position of the laser ranging unit. Instead of temporally installed GPS ground stations, reference data provided by a fixed GPS reference station network can be used. The orientation of the ALS system is described by the pitch, roll and heading of the aircraft, which is measured by an inertial navigation systems (INS), also referred to as inertial measurement units (IMU). Furthermore, the beam direction relative to the ALS system is recorded for each laser measurement.

2.2.5. Control, processing and storage unit

The measured data from all units are time marked and saved in the storage unit. The control and processing unit provides the system set-up, monitoring and control of the whole ALS system components.

2.3. Physical principles

In this section a short introduction in physical principles of airborne laser scanning is given. Detailed collections of physical formulas and basic relations concerning ALS can be found in Baltsavias (1999a), Wehr and Lohr (1999) and Wagner et al. (2003). An extensive physical description of a small footprint, full waveform digitising airborne laser scanner is given by Wagner et al. (2006b).

2.3.1. Laser light properties

The physical principles of LiDAR are similar to those of RADAR (RAdio Detection And Ranging) but for LiDAR short pulses or beams of laser light instead of a wide range of radio waves are used. Airborne laser scanner systems use the infrared portion of the electromagnetic spectrum as this wavelength provides the strongest signal response from terrestrial surfaces and gives clearly recordable return signals after diffusion and reflection on the ground (Ackermann, 1999).

Furthermore, Wagner et al. (2003) summarised the exceptional properties of laser light compared to natural light. For example, laser light is to a high degree monochromatic (exactly defined frequency, narrow bandwidth), highly directional (relatively narrow beam in a specific direction) and coherent (waves swing in phase). In addition, laser light can excite an extremely high pulse power by using a process which is called optical pumping. Finally, they stated that the high pulse power, the short pulse duration, the high pulse firing rate, the small beam divergence and the narrow bandwidth of laser light are advantageous for ALS applications. For example, the high pulse power allows to fly at high altitudes and therefore, larger areas can be covered. Short pulse durations are needed to improve range discrimination and the small divergence of the laser beam is important for small footprint sizes. State-of-the-art ALS systems have a beam divergence of 0.2 to 2.0 mrad, resulting in a footprint size of 0.2 to 2.0 m for a flying height of 1,000 m. Due to the narrow bandwidth of laser light optical interference filters can be installed in the receiver path, which suppress disturbing background radiation (e.g. backscattered sunlight) (Wehr and Lohr, 1999).

2.3.2. Sensor characteristics

For the generation of the laser light semiconductor diode lasers or Nd:YAG lasers pumped by semiconductor laser, with pulse widths less than 10 ns are commonly used. These lasers operate in wavelengths between 800 nm and 1 600 nm of the electromagnetic spectrum and have a pulse energy in the order of 100 µJ. In general, the selection of the wavelength and the peak power is related to the overall ALS system design and to eye safety considerations (Wehr and Lohr, 1999). An important component of an ALS system is the used detector. According to Wehr and Lohr (1999) the most sensitive detectors are available for wavelength between 800 nm an 1,000 nm. Therefore, a wavelength of 900 nm was used for the first ALS systems. Due to the low power of the backscattered echoes higher laser pulse energy is required, which is incompatible with eye safety considerations. Therefore, current ALS systems use wavelengths of 1.064 µm and 1.535 µm respectively for which eyes are less sensitive and thus, higher energy levels can be used. Although the sensitivity of the useable photodiodes for these wavelengths is lower, the higher pulse energy leads to an improved ALS ranging performance. However, for the practical planning of ALS flight campaigns (e.g. used ALS system, flying height) one have to consider the different target reflectivity for different wavelengths and the fact that the power of a laser echo decreases with the square of the distance.

2.3.3. Scanner characteristics

The distribution of the transmitted laser beams across the flight direction is done by the opto-mechanical scanning unit whereas the flying speed of the aircraft is responsible for the point distribution in flight direction. Depending on the used deflection system and the flying height above ground h the swath width SW is given by Eq.(2.1).

$$SW = 2\,h\,\tan\left(\frac{\theta}{2}\right)$$
(2.1)

where θ is the scanning angle. For current ALS systems the scanning angles are in the range of $\pm 20°$ to $\pm 30°$, resulting in a swath width of about 730 m and 1 150 m respectively for an average flying altitude of 1 000 m. Today, the pulse repetition frequencies vary between 5 kHz and 150 kHz depending on the used ALS system and flying height above ground. An important characteristic in ALS is the point density, which significantly influences the accuracy of derived topographic models. Typically, for large scale terrain mapping point densities between 1 p/m² and 4 p/m² are used. For the surveying of special objects (e.g. buildings, power lines, etc.) point densities up to several dozen of points per square meter can be measured. A summary of the most important characteristics of typical commercial ALS systems is given in Table 2.1.

2.3.4. Range measurement

For a pulsed airborne laser scanner system the principle of range measurement is based on measuring the time between the transmission of a short laser pulse and the reception of the backscattered echo. Knowing the round-trip time t of the laser pulse the range R between the sensor and the target is given by

$$R = \frac{v_g\,t}{2}$$
(2.2)

where v_g is the group velocity of the pulse. According to Rees (2001) the group velocity describes the velocity of the propagating waveform and is for atmospheric conditions about 299 710 484 ms^{-1}, which is about 0.03% slower than the speed of light (c = 299 792 458 ms^{-1}). Due to the fact that current LiDAR systems use a single telescope for transmission of laser pulses and reception of backscattered echoes only one pulse is travelling at a time and therefore, no overlapping of pulses is allowed. Depending on the flying altitude above ground this determines

the maximum possible Pulse-Repetition-Frequency (PRF). For example, the maximum possible PRF is 150 kHz for a flying altitude above ground of 1 000 m and 74.9 kHz for 2 000 m.

A transmitted pulse can not only be scattered from several targets on the Earth's surface but also from the molecules and particles in the air. Therefore, the returned signal can be complex and is extended in time with several short peaks for each target and a much weaker, but temporally extended signal from the air. One of the most crucial factors for an exact range measurement is the used echo detection algorithm. For multiple return ALS systems several algorithms (e.g. threshold, centre of gravity, maximum, zero crossing of the second derivative and constant fraction) can be used. As pointed out by Katzenbeisser (2003) the most frequently used algorithms are based on threshold approaches which trigger an echo if the rising edge of the received signal exceeds a defined threshold. For novel small footprint, full waveform ALS systems, Wagner et al. (2006b) presented a technique referred to as Gaussian decomposition to model the whole waveform as a series of Gaussian pulses. As a result the range, amplitude and width for each echo can be extracted.

In addition to the echo detection method the accuracy of the range measurement is also influenced by the resolution of the time counter used for the measurement of the round-trip time. Typically, the time resolution is about $\Delta t = 1$ ns. Using Eq.(2.3) the range error ΔR can be calculated and is in the order of 0.15 m.

$$\Delta R = \frac{v_g \, \Delta t}{2} \qquad\qquad (2.3)$$

Finally, for an ALS system the range resolution is an essential parameter, which depends mainly on the duration τ of the transmitted pulse. Therefore, a successful separation of two neighbouring targets along the pulse path requires a minimum distance d between the targets given in the following Eq.(2.4).

$$d = \frac{v_g \, \tau}{2} \qquad\qquad (2.4)$$

Thus, a pulse duration of 10 ns leads to a range resolution of 1.5 m. If the distance between the targets is less than d, only one dispersed target can be detected.

Currently, most of the available ALS systems are able to record in addition to the range at least the intensity (multiple return systems) or even the amplitude and echo width (full waveform systems) for each backscattered echo. Detailed physical information about these additional ALS capabilities can be found in Katzenbeisser (2002) and Wagner et al. (2006b).

Table 2.1: Summary of relevant characteristics of typical commercial ALS systems. The information are based on Baltsavias (1999b), Briese (2004a), Optech (http://www.optech.ca), Riegl (http://www.riegl.com) and Leica (http://www.leica-geosystems.com).

Specification	Multiple return systems	Full waveform systems
	Typical values of commercial available ALS systems	
Laser ranging unit		
Operating altitudes above ground	100 to 6 000 m	30 to 1 500 m
Wavelength	0.8 to 1.56 µm	NIR
Pulse duration	5 to 10 ns	4 ns
Pulse energy	100 to 200 µJ	8 µJ
Beam divergence	0.2 to 2.0 mrad	0.5 mrad
Footprint size on the ground (flying height: 1,000 m above ground)	0.2 to 2.0 m	0.5 m
Pulse repetition frequency (PRF)	5 to 150 kHz	<100 kHz
Discretisation of backscattered echoes	up to 5 returns	1 ns
Additional recordable information	intensity	Amplitude, number of echoes, echo width, cross section
Opto-mechanical scanner unit		
Scanning angle	±14 to ±75°	±22.5°
Scan rate	25 to 650 Hz	<160 Hz
Position and orientation unit		
GPS frequency	1 to 2 Hz	
INS frequency	50 to 200 Hz	

2.4. Georeferencing

As already mentioned in section 2.2.4, an airborne laser scanner system measures not only the range between the sensor and the target, but also the position and orientation of the sensor. The three-dimensional (3D) positions of the targets are calculated in a post-processing mode, whereas all different data sources are linked using time marks. The dGPS and IMU are used to measure the time dependent position and orientation of the airborne platform and therefore, their trajectory can be computed. The accuracies of the trajectories are thereby significant influenced by the measurement frequencies of dGPS and IMU (Table 2.1). Finally, the ranges are converted to 3D elevation data using the instrument mounting parameters and the aircraft trajectories. The results of these calculations are strip-wise 3D points in a global coordinate system, e.g. WGS84.

As mentioned by several authors (Ackermann, 1999; Kraus, 2003a; Maas and Vosselman, 2004; Wehr and Lohr, 1999) topographic data (e.g. digital terrain models, digital surface models) derived from ALS measurements as well as value-added products (e.g. city models, vegetation parameter, etc.) serve as geo-basis data for many applications. Therefore, the geometric accuracy requirements are large and it is essential to transform the data from the WGS84 to a desired local coordinate system. First of all, geometric error sources can be found in possible inaccuracies in all

ALS system components, leading to discrepancies in height and planimetry of the ALS data. Secondly, a possible error source is the insufficiently description of the geoid (Kager, 2004), which is an essential input information for the transformation to the local coordinate system.

An approach to minimise all these inaccuracies was presented by Kager (2004). His method employ an adjustment strategy for correcting the exterior orientation elements as recorded by dGPS and IMU, as well as interior orientation elements concerning the Scanner-dGPS-IMU system. The method applies correction polynomials in the time domain to all degrees of freedom as determined by the dGPS-IMU components and to the relative orientation parameters between those and the laser scanner-device itself. All these parameters are determined simultaneously with hybrid block adjustment by least squares. The result of this pre-processing step is a high quality georeferenced 3D point cloud, which minimises the discrepancies between overlapping laser scanner strips and ground controls. Further information about georeferencing methods can for example be found in Burman (2002), Crombaghs et al. (2000), Kilian et al. (1996), Kraus and Pfeifer (2001), Pfeifer et al. (2005), or Vosselman and Maas (2001).

2.5. *Digital models from ALS data*

The basic ALS data sets consist of point clouds derived from e.g. last-echoes, first-echoes and depending on the used ALS system intermediate-echoes. As ALS is not capable to measure particular objects or object features the resulting 3D points are irregularly dispersed. The great advantage of ALS data lies in the high accuracy and in the high sampling density and therefore, they provide ideal input data for the continuous description of topographic surfaces. As summarised in Briese (2004a) many different surface modelling techniques exist which can be divided in topological and functional modelling approaches.

For topologic modelling approaches surfaces are described based on observed ALS points and additionally determined topological information (e.g. breaklines, formlines, etc.). The main aim of these approaches is to build up a topology, which can be done with different algorithms (e.g. Delaunay triangulation (Kraus, 2000), greedy triangulation (Dickerson et al., 1997). Commonly, triangular irregular networks (TINs) are used to represent the surfaces. In contrast to topologic methods functional approaches use mathematical functions to describe surfaces (Briese, 2004a). In general, functional modelling techniques can be subdivided in interpolation and approximation methods. For both methods the mathematical functions are determined on the basis of the original observed ALS points and additionally determined geometric information (e.g. breaklines, formlines, etc.). The determined functions of interpolation methods exactly describe the measured

ALS points, whereas the functions of approximation methods just approximate the ALS points. This allows removing measurement errors of the ALS system and leads to smooth surfaces. As pointed out in Briese (2004a) the most commonly used interpolation methods are moving least squares (Lanchaster and Salkauskas, 1986), finite elements (Hoschek and Lasser, 1993) and the statistical based kriging (Journel and Huijbregts, 1978) similar to the least squares interpolation (also referred as linear prediction) (Kraus, 1998; Kraus and Mikhail, 1972). The determined functions can either be stored as mathematical function or can be discretised. The elevations of the discretised functions are commonly stored in raster, grid, or hybrid grid data structures. The hybrid grid model allows the integration of irregularly distributed vector information into the grid data structure (Kraus, 2000). A detailed overview of advantages and disadvantages of topological and functional modelling approaches as well as their preferred area of applications can be found in Briese (2004a) and Ackermann and Kraus (2004).

Apart from the used modelling technique several different models can be generated from ALS data. The most important model is the digital terrain model (DTM), which describes the elevation of the ground surface. Synonymously the term digital elevation model (DEM) is in use, which describes height information in a more general fashion. In contrast to the DTM the digital surface model (DSM) represents the top most surface which can be seen from the aeroplane. According to Pfeifer (2003) the elevation of the DSM in open areas like streets, agricultural fields without vegetation, grassland with short vegetation, or areas with bare soil is equivalent with the elevation of the DTM. For buildings the DSM describes the roofs whereas the DTM describes the terrain without buildings. In forested areas the DTM represents the ground surface and the DSM the elevation of the top most canopy surface (Figure 2.2).

For the generation of the DTM the observed ALS point cloud must be classified in terrain and off-terrain points, which is commonly referred to as filtering (Kraus and Pfeifer, 1998). This is not a simple task because current ALS systems provide only geometric information from unknown targets, encountered by the laser beam. Due to the missing semantic information it is unknown where the recorded echoes are coming from. Therefore, physically based approaches are not feasible. This necessitates the use of statistical approaches that model, in some way or other, the spatial relationship of the data cloud. Commonly used filtering algorithms are the morphological filtering, the progressive TIN densification, or the robust filtering. An extensive overview of different filtering approaches can be found in Sithole and Vosselman (2004). All of these filtering methods assume that objects on the ground, such as trees, cars or buildings, are usually higher than those of the surrounding ground points (Pfeifer, 2003; Zhang et al., 2003). Therefore, points are more likely to be classified as off-terrain points if they "stick out" from the neighbouring point cloud. With novel ALS systems, which record the full waveform of the backscattered echo, it is

possible to provide additional, more physically based criteria for the classification of the point cloud (Wagner et al., 2006a; Wagner et al., 2006b). Furthermore, the use of intensities of laser echoes for the filtering process could improve the classification accuracy. However, the use of this information requires an appropriate calibration, which is an ongoing research (Kaasalainen et al., 2005).
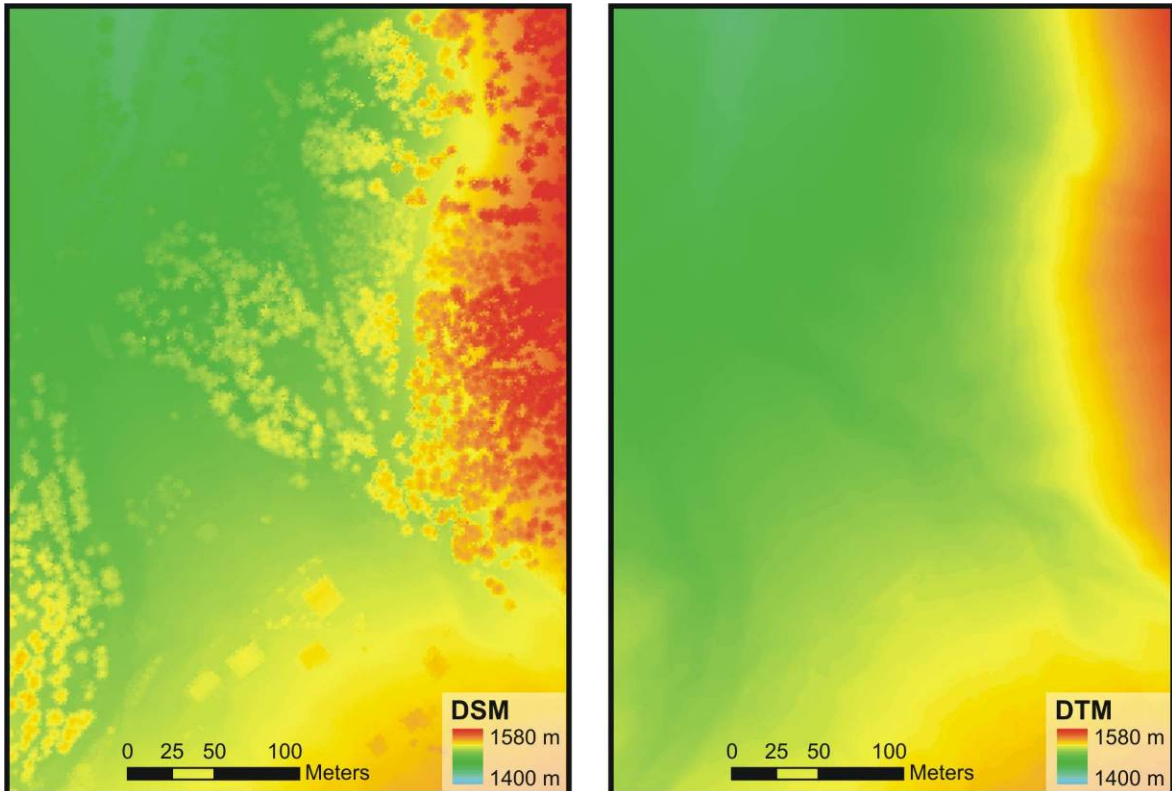
Figure 2.2: Digital surface model (DSM) versus digital terrain model (DTM).

Today, typical ALS data consist of first- and last-echo points. Thus, the reconstruction of DTMs, using topological or functional modelling approaches, is based on terrain points extracted from last-echo data by means of filtering. The generation of DSMs is commonly based on the highest first-echo points within a defined grid box, whereas simple interpolation methods (e.g. moving planes) can normally be used. A typical subsequent product from a DTM and a DSM is a so-called normalised digital surface model (nDSM) calculated by subtracting the DTM from the DSM (Figure 2.3). For forestry applications the nDSM is commonly referred to as digital crown model or canopy height model (CHM) (Hyyppä and Inkinen, 1999; Popescu et al., 2002).
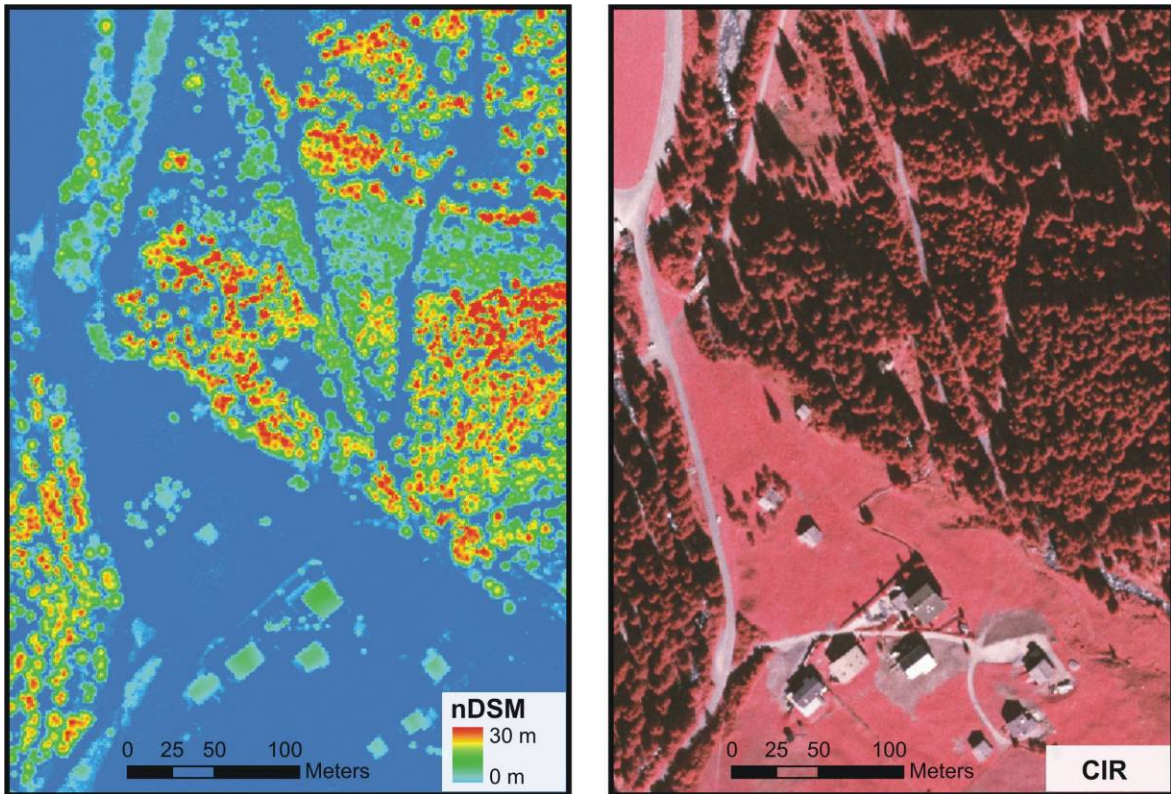
Figure 2.3: Normalised difference surface model (nDSM) versus colour infrared (CIR) orthophoto. The nDSM is also called canopy height model (CHM) and is calculated by subtracting the DTM from the DSM. The spatial resolution of the nDSM is 1.0 m and 0.25 m for the CIR orthophoto.

The accuracy of the derived topographic models is influenced by the ALS system components, the modelling method, environmental conditions and the covered area. As already mentioned in section 2.3.4 the accuracy of the laser range measurement is a function of the flying height, the quality of the dGPS and IMU data, the laser beam diameter and the used post-processing algorithms. However, depending on the used ALS system vertical errors of ±15 cm can occur (Hodgson and Bresnahan, 2004; Kraus et al., 2004; Wagner et al., 2003). Beside these factors concerning the system components the land cover and the topography have a major influence on the achievable model accuracy. According to Kraus et al. (2004), the DTM accuracy decreases with increasing terrain slope and decreasing ground point density. As summarised in Kraus and Pfeifer (1998) the penetration rate of laser beams within deciduous forests (e.g. Vienna Woods – Wiener Wald) can drop to 20 to 30%. Thus, for planning ALS flight campaigns over forested areas the low penetration rates of laser beams have to be considered. Several studies (Hodgson and Bresnahan, 2004; Hollaus et al., 2006; Hyyppä et al., 2005; Takahashi et al., 2005a) show that DTMs achieve accuracies in the order of ±10 to ±25 cm for smooth surfaces with low slopes and decrease to several decimetres for surfaces with high slopes.

2.6. Airborne laser scanning for hydrologic applications

2.6.1. Introduction

Modelling tools for simulating spatially distributed hydrological processes are in use, that allow more detailed analysis in decision-making than lumped models. The quality of simulation and spatial process representation is crucially dependent on the input data that describe the variability of the natural conditions in an appropriate form. Therefore, a great demand for such information exists to minimise the uncertainties of the simulation results. A similar trend can be observed in the hydraulic modelling of floodplain flows. As reported in Marks and Bates (2000) two-dimensional (2D) hydraulic surface flow models are mostly constrained by inadequate parameterisation of topography and roughness coefficients, primarily due to insufficient or inaccurate data.

For all above-mentioned model types DTMs and their derived parameters such as slope, aspect and drainage network form the basic model-input. Therefore, the accuracy of the DTM has a crucial influence on the model output. Advances in remote sensing techniques made it possible to generate high resolution DTMs for whole watersheds at reasonable costs. In the past, DTMs were generated from stereoscopic analysis of aerial photographs or satellite imagery. In the last few years the technology of ALS has emerged, which allows to produce DTMs with high quality as mentioned in section 2.5. Several authors summarised possible uses of products derived from ALS data for hydraulic applications. Charlton et al. (2003) analysed the potential of ALS for mapping gravel-bed river environments for gathering high-resolution topographic data. Kraus (2003c) studied the use of laser scanner DTMs for modelling flood risk areas. Pereira and Wicherson (1999) reported that laser scanning was a suitable technique to collect relief information for river management.

Airborne laser scanners also provide data for describing the landscape roughness of the earth's surface. As described by Schmugge et al. (2002) landscape roughness affects the transport of hydro-meteorological fluxes between the land surface and atmosphere as well as below the surface. Therefore, precise topographic information can be used to understand and calculate the effects of landscape roughness on evaporation, soil moisture, runoff and soil erosion at field and landscape scale. Govers et al. (2000) summarised that soil roughness does not only affect the runoff amount due to depression storage, but also affects the volume and rate of infiltration.

In the case of 2D hydraulic flood models information describing the roughness of streams are needed. Cobby et al. (2001) described an approach for estimating low vegetation heights using a logarithmic regression relationship that predicted the vegetation height from the standard

deviations of detrended ALS heights in a small surrounding area. Mason et al. (2003) had reviewed approaches in literature how vegetation height data measured by ALS could be transformed to roughness coefficients. Finally, Cobby et al. (2003) analysed the different frictional properties of floodplain vegetation features such as hedges and trees.

These studies have shown that the potential of ALS to estimate vegetation properties and roughness coefficients of streams is high, but still, several deficits in the physical interpretation and processing of ALS data remain. For example, Mason et al. (2003) mentioned that the estimation of vegetation heights may cause problems, especially in areas of overlap between adjacent ALS swaths. Nevertheless, substantial progress has been made with georeferencing of ALS data, particularly with the minimisation of discrepancies between overlapping laser scanner strips. These discrepancies - in height as well as in planimetry - are unsatisfactory phenomena for end-users of ALS data. An adjustment strategy was developed by Kager (2004) as described in section 2.4.

Therefore, the algorithms for processing large ALS data are available and provide together with CIR orthophotos a valuable data source for the parameterisation of hydraulic / hydrologic models. The complementary informational content of ALS data and CIR orthophotos, as described in the following section 2.6.2, is well suited for object-oriented land cover classifications described in 2.6.3.

2.6.2. Airborne laser scanning versus aerial photography

The following short overview of airborne laser scanning and photogrammetry is based on Baltsavias (1999c), Kraus (2003b) and Maas and Vosselman (2004). Airborne laser scanning systems are characterised by pointwise sampling mechanisms, whereas photogrammetry delivers full area coverages. As a passive system, photogrammetry is strongly depending on weather conditions. The fundamental advantages of photogrammetry are the spectral / textural information content of the images, the large area coverages, the high spatial resolution, the very high position accuracy, and the possibility of direct identifications and measurements of objects. Furthermore, the gathered imagery can be used for generation of orthoimages, DTMs and digital surface models (DSMs). On of the disadvantages is the poor visibility inside the canopy. Additional drawbacks are the fact that for stereoscopic analysis (DTM and DSM generation) the point on the surface must be visible from two different locations and the very time-consuming interpretation work.

In contrast to photogrammetric systems, ALS ones are characterised by a simple measurement geometry meaning that the 3D-position of a point on the surface is measured from one location. This allows the generation of precise DTMs also for urban areas with narrow alleys and wooded

areas, where the penetration rate through the tree canopy mainly depends on the density of trees and the season. However, the high point density achievable with ALS systems permits the generation of high accuracy DTMs and DSMs. In forested areas the difference between the DSM and the DTM is the CHM (Figure 2.3, Figure 2.4), which enables the derivation of other important parameters like tree heights or biomass. Furthermore, the mapping of surfaces with very little / no texture is possible with ALS. Finally, a high degree of automatisation for analysing the ALS data can be achieved.
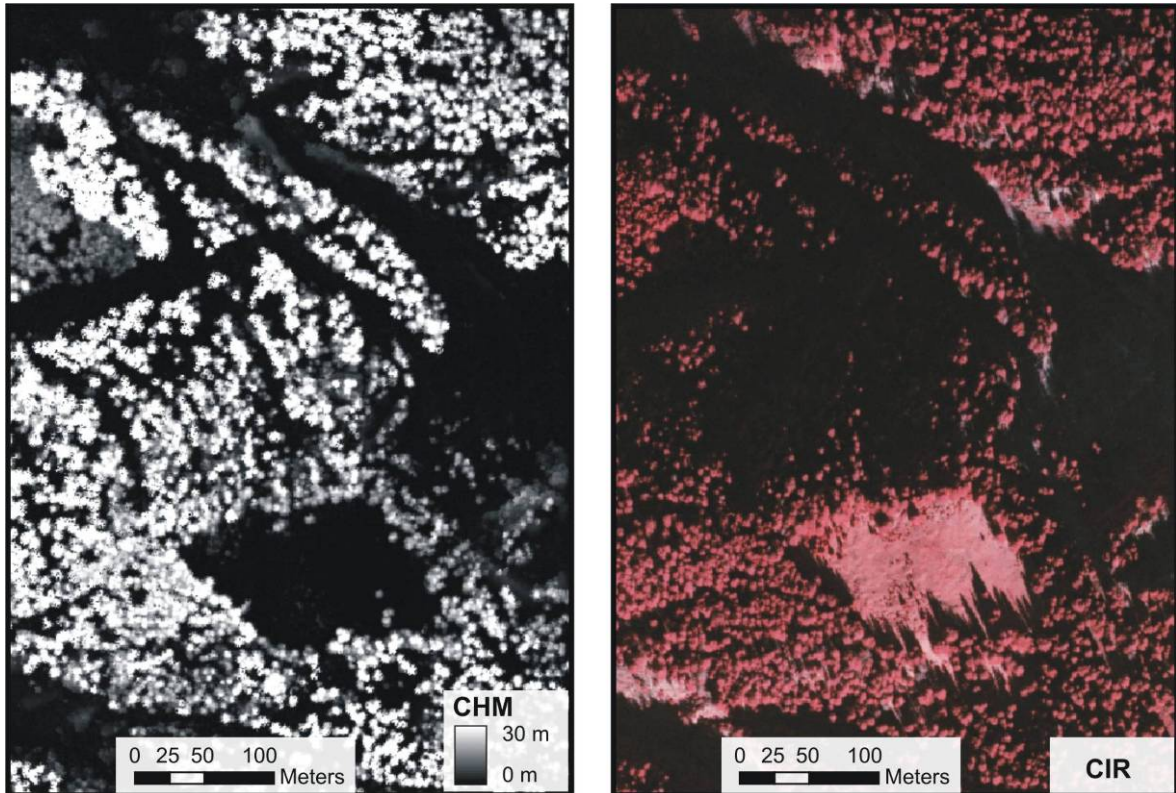
Figure 2.4: Comparison of ALS derived canopy height model (CHM) and CIR orthophoto. The spatial resolution of the CHM is 1.0 m and 0.25 m for the CIR orthophotos.

2.6.3. Land cover classification with respect to hydrologic applications

Deriving land cover information from remotely sensed data is one of the most important tasks in earth observation. Since the first Landsat satellite, launched in 1972, remote sensing has made enormous progress in terms of data availability and improved spatial and temporal resolution. In the field of ALS substantial progresses has been made during the last decade. Cobby et al. (2003) reported the usefulness of ALS data for 2D river flood models providing spatially distributed floodplain topography for model bathymetry and vegetation heights for the determination of roughness coefficients. Normally the roughness is described by Manning's roughness coefficients that can be expressed as a function of land cover (De Roo et al., 2001; Van der Sande et al., 2003). Unfortunately, detailed, actual and hydraulic relevant land cover information is normally not available. Since DTMs are generated from ALS data more frequently, there is now the possibility to use this data source together with orthophotos for land cover classifications.

As the primarily result of laser scanning is a 3D point cloud, additionally information for the classification and identification of objects is necessary. Therefore, several authors (Ackermann, 1999; Baltsavias, 1999c; Kraus, 2003b) proposed the use of the synergetic informational content of photogrammetrically derived imagery and ALS data. Especially for shaded areas ALS data provide useable information (Figure 2.4), which leads to enormous improvements of land cover classifications in those areas. Furthermore, this information can be used for the determination of roughness coefficients.

In order to obtain the largest benefit of combined analysis, the data should be gathered simultaneously or within short time intervals. Due to cost and the fact that many datasets are already available from several projects, the data processing algorithms have to consider the different qualities and properties of the available data.

However, for exploring the full informational content of these data traditionally pixel-based classification algorithms are not suitable. Therefore, object-oriented approaches were proposed from several authors during the last years (Benz et al., 2004; Blaschke and Strobl, 2001; Darwish et al., 2003). The practical realisation of the object-oriented approach postulates the existence of objects. In this context an object is characterised by an amount of spatial connected pixels that represents a meaningful, homogeneous landscape patch. The process for building these objects is normally called segmentation and was the research area of many groups in the past. Unfortunately, most of the algorithms were developed for research experiments only. The commercial available software package eCognition (eCognition, May, 2006) has realised a multi-resolution segmentation approach together with an object-based fuzzy logic classification algorithm. Detailed descriptions of the multi-resolution segmentation approach can be found in Baatz and Schäpe (2000).

2.7. Large scale forestry applications

2.7.1. Introduction

Mapping of forests in alpine environments is a challenging undertaking. Field surveys are hampered by steep and difficult-to-access terrain, which increases labour efforts and costs. A significant portion of the alpine forest area is even inaccessible. For example, Schadauer et al. (1997) noted that about a quarter of Austria's protection forest, an area of about 175 000 ha, can not be accessed. Protection forests can be found in steep slopes and provide protection against natural hazards such as rockfall and snow avalanches. Therefore, remote sensing is often the only viable method for obtaining information about alpine forests. However, complex topography also poses significant challenges to remote sensing, affecting the complete processing chain from data acquisition to data analysis. This, in combination with the limited thematic content of remotely sensed data, has so far delayed a more widespread use of remote sensing techniques for large scale forestry applications in alpine environments.

2.7.2. Field measured forest inventories

In Austria and in many other countries outside the tropics continuous national forest inventories (NFI) are in use and provide forest parameters with high precision. In Austria, the existing NFI is based on a permanent point sampling approach, whereas the sampling units are distributed regularly over the entire territory with a distance of 3,89 km. Due to the sampling design of those inventories the derived parameters are only representative for relatively large administrative units. For example, in Austria the whole federal territory is divided in 88 forest districts ranging between 112 and 2 790 km^2. For each district, representative forest parameters are statistically calculated based on the measured forest inventory data (BFW, May, 2006). Houghton (2005) reported that such forest parameters derived from NFIs are often not compatible with local forest management activities and local land use changes and that the use of average values would bias the calculated sources and sinks of carbon. In Austria, approximately 80% of the forest is privately owned. More than 170 000 forest owners with a maximum area of 200 ha each, manage about 54% of Austrian's forest (Russ, 2004). The minority of these private forest owners operate a continuous forest inventory for their own forest. For such small forest areas the NFI parameters are not representative. Therefore, reliable forest planning data are lacking for a significant percentage of forested areas in Austria. Remote sensing methods offer the potential to acquire this information in a cost- and time-effective way.

2.7.3. Aerial photographs for forestry applications

Despite major advances in satellite technology, still today the most widely used remote sensing technique for operationally mapping alpine forests in Austria is airborne colour-infrared (CIR) photography. Furthermore, Holmgren (2003) reported that aerial photos in combination with field surveys are still the dominant data sources for forest stand mapping and forest variable assessment in Sweden. Especially for local forestry applications CIR images have the advantages that they are available at reasonable costs and that they are accepted within the forestry community as valuable data source. This is because aerial images have a high spatial resolution (<25 cm), which allows recognition of differences in forest canopy structure and relatively large free-standing trees. A further advantage of orthophotos is the spectral information content as already described in section 2.6.2. Thus, a trained photointerpreter with good knowledge of site conditions can distinguish different forest types or even estimate forest attributes such as tree height or crown diameter. The disadvantages are the high degree of manual processing and interpretation work and the low information content about the vertical structure of forests. A more expensive alternative to orthophotos analysis is the stereoscopic analysis of aerial images. However, for both data sources strong limitations exist for deriving parameters regarding the vertical forest structure. This is especially the case for dense forests or for forests located in difficult topography, which is the case in most of the forested areas in the Alps. A reliable and direct measurement of tree height or canopy height, which represents a fundamental input parameter for the estimation of stem volume, is therefore, hardly possible.

However, these approaches are highly subjective and software solutions, which try to mimic the expert's decisions, produce barely satisfactory results. Therefore, there is on the one side the continued need to develop more automatic methods for classifying high resolution imagery. On the other side, there is a need to develop novel remote sensing techniques which allow deriving quantitative forest attributes more directly.

2.7.4. Operational applications of airborne laser scanning in forestry

Today, ALS is one of the most promising remote sensing techniques for forestry applications. As an active remote sensing technique, it provides three dimensional point clouds, where over vegetated terrain some of the points are caused by reflections in the vegetation canopy and some by reflections at the ground surface. Therefore, detailed information not only about the horizontal distribution of the forest but also about the canopy, the vertical structure and about the terrain in forested areas can be derived from ALS data. For this thesis, small-footprint ALS systems were considered. Large footprint systems, which can also be used for deriving forest attributes (Lefsky et al., 1999a; Lefsky et al., 1999b; Means et al., 1999), were not discussed here.

During the last decade several studies for deriving forest parameters from small-footprint ALS data have been carried out. These have shown the great potential of the developed algorithms for measuring and modelling various forest attributes. The available algorithms can be divided in area based (e.g. stand, plot) and single tree based approaches. According to Hyyppä and Inkinen (1999), the modelling of single trees (e.g. tree crowns) within a boreal forest can be done with ALS point densities with approximately 10 p/m². As the commonly used ALS data in large-area mapping projects have sampling densities of 0.5-3.0 p/m², area based approaches are currently the most appropriate ones for deriving forest parameters. A comprehensive survey of accomplished projects concerning the use of ALS in forestry is given by Lim et al. (2003) and Hyyppä et al. (2004). Furthermore, Næsset et al. (2004) summarise available applications of ALS for operational forest inventories in Norway, Sweden and Finland. They summarise available algorithms to derive, for example, sub-canopy topography, canopy height, canopy volume, tree height, stem diameter, stem volume, basal area or biomass.

The application of ALS in complex alpine terrain is lacking behind, at least partly due to the technological challenges of ALS operations and data processing in these environments. During the last years, a few studies (Heurich and Weinacker, 2004; Hirata, 2004; Morsdorf et al., 2004; Schardt et al., 2002; Takahashi et al., 2005a; Takahashi et al., 2005b) have been published, which use small footprint ALS data for forestry applications in mountainous areas. In general, the results of these studies show good accuracies for the derived forest parameters. But it needs to be recognised that these studies were limited to very small test sites, the reference data were measured during extensive field campaigns, and the ALS data used were acquired with homogenous system configurations. For operational applications of large areas, ALS data are normally acquired during several flight campaigns with different sensors, flying heights, footprint sizes and point densities. Furthermore, required snow-free and leaf-off conditions can hardly be achieved in one flying date

for large alpine areas and therefore, the phenology can change within an ALS data set. Thus, the algorithms used to derive forest attributes have to handle these different conditions.

The retrieval of forest parameters from ALS data is commonly based on regression analyses, which require reference data. From an economic point of view extensive measurements of reference data are not practicable for large areas. In reality nationwide forest inventories as well as inventories from private forest owners exist, which can be used as reference data. These inventory data have the advantage of being readily available and do not lead to additional costs for extensive field works. Their major disadvantages are the inappropriate inventory designs, which are not optimised to use these data as reference data for remotely sensed data analyses. Therefore, objectives of this thesis were to analyse and to discuss the usability of such forest inventory data as reference data for the retrieval of forest parameters from small footprint ALS data with the focus on the estimation of canopy heights (2.7.5) and stem volume (2.7.6).

2.7.5. *Extraction of canopy heights from airborne laser scanning data*

The canopy height is the primary quantity, which can be measured by ALS. The canopy height is defined as the vertical extent of the vegetation canopy from the ground surface to the top of the canopy, given in meters. Before the advent of ALS it had been nearly impractical to measure canopy heights over a regular grid for larger areas. Rather, it had been much easier to measure the heights of individual trees and plants using clinometers, hypsometers (e.g. Vertex), electronic total stations or other instruments, even though it is quite hard to identify single-tree tops from the ground in dense and especially deciduous forests. Conversely, ALS does not allow determining tree heights directly. This is because, firstly, the sampling pattern is irregular and most pulses hit the branches rather than the treetops. Secondly, the footprint size of the laser pulse is in the order of half a meter. Hence, it is not possible to focus on the treetop as a forester does when measuring tree height from the ground. Laser beams penetrate into the canopy and the first echo is not triggered until the backscattered echo is strong enough. Detailed information about the penetration of small footprint laser beams into the canopy can be found in Gaveau and Hill (2003).

For a comparison between ALS derived canopy heights and field measured forest inventory data the canopy height can be expressed as a single-tree based quantity (e.g. single tree heights) or as an area-based one (e.g. Lorey's mean heights). The Lorey's mean height is a commonly used quantity in forestry and corresponds to the basal-area weighted mean tree heights.

For the retrieval of canopy height information from ALS data it is necessary to firstly generate a DTM, a DSM and a CHM (2.5). In order to estimate tree heights it is necessary to detect

individual trees in a CHM, orthophoto or high spatial resolution satellite image and then to find the highest first-echo ALS point or raster cell of the CHM within the crown area. Hyyppä and Inkinen (1999) reported that the modelling of single trees can successfully be done based on ALS data with a point density of 10 p/m². As the commonly used ALS data in large-area mapping projects have sampling densities of 0.5-3.0 hits per m², single-tree-based methods are replaced by area-based approaches. The problems with single-tree-based approaches are that only dominant and free-standing trees can be detected with high correctness and that the tree height is slightly underestimated. A comprehensive overview of the available studies about tree height and canopy height estimation from small footprint ALS data is given by Hyyppä et al. (2004). Furthermore, Gaveau and Hill (2003) reported that the use of interpolated grid-based CHM propagate these underestimation errors. For area-based approaches basal-area weighted mean tree heights (Lorey's mean heights) or mean tree heights are commonly used as reference heights for regression analyses (Næsset, 1997a; Popescu et al., 2002). Holmgren et al. (2003) analysed area- and single-tree-based methods for the estimation of tree heights and found that the detection of single-trees did not improve the tree height estimates by using TopEye laser data with a point density of approximately 1 p/m². As summarised in Hyyppä et al. (2004) the underestimation of tree heights depends on several factors such as the laser point density and footprint size, the tree species, the existence and height of under-vegetation, the algorithms used in the laser signal processing and the algorithms used to calculate the DSM and DTM. For complex terrain, one of the most crucial questions for the correct determination of forest canopy height is if there are enough ground hits to reconstruct the DTM below the canopy (Wagner et al., 2004a). Since laser pulses do not penetrate through leaves and branches, the number of terrain points depends on the presence of openings within the forest canopy. In literature, information about the accuracies of terrain heights below tree crown areas can scarcely be found. Takahashi et al. (2005a) achieved surprising terrain height accuracies of -0.20 (25 to 48 degree slopes) to 0.11 m (11 to 21 degree slopes) with and average distance between footprints of 0.42 m. Yu et al. (2005) achieved for boreal forest overestimations of terrain heights of 0.09 to 0.30 m depending on tree species, terrain slope, vegetation cover and density of the ALS points. Especially for mountainous terrain with rough surfaces, steep slopes and low laser pulse penetration rates the published accuracies seem to be very optimistic. The generation of DTM heights below dense tree crowns is usually done by interpolating the terrain height among the nearest available terrain points. Therefore, the task of reconstruction the DTM below a forest canopy is less problematic over relatively sparse lowland forests (e.g. boreal forests) compared to mountainous environments, where dense forests (e.g. protection forests) are often situated in steep rough terrain.

In this thesis the capability of state-of-the-art small footprint ALS technology for mapping canopy heights of alpine forests with complex topography was investigated. Rather than employing

data and methods tuned for this particular task within a small test site, solely data and methods which already serve other operational applications were used.

As described in section 3, ALS data of a 128 km^2 region in Vorarlberg, Austria, were used. The ALS data were acquired within the framework of an operational DTM mapping activity. The acquisition of the ALS data took place in two different seasons with varying ALS system configurations. Therefore, the effects of these different conditions on the derived products were analysed and discussed for two small test areas which were covered by both flight campaigns. For processing the ALS data only methods that are already implemented in commercially available software packages were used. Last but not least, existing forest inventory data and ground control points were used for validating the derived terrain and canopy heights (single-tree and Lorey's mean heights). In this way it was ensured that the results obtained in this thesis are of practical relevance.

2.7.6. Estimation of stem volume based on airborne laser scanning data

The estimation of stem volume is of special interest for planning, management and decision-making purposes in forestry. Stem volume is a key parameter and forms the basis for assessing forest biomass and carbon stock, which are essential input quantities for the Kyoto protocol reporting.

A widely used method to estimate stem volume is the multiplicative regression model, developed by Næsset (1997b; 2002; 2004b). It uses a multitude of statistical quantities derived from ALS first- and last-echo data like mean values, coefficients of variation, percentiles of heights and canopy densities. Several studies have shown that for boreal forests the estimation of stem volume using ALS leads to higher accuracies compared with traditional methods. For alpine forests this method has not been used until now. Therefore, an objective of this thesis was to evaluate the potential of this approach for a large alpine test site in Austria. Due to the former forest management in the study region very high stem volumes, which achieve more than 1 000 m^{3}ha^{-1}, are present. Furthermore, the difficult topography and the fact that the structures of alpine forests significantly differ from boreal ones raised the question if this approach is easily transferable.

In general, methods for mapping stem volume using ALS techniques are only beneficial for operational applications if they are transferable to different regions without extensive modifications. That means that the models should preferably be as simple as possible, that homogenous parameter sets should be used for different regions and that the calibrated coefficients should be physically interpretable. As shown in Næsset et al. (2005), the multiplicative regression

model tends to include different parameter sets in the final regression function of different regions. Alternatively to this approach a simple linear model to combine forest inventory and ALS data was developed. A linear function for mapping stem volume, which only includes canopy volumes derived from ALS data was applied. The canopy volumes were calculated for sample plot sub areas depending on predefined, fixed canopy heights.

For the calibration of the models reference data are needed, which are normally gathered in extensive field campaigns. Such reference data are usually measured within circular sample plots. Nilsson (1996), Næsset (2002), Popescu et al.(2003) and Holmgren and Jonsson (2004) used reference data, where the diameter at breast height (d_{bh}) had been measured for all trees, or for trees with a diameter at breast height greater than a defined threshold of 4 to 13 cm within circular plots with constant diameters ranging from 15 to 20 m. Inside a dense forest the measurement of tree heights is much more complex and is therefore reduced to few representative sample trees within a plot. The remaining tree heights are calculated using various height-diameter functions. Operational uses of such methods for large regions require the reduction of these time consuming and expensive field measurements. Therefore, a further objective of this thesis was to analyse the usability of already existing forest inventory (FI) data as reference data.

Due to the fact that the ALS data were acquired with different ALS system parameters, a further objective of this thesis was to investigate the effects of the different laser scanner system parameters on the obtained stem volume accuracies. Finally, the potential of the ALS for mapping stem volume for the whole 128 km^2 study area was analysed.

3. Study area and data

The selection of the study area was based on the availability of the ALS and forest inventory data. The topography of the region and the complexity of the study area as well as the ALS data made this area to an ideal test site to analyse large scale applications of ALS for complex mountainous environments.

3.1. Study area

The study site is situated in the western part of the Austrian Alps and covers 128 km² of alpine area. Figure 3.1 shows the location of the study site in the southern part of the federal state of Vorarlberg, in the so-called "Montafon". The complex mountainous landscape of the study area shows many different facets and is characterised by hilly to high alpine terrain, with altitudes rising from 720 m to 2 875 m. Approximately 10% of the territory is valley area and is mainly used for agricultural purposes and for settlements. The land cover is composed of alpine land cover types (e.g. shrubs, meadows, bare soils, etc.), forested areas (e.g. coniferous and mixed forests) and sparsely settled areas in the valley floors (e.g. agricultural and urban land). Several small mountain streams run through the study area whereas the two main streams are the Suggadinbach (south to north) and the Ill (south-east to north-west).

Within the whole test site the total forested area sums up to ~30.7 km². According to "Stand Montafon Forstfonds" (May, 2006) the main tree species in the area are spruce (*Picea abies*) with 96% and fir (*Abies alba*) with 3%. The rest consists of red beech (*Fagus sylvatica*), other deciduous species and larch. Especially in valleys and sunny slopes, mixed forests with the species red beech can be found. The average stem volume is approximately 465 m^3ha^{-1}, which is high compared to 325 m^3ha^{-1} (BFW, May, 2006) representing the average Austrian stem volume. Two thirds of the forests are located above 1 000 m sea level, whereas the timberline is at about 1 950 m. As a result of the mountainous terrain 6% of the forest grow on a slope inclination of more than 45°, 61% between 30° and 45°, 28% on slopes between 15° and 30° and only 5% on slopes less than 15° (Figure 3.2). In the "Montafon" region the growing conditions of forests depend strongly on the altitude and therefore, on the precipitation (e.g. the mean yearly precipitation vary between 1 200 to 1 800 mm) and on the temperature (e.g. the mean yearly temperature vary between 8 to -4 degree Celsius).
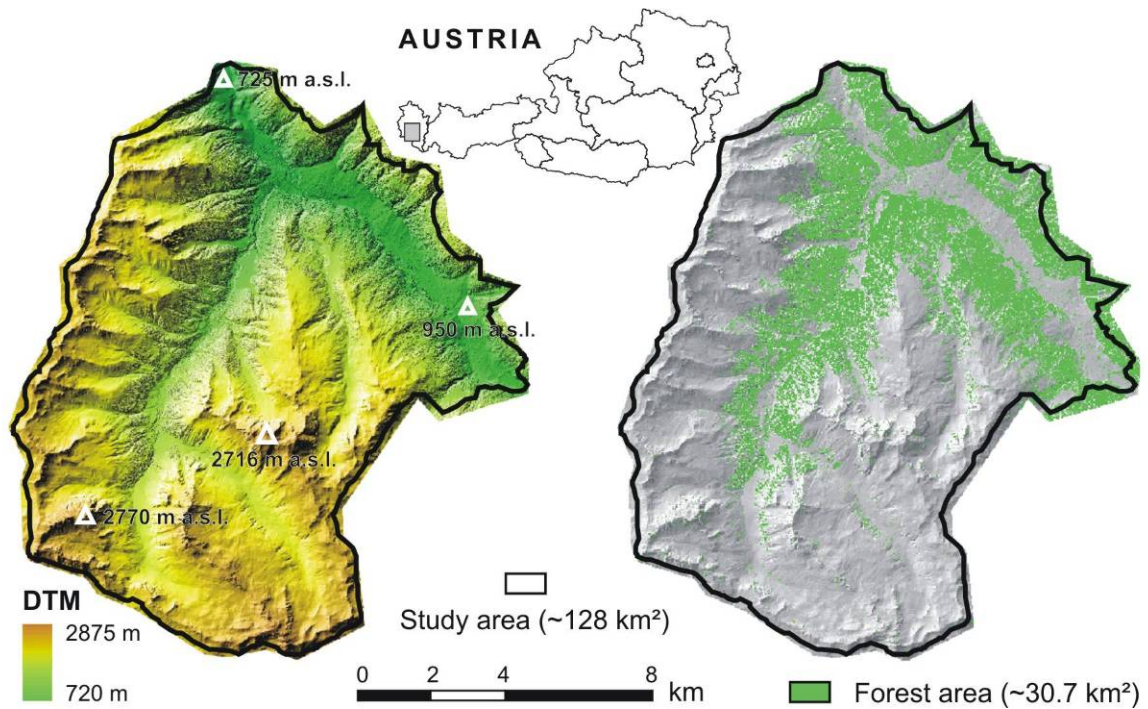
Figure 3.1: Location of the study area. The left image shows a coloured, shaded DTM derived from ALS data. The right image shows a shaded DTM overlain with forested areas.
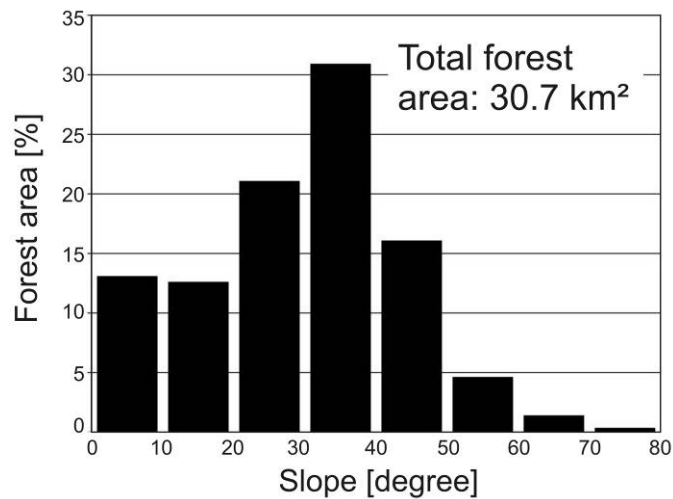
Figure 3.2: Distribution of the forested area depending on the terrain slope.

About half of the forest area in the study area is managed by the forest administration "Stand Montafon Forstfonds" (May, 2006), which is the largest forest owner in Vorarlberg. This forest administration manages a total forest area of 6 490 ha in the "Montafon" region, of which about 80% is managed forest with protection function (protection forest with yield), 10% is managed forest (commercial forest) and the rest is unmanaged protection forest (protection forest without

yield) on extreme sites or at the timberline. Therefore, the forest is of great importance for protecting inhabited areas and transportation routes against natural hazards such as snow avalanches and rock falls. The average forest stand size of the forest administration "Stand Montafon Forstfonds" is approximately 3.5 ha and represents therefore the average size of private owned forests in Austria. As a consequence of this small forest stands the whole forest within the study region is highly structured. Since 1988, this forest administration operates a precise forest inventory, which provides the field data used in this study.

Within the study area two small test sites were selected to investigate the properties of the winter (leaves-off) versus the summer (leaves-on) ALS data. The test site Winkel (675×475 m^2) was mainly covered with deciduous forests whereas the forest of the test site Valisera (850×700 m^2) was dominated by deciduous trees. Both test sites were covered by the summer and the winter ALS flight campaign (Figure 3.3).

3.2. Data

3.2.1. Airborne laser scanner data acquisition and georeferencing

The ALS data were acquired in the framework of a commercial terrain mapping project during two flight-campaigns (Figure 3.3). Both flights were performed by the company TopScan, Germany. The first flight took place on December 10, 2002, the second on July 19, 2003. These two flight campaigns were carried out in an effort to map the complete area under snow free conditions, i.e. the lower lying parts were covered by 24 flight lines during the winter campaign under snow-free and leaf-off conditions, while the higher altitudes up to about 3 000 m were covered by 52 flight lines during the summer campaign under snow-free and leaf-on conditions. TopScan employed first-/last-echo Airborne Laser Terrain Mapper (ALTM) systems from Optech Inc., Canada. During the winter flight the pulse repetition rate was 25 kHz, for the summer flight it was 50 kHz. Consequently, the average point density on ground was higher for the summer campaign (2.7 p/m^2) than for the winter campaign (0.9 p/m^2). For both flights the flying heights above ground ranged between ~650 m and 2 000 m, whereas the average flying height was 1 000 m. The maximum scanning angle was ±20 deg. The resulting swath width was about 725 m and the overlap between flight lines was 425 m. The ALTM system operates at a laser wavelength of about 1 µm (Baltsavias, 1999b). The beam divergence of the ALTM system is 0.3 mrad, which results in a mean footprint size of 0.3 m in diameter at an average flying height of 1 000 m. The total amount of laser scanner points for the two flight-campaigns is 650 millions, including first- and last-echoes.

Due to the complex flight pattern, both in terms of the number of flight lines and variable flying heights above ground, the georeferencing of the ALS data is a demanding task. For the georeferencing of the data the method developed by Kager (2004) was applied. A summary of the method is given in section 2.4; a detailed description can be found in Kager (2004). The georeferenced 3D point clouds were used to calculate the DTM, the DSM, the CHM and canopy height points as described in chapter 4.1.

☐ Test Site Winkel

☒ Test Site Valisera

Kilometers
0   5   10

-- Winter Flight
— Summer Flight

• 22,000 Ground Control Points
○ 143 Forest Inventory Points
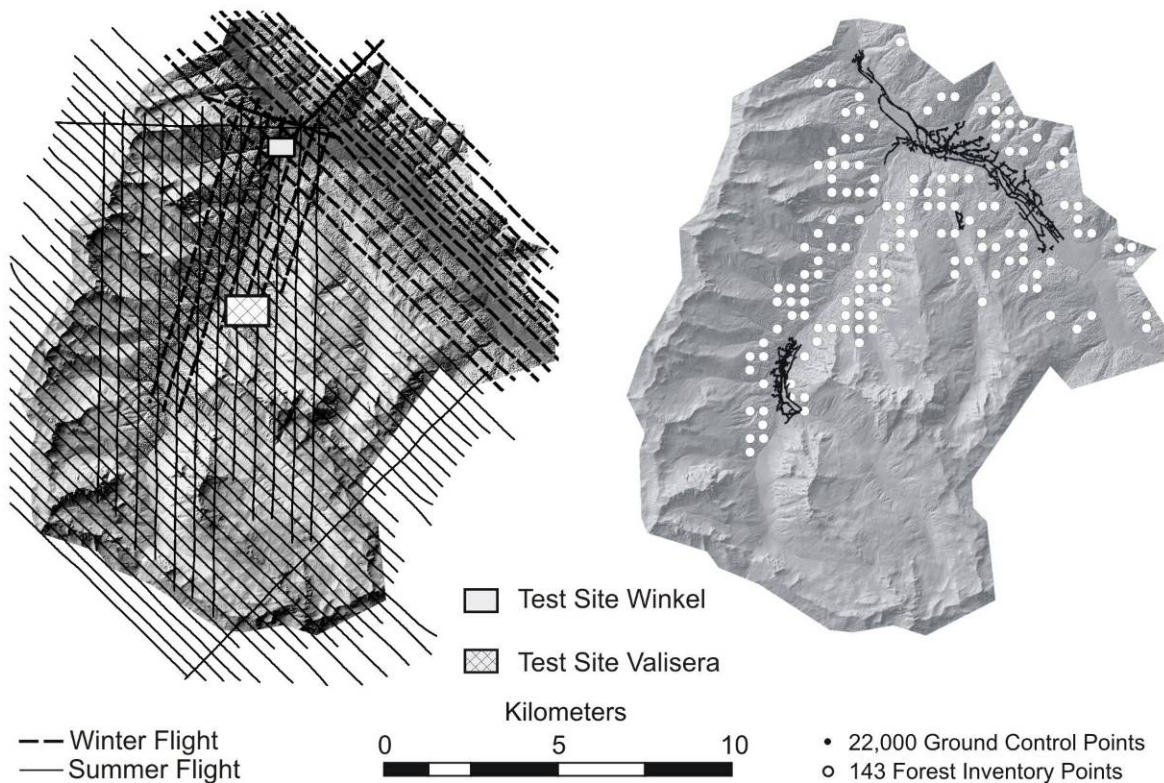
Figure 3.3: The left image shows the flight lines of the airborne laser scanner acquisition during the winter and summer campaign, overlain over the shaded terrain model. It also shows the location of the small Winkel and Valisera test sites, which were used for analysing the different properties of summer and winter ALS data. The right image shows the location of the 22 000 ground control points for validating the digital terrain model and the 143 forest inventory plots for checking the quality of the canopy height model.

3.2.2. Orthophotos

For the whole study area colour infrared (CIR) digital orthophotos with a ground resolution of 0.25 m were available. The orthophotos were acquired in 2002 and were provided by the provincial government Vorarlberg. Figure 3.4 shows a mosaic of the CIR orthophotos for the study area.
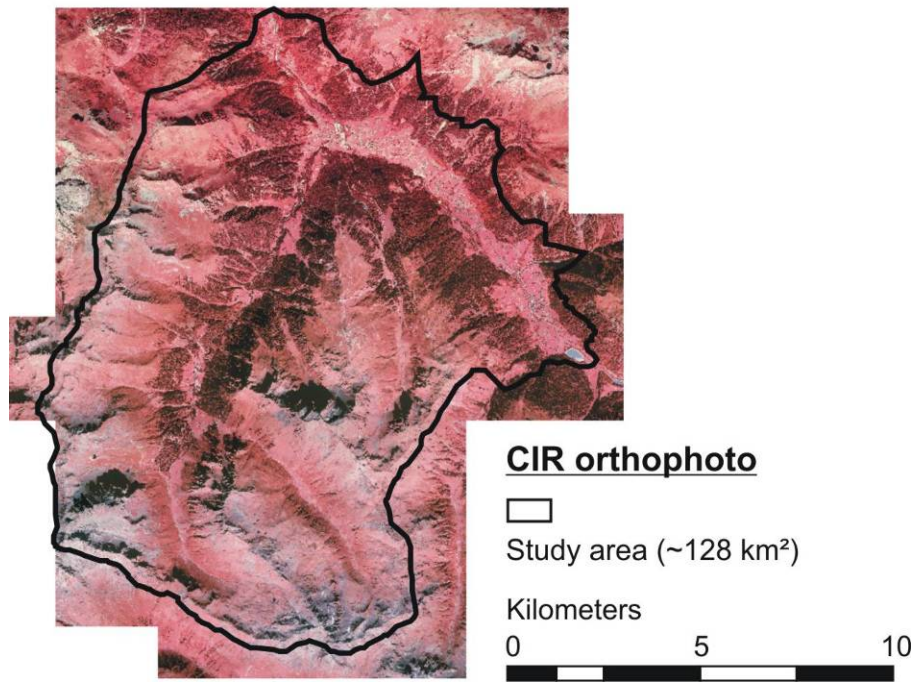
Figure 3.4: Mosaic of CIR orthophotos for the entire study area. The spatial resolution is 0.25 m.

3.2.3. *Forest inventory data*

The forest inventory data were provided by the forest administration "Stand Montafon Forstfonds", which operates a precise inventory for a 6 570 ha large area in Vorarlberg, Austria. The inventory is based on permanent sample plots distributed in a regularly 350 m grid, whereas sample plots are only situated in forested areas that are managed by the forest administration. Thus, for the study area, 143 inventory sample plots were available as shown in Figure 3.3. The used forest inventory data were measured in 2002.

For each plot trees were collected based on a Bitterlich plot (Figure 3.5). A Bitterlich plot is characterised by a variable sample plot size. A relascope with a relascopic factor of four (angle gauge) was used for the selection of sample trees within each sample plot. This is a so-called probability-proportional-to-size sampling method meaning the probability of selection is proportional to tree basal area (Shiver and Borders, 1996). It is a point sampling method and, therefore, it does not refer to a certain sample plot area.

For all selected trees the tree species were determined and the diameter at breast height *dbh* was measured with a tree calliper at the breast height of 1.3 m. For trees with a *dbh* greater than 100 cm the *dbh* were measured with a diameter tape. Trees with a *dbh* less than 10 cm were excluded from this forest inventory.
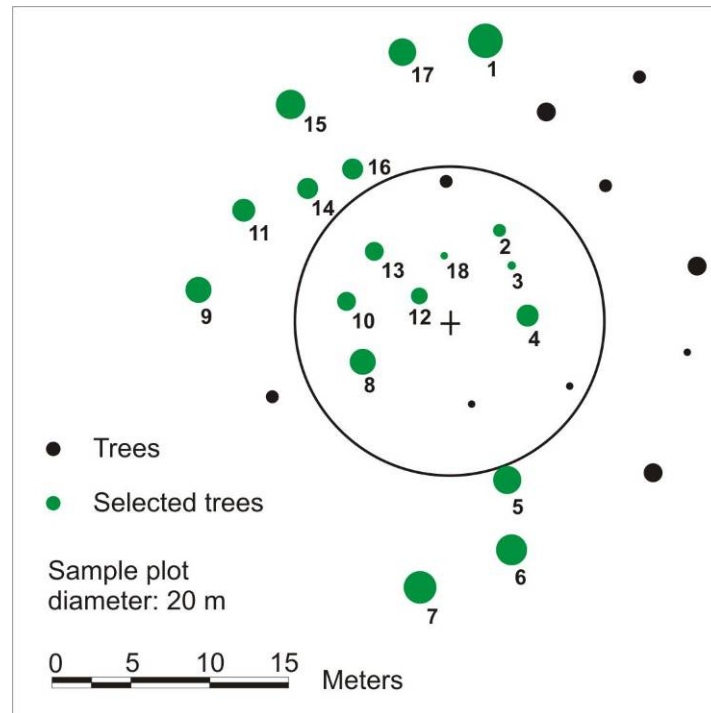
Figure 3.5: Bitterlich plot. Selected trees are shown in green.

For each sample plot one tree height *h* for each tree species was measured with a Vertex III hypsometer (http://www.haglofsweden.com/products/VertexIII/). For the selection of the tree, whose height was measured, the 50% mark in the stand basal area distribution was used. Thus, it is assumed that the measured tree height correspond to the median tree height. If there were more than 10 trees with the same tree species, the heights of two trees were measured. If the selected trees within a sample plot were grouped to two clearly differentiable tree height clusters, for each height cluster one tree height was measured. The accuracies of the measured tree heights were not validated for this study. However, to get an approximation of the achievable accuracies literature information can be used. Rössler (May, 2000) reported, that the accuracy of tree height measurements of 67 spruces ranged between -0.6 to 0.8 m. If one considers that this reported accuracies were derived under ideal conditions (e.g. for the measurements the Vertex was mounted on a tripod, the trees were precisely vertically and the tree tops were clearly visible) the expected accuracies for the current tree height measurements are in the range of ±1.0 to ±2.0 m. A further increase of the uncertainties of the measured tree heights can be expected, as the measurements were done by several persons. The heights of the remaining sample trees were calculated by means of height curves, which describe the correlation between *h* and *dbh*. For the available forest inventory data the height curve according to Keylwerth (1954) was used, which is defined by the following mathematical function:

$$h = e^{a_0 + \frac{a_1}{dbh}} + 1.3 \qquad\qquad (3.1)$$

where h is the tree height in meters, a_0 is a variable coefficient, a_1 is a constant coefficient and dbh is the tree diameter at breast height (1.3 m) in centimetres. The coefficient a_0 depends on the site quality and was calculated by means of the measured h-dbh pair for each sample plot and each tree species separately. Knowing a_0 for each sample plot, all the missing tree heights within the plot could be calculated. The expected standard deviation of the estimated heights ranged between 1.3 and 1.9 m (Prodan, 1965).

For the validation of the ALS derived canopy height model (CHM) the basal-area weighted mean tree heights h_L, commonly called Lorey's mean heights, were used. According to Prodan (1965) h_L corresponds to the mean height of the selected trees within the Bitterlich plot and can be calculated with the following formula:

$$h_L = \frac{\sum\limits_{i=1}^{n} h_i}{n} \qquad\qquad (3.2)$$

where h_i is the single-tree height of the tree i and n is the number of measured trees per sample plot.

For the regression analyses the stem volumes per unit area were used as ground reference quantities. The estimation of stem volume was based on regional volume equations of the Bavarian forest inventory, as these reflect the growth pattern of spruce in the province of Vorarlberg best. These volume equations are based on a so-called form height concept, which means that the stem volume of a single-tree is described by a cylinder. The diameter of the cylinder corresponds to the dbh and the height (form height FH) was calculated by means of the following formula (Pollanschütz, 1974):

$$FH = \exp(A_1 + A_2 \cdot \log(h) + A_3 \cdot \log(h)^2) \qquad\qquad (3.2)$$

$$A_1 = c_{11} + c_{21} \cdot \log(dbh) + c_{31} \cdot \log(dbh)^2 \qquad\qquad (3.3)$$

$$A_2 = c_{12} + c_{22} \cdot \log(dbh) + c_{32} \cdot \log(dbh)^2 \qquad\qquad (3.4)$$

$$A_3 = c_{13} + c_{23} \cdot \log(dbh) + c_{33} \cdot \log(dbh)^2 \qquad\qquad (3.5)$$

where FH is the form height in meters, c_{ij} are the constants for the different tree species taken from a inventory-evaluation software of Süß (1984).

According to Sterba (1991) the stem volume ($v_{stem,fi}$) per hectare can be calculated with the following formula:

$$v_{stem,fi} = k \cdot \sum_{i=1}^{n} FH_i \hspace{5cm} (3.6)$$

where $v_{stem,fi}$ is the stem volume in m^3 per hectare, k is the relascopic factor and has the value 4 and n is the number of measured trees per sample plot unit.

The calculated $v_{stem,fi}$ corresponds to the commercial useable timber volume and is therefore not equal to the real biological available stem volume, represented for example by ALS data. In contrast to the commercial useable timber volume, the biological one includes additional small trees ($dbh < 10$ cm) and old trees in bad condition.

Although the forest inventory is based on permanent sample plots the accuracies of the available coordinates of the sample plot centres vary and are in the range of several meters. Several reference measurements with differential GPS (dGPS) have shown that the average position error is approximately 10 m, which is quite large related to the 20 m diameter of the sample plots used for the ALS data analyses. To overcome the problems with these spatial inaccuracies a manual co-registration to the ALS data was carried out. For this purpose positions of single trees were needed, which were measured during the forest inventory field campaign. For all sampled trees the polar coordinates relative to the sample plot centre were measured with a compass in combination with an ultrasonic range instrument. The expected accuracies of the measured polar coordinates were in the range of 0.3 to 0.5 m. As shown in Figure 3.6 the position of each sample plot centre had been manually changed so that the measured single-tree positions best fitted to the visual detectable tree positions in the ALS canopy height model (CHM) and that the measured tree heights best fitted to the CHM heights. The relative positions of the single-trees within one sample plot were not changed at the manual co-registration. The co-registration was done with commercial available GIS software. The canopy height model was calculated by subtracting the terrain model from the surface model as described in section 4.1.1. In this way the sample positions of 103 of the 143 available sample plots could be clearly co-registered to the ALS data. Thus, for the further analyses the calculated $v_{stem,fi}$ of these 103 FI sample plots were used as reference data.

Within the 103 sample plots the *dbh* for 925 trees were measured, whereas the *dbhs* varied between 10 and 127 cm. The tree heights varied between 5.4 and 42.2 m and were measured for 196 trees within the co-registered sample plots. The distances of the trees from the sample plot centres varied between 0.5 and 24.5 m as shown in Figure 3.7. The average distance was 7.6 m and

the standard deviation was 4.2 m. The summary of the available forest inventory data is shown in Table 3.1.
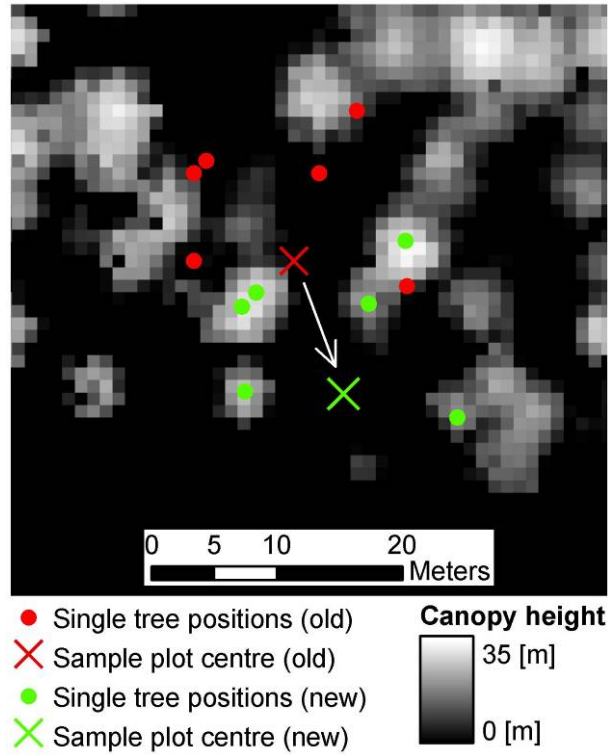
Figure 3.6: Manual co-registration of the FI sample plots to the ALS data. The centre coordinates of each sample plot had been changed, that the measured single tree positions fitted best to the visually detectable tree positions in the ALS canopy height model.
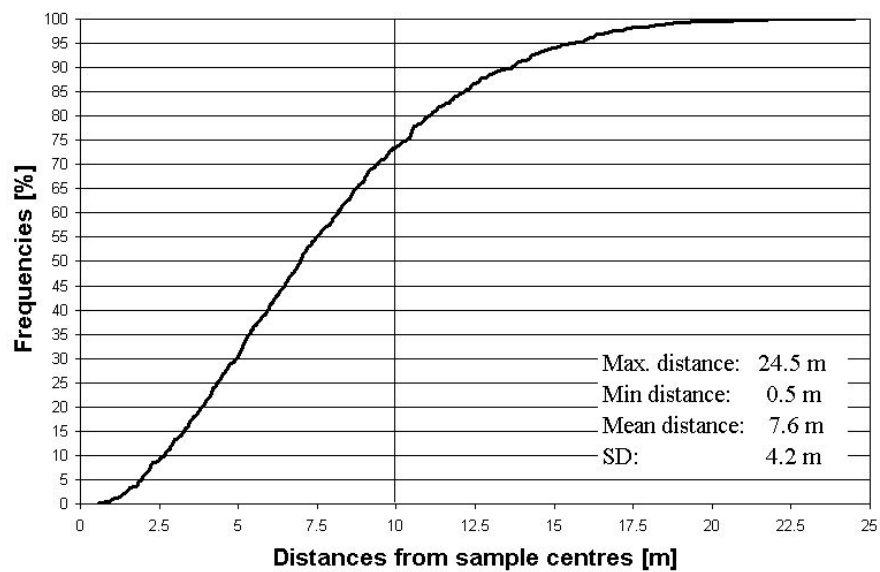
Figure 3.7: Distribution of distances of all 925 measured single trees from the FI sample plot centres.

Table 3.1: Summary of forest inventory data of 103 sample plots. In addition to the range of the values (min, max) the mean values (mean) and the standard deviations (sd) are shown.

Variable	min	max	mean	sd
Diameters at breast height (925 measured trees) [cm]	10.0	127.0	47.6	18.7
Tree heights (925 trees) [m]	5.4	42.2	27.1	6.8
Tree heights (196 measured trees) [m]	6.0	42.5	27.5	6.8
Lorey's mean tree heights (103 sample plots) [m]	6.0	38.6	26.2	6.9
Number of trees per plot (103 sample plots)	1	22	9.0	4.5
Number of trees per hectare (103 sample plots)	11	1 875	381	392
Calculated stem volume (103 sample plots) [m^3 ha^{-1}]	15.7	1 137.7	423.4	239.0

4. Methods

4.1. Airborne laser scanning data processing

4.1.1. Derivation of surface models

In this section the generation of the DTM and the DSM is described. As mentioned in section 2.5, for the generation of the DTM the observed ALS last-echo point cloud must be classified in terrain and off-terrain points, which is commonly referred to as filtering (Kraus and Pfeifer, 1998). For this thesis the widely-tested hierarchic robust filtering technique described in Kraus and Pfeifer (1998), Pfeifer et al. (1998a) and Briese et al. (2002) has been employed to generate the DTM. The hierarchic robust filtering technique is based on the georeferenced 3D ALS points, which has the advantage that the original elevation values are preserved. In the first run, an average surface of thinned out data set is calculated, whereas all used points have the same weight. It is expected that the true terrain points have negative residuals, while the vegetation points have small negative or positive residuals. In a next calculation step these residuals are used to compute weights ranging between 0 and 1 for each laser point. To identify if a point is a terrain point or an off-terrain point several methods exist, which are all based on the analysis of the histogram of the residuals. These weight functions give high weights to ground points and low weights to vegetation points. Details about these weight functions can be found in Pfeifer et al. (1998b). Considering the calculated weights a new surface is calculated. Finally, in an iterative process the mentioned calculation steps are repeated using for each step a higher point density. The hierarchic robust filtering approach is implemented in the commercial software package Scop++ (May, 2006). Comprehensive information about the performance of this hierarchic robust filtering approach in comparison with several other available approaches can be found in Sithole and Vosselman (2004).

While this was a computationally demanding task, the DSM was quickly generated by using a moving planes interpolation of the highest first-echo points within a pre-defined grid of one meter. The moving planes interpolation fits tilted planes into the eight nearest first-echo points by using a least square approach. Furthermore, the heights are weighted inversely proportional to the distance from the grid point. The moving planes interpolation is also implemented in Scop++.

For the calculation of both, the DTM and the DSM, the ALS data from both flight campaigns were merged to one data set. The grid size for all calculated models was 1.0 m.

4.1.2. Calculation of canopy heights

Within this work the canopy heights were represented as interpolated canopy height model (CHM) and as point-based canopy heights. As mentioned in section 2.5 the canopy height can be defined as the vertical extent of forested areas between the ground surface and the highest surface of the canopy, given in meters.

For the calculation of the canopy heights the DTM and first-echo data were used. In contrast to a last-echo point a first-echo point is known to be reflected by the first object on the laser beam's travel path. Of course, depending on the surface a certain amount of penetration can occur. For example, if the laser beam hits to a very dense canopy the penetration depth will be very small. Otherwise, if the laser beam hits a sparse forest canopy (e.g. deciduous forest without leaves) the penetration depth can be enlarged to several meters (Gaveau and Hill, 2003). Furthermore, the penetration depth also depends on the footprint size of the laser beam. However, for last-echoes it is unknown if the return signals are reflected from the canopy or from the ground. Detailed information about the interaction of the laser beam with complex targets can be found in Wagner et al. (2006b). In conclusion, first-echo points represent the highest canopy surface better than last-echo points.

The CHM could easily be calculated by subtracting the DTM from the DSM. The last hindrance to generating the CHM was that the difference model DSM - DTM not only contained trees and other vegetation, but also buildings, cars and other objects (Figure 4.1). The detection of buildings is the focus of many research groups and therefore, several detection algorithms are available (Haala and Brenner, 1999; Matikainen et al., 2003; Rottensteiner et al., 2005b). For the calculation of the current CHM the algorithm from Rottensteiner et al. (2005b) was used to extract building areas. The heights of CHM pixels were set to zero if they were covered by buildings. The other objects, which do not correspond to forest, should be removed in subsequent steps, e.g. with the help of mathematical morphology. However, potentially adverse effects of such morphologic operations especially over young, dense forested areas are not well understood until now. Therefore, no such removal-techniques were applied for the used CHM.

Similar to the calculation of the CHM the calculation of the point-based canopy heights were based on the first- and last-echo ALS data but used the 3D first-echo points instead of the interpolated DSM. This means that for each first-echo points the terrain heights were subtracted. The resulting canopy height points were used for the calculations described in the following sections. The used algorithms are implemented in Scop++.
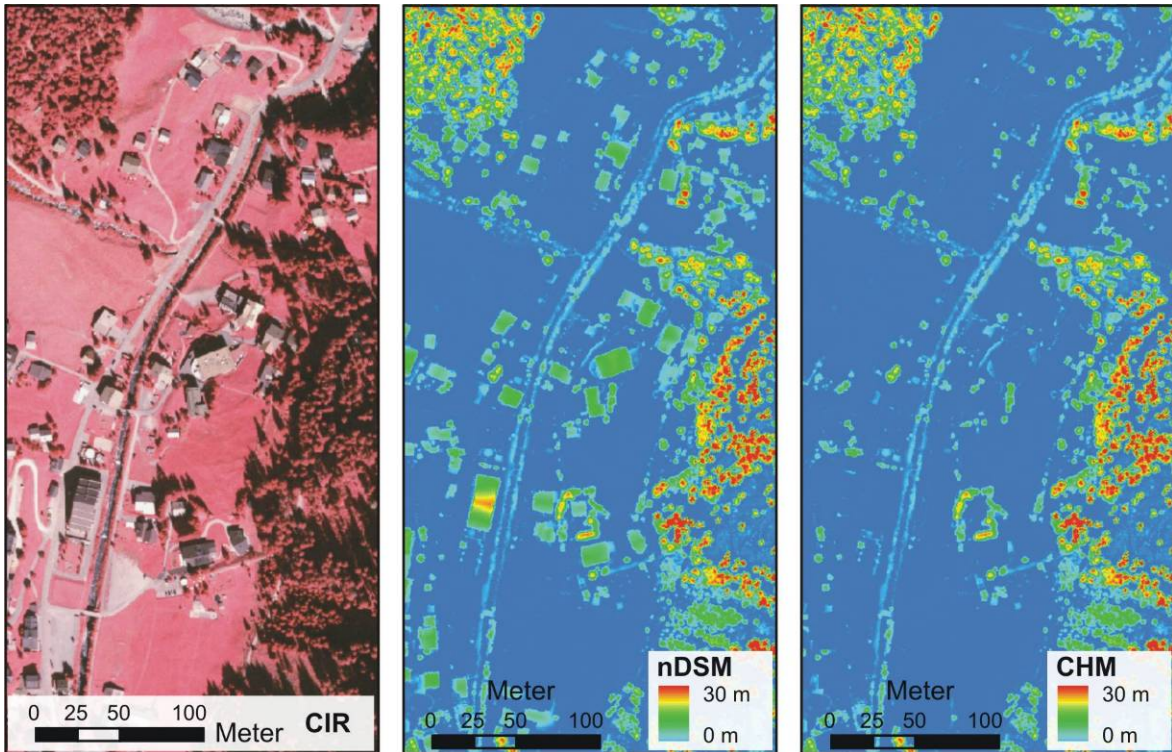
Figure 4.1: CIR orthophoto in comparison with the normalised digital surface model (nDSM) and the canopy height model (CHM). In the CHM building heights were set to zero whereas heights of other man-made objects were not removed for this study.

4.2. Land cover classification with respect to hydrologic applications

In the current work a land cover classification was done based on the complementary information of the ALS data and the CIR orthophotos. As input data the CHM and the building layer were used, whereas the building layer was generated using the algorithm from Rottensteiner et al. (2005b). Both data sets had a spatial resolution of 1 m and were derived from the ALS data as described in section 4.1.2. In addition to the ALS data the normalised difference vegetation index (NDVI), calculated from the CIR orthophotos was used for the classification. The NDVI image had a spatial ground resolution of 0.25 m.

The selection of the land cover classes was motivated entirely by hydraulic relevant roughness coefficients corresponding to the following land cover classes:

- buildings,

- sealed surfaces (roads, parking places),

- bare soils (smooth),

- gravel / riprap (rough),

- pastures / meadows (short-, high-grass),

- scrubs (sparse, dense),

- forests (sparse, dense) and

- young forests (sparse, dense).

Due to the high spatial resolution of the input data an object-oriented classification approach was chosen. The commercial software eCognition (May, 2006) was used to derive the hydrologic relevant land cover classes. The design of the knowledge-based classification rules was driven by the complementary information content of the two data sources as described in section 2.6.2.

4.3. Accuracy of canopy height products

4.3.1. Validation of the DTM

Since the CHM was obtained by subtracting the DTM from the DSM, errors in both the DTM and the DSM directly propagated into the CHM. No suitable reference data for validating the DSM exist, but for a quantitative accuracy assessment of the DTM 22 000 ground control points were available. As can be seen in Figure 3.3 these ground control points were predominantly available along roadsides in the valley, but some were acquired also along steep mountain roads. Therefore, it was possible to assess the accuracy of the DTM in dependence of the local slope from flat to very steep terrain, albeit unfortunately only for non-forested terrain.

4.3.2. Validation of the canopy heights

A truly quantitative assessment of the ALS derived canopy heights with the data from the 103 inventory plots, each representing a roughly circular area with a varying diameter (Bitterlich plot), was done on a single-tree and an area-based approach. To investigate the effects of the interpolated DSM, the canopy heights were extracted from both the first-echo point cloud and the grid-based CHM separately.

Single-tree based validation

For the single-tree based validation only those trees were used whose heights had been measured with the Vertex III hypsometer. As the positions of these trees were known the highest first-echo point/DSM pixel within a distance of 1.0, 1.5 and 2.0 m was extracted for each tree. In a further calculation step the tree height was calculated by subtracting the terrain height from the extracted height. For the extraction of the tree heights from the CHM the highest pixel value from a 3x3 pixel window was used.

Due to the difficult terrain it was analysed if there was a connection between terrain slopes and single-tree heights derived from the first-echo ALS data as well as from the canopy height model.

To investigate the influence of the ALS point density on the derived single-tree heights the ALS data were thinned out with different percentages (25%, 33%, 50%, 66% and 75%). The thinning out was done systematically, which means that a thinning out percentage of 25% deleted every fourth ALS point. Using each thinned out data set the above described analyses were done. These analyses were only done for the estimation of the single-tree heights from the first-echo points.

Area based validation

The area-based validation was done with the Lorey's mean heights h_L of the 103 sample plots as reference data. As mentioned in Næsset (2005) height percentiles are the most commonly used canopy height-related metrics. Thus, for the estimation of the h_L from the ALS data, percentiles of first-echo point/CHM pixel height distributions were used. To guarantee that ground points and canopy heights from stones and low vegetation like grasses and bushes did not disturb the canopy height distribution a height threshold of 2.0 m (Næsset, 1997a) was used. In this study the influence of this height threshold was investigated. Therefore, three different height thresholds (0.0 m, 2.0 m and 4.0 m) were investigated. For the calculation of the height distribution only those points / pixels wee used which were above the threshold. As the optimal canopy height percentile was not known in advance, it had been estimated for each sample plot separately. In a second step the h_L was extracted from the ALS data based on the averaged optimal canopy height percentiles. Due to the fact that the measurements of the forest inventory data wee based on Bitterlich plots, the sample plot areas were variable. Therefore, five different sizes of circular sample areas (Ø 21, Ø 23, Ø 25, Ø 27 and Ø 29 m) were used to analyse the calculation of the canopy height percentiles.

Also for the estimation of the Lorey's mean heights the influence of the ALS point densities on the achievable accuracies was investigated. These analyses were only been done for the estimation of the Lorey's mean heights from the first-echo points.

4.3.3. Effects of winter versus summer ALS data on the derived canopy heights

To investigate the properties of the winter (leaves-off) versus the summer (leaves-on) data the validation approaches, as described in section 4.3.2 were performed for both data sets (winter/summer) separately. Furthermore, small experiments over the Winkel and Valisera test sites were conducted. Both test sites were covered by the winter and the summer flight (Figure 3.3). As done before for the merged winter/summer point cloud, the data werr filtered and the different models (DTM, DSM, CHM) were calculated for winter and summer separately. Since the Winkel test site contained many deciduous trees, it was possible to investigate the different appearance of deciduous versus coniferous trees in summer and winter ALS data. For the Valisera test site, where coniferous trees dominated, the penetration capability of the laser beam depending on winter/summer conditions was studied. First of all the DTMs based on the merged winter/summer ALS data were calculated. In a second step the penetration rate of ALS first-echo points was calculated for both data sets separately. The penetration rate was described as the percentage of ALS points with height differences to the terrain surface less than 0.5 m.

4.4. Stem volume estimation

In the current thesis two different approaches for mapping stem volume were tested, which both combined the information from 103 forest inventory plots and the ALS data. Due to the low ALS point densities (0.9 and 2.7 p/m^2) area-based methods were used for the analyses. For the calibration of the models the statistically calculated stem volumes per hectare $v_{stem,fi}$ acted as reference data. The calculation of $v_{stem,fi}$ is described in section 3.2.3.

Both approaches had to account for different ALS properties (e.g. point densities and footprint sizes) and the disadvantages of the forest inventory data, such as variable sample plot sizes, the fact that the measured trees were selected by an angle count method and that $v_{stem,fi}$ did not correspond to the biological timber volume. The calculations of the ALS derived parameters were based on ALS point clouds instead of a calculated canopy height model. The major reason for this was that the interpolation process introduces errors into the canopy height model depending on the chosen grid size and the interpolation method itself (Smith et al., 2004). A further reason for using point

clouds was the different point density of the two ALS data sets, which would lead to different interpolation errors. The calculations of ALS parameters were based on circular areas with a constant diameter. If a sample plot was covered by both ALS flights, the merged ALS data were used for the parameter calculations. Within the study area the forests were dominated by coniferous trees (~99%) as described in section 3.1. Therefore, for the whole study region homogenous regression functions could be used for both methods.

4.4.1. Method A

Method A is the multiplicative model for estimating stem volume developed by Næsset (2004b), which is shortly described here. For the multiple regression analysis first- and last-echo ALS data are needed. A multitude of statistical quantities needs to be calculated including mean values, coefficients of variation, percentiles of heights and canopy densities for several height intervals. The calculations are based on circular sample plot areas with constant diameters. The multiplicative model is formulated as

$$
\begin{aligned}
Y = \beta_0 \; h_{0f}^{\beta_1} \; h_{10f}^{\beta_2} ... h_{90f}^{\beta_{10}} \; h_{0l}^{\beta_{11}} \; h_{10l}^{\beta_{12}} ... h_{90l}^{\beta_{20}} \; h_{mean\,f}^{\beta_{21}} \; h_{mean\,l}^{\beta_{22}} \\
\times h_{cvf}^{\beta_{23}} \; h_{cvl}^{\beta_{24}} \; d_{0f}^{\beta_{25}} \; d_{1f}^{\beta_{26}} ... d_{9f}^{\beta_{34}} \; d_{0l}^{\beta_{35}} \; d_{1l}^{\beta_{36}} ... d_{9l}^{\beta_{44}}
\end{aligned}
\tag{4.1}
$$

where Y is the $v_{stem,fi}$ in m^3ha^{-1}; h_{0f}, h_{10f}, …, h_{90f} are percentiles of the first-echo laser canopy heights for 0%, 10%, … , 90% in meters; h_{0l}, h_{10l}, …, h_{90l} are percentiles of the last-echo laser canopy heights for 0%, 10%, … , 90% in meters; h_{meanf}, h_{meanl} are mean of the first- and last-echo canopy heights in meters; h_{cvf}, h_{cvl} are coefficients of variation of the first- and last-echo canopy heights in percent; first- and last-echo returns with heights less than 2 m were classified as ground hits and therefore, the heights were set to zero; d_{0f}, d_{1f}, …, d_{9f} are cumulative canopy densities of first-echo laser points for the fraction no. 0, 1, …, 9; d_{0l}, d_{1l}, …, d_{9l} are cumulative canopy densities of last-echo laser points for the fraction no. 0, 1, …, 9. The 10 fractions are of equal height and are calculated by dividing the difference between the highest and the lowest (2 m) canopy height by 10. For each fraction no. 0, 1, …, 9 (> 2 m) the proportion of laser hits above the fraction limits to the total number of laser hits are calculated for both, first- and last-echo points.

The model parameters of Eq.(4.1) can be estimated with the linear form of the equation using logarithmic variables as shown in the following formula:

$$
\begin{aligned}
\ln Y = \ln \beta_0 &+ \beta_1 \ln h_{0f} + \beta_2 \ln h_{10f} + ... + \beta_{10} \ln h_{90f} + \beta_{11} \ln h_{0l} + \beta_{12} \ln h_{10l} + ... \\
&+ \beta_{20} \ln h_{90l} + \beta_{21} \ln h_{meanf} + \beta_{22} \ln h_{meanl} + \beta_{23} \ln h_{cvf} + \beta_{24} \ln h_{cvl} + ... \\
&+ \beta_{25} \ln d_{0f} + \beta_{26} \ln h_{1f} + ... + \beta_{34} \ln d_{9f} + \beta_{35} \ln d_{0l} + \beta_{36} \ln h_{1l} + ... + \beta_{44} \ln d_{9l}
\end{aligned}
\tag{4.2}
$$

Regression analyses

For the development of the final models stepwise multiple regression analyses were used for method A. Starting with the regression equation, (Eq.(4.2)), including all independent variables, a backwards working approach was used, in which variables were dropped out from the equation one at a time if the significance level of the partial F statistic was greater than 0.05. Finally, a collinearity measure was used for selecting the final variable set, whereas only models whose condition number $\kappa < 30$ were accepted. For the stepwise multiple regression analyses the open source software "R" (R Development Core Team, 2005) was used.

Correction of the logarithmic transformation bias

For the multiple regression analysis of method A the multiplicative model (Eq.(4.1)) is transformed to a logarithmic scale (Eq.(4.2)). This common procedure has the advantage that the complex multiplicative model can be expressed by a linear one. Thus, a simple least square method can be applied in order to estimate the model parameters. For the final prediction of the stem volume a conversion of the log-linear model parameters to the original untransformed scale is necessary. This procedure introduces a bias because the large values are compressed on the logarithmic scale and thus tend to have less leverage than small ones (Beauchamp and Olson, 1973). Thus, the bias is not an arithmetic constant but a constant fraction of the estimated value (Snowdon, 1991). Several procedures to correct this bias in logarithmic regression estimates are advocated in literature. An extensive theoretical basis for correcting bias in logarithmic regressions can be found in Flewelling and Pienaar (1981). Smith (1993) gives an overview of available parametric and nonparametric algorithms for correcting transformation bias. In the current study the empirical ratio estimator (RE) approach developed by Snowdon (1991) was applied. The study from Snowdon (1991) demonstrated that this method is more reliable than corrections estimated from variance as for example described by Baskerville (1972) or Sprugel (1983). The correction

factor for this RE method is calculated by dividing the mean of the observed values by the mean of the predicted (retransformed) values as shown in Eq.(4.3):

$$RE = \sum_{i=1}^{n} v_{stem,fi,i} \Big/ \sum_{i=1}^{n} v_{stem,i} \qquad (4.3)$$

where RE is the correction factor; $v_{stem,fi}$ are the observed values (stem volume calculated from the FI data) in $m^3 ha^{-1}$; v_{stem} are the predicted values (stem volume) in $m^3 ha^{-1}$, retransformed back to the original untransformed scale without bias correction; and n is the number of sample plots.

Finally, the bias corrected, predicted stem volumes is calculated by multiplying the predicted values v_{stem} with the correction factor RE.

4.4.2. Method B

For the second approach, denoted as method B, a less complex model is proposed using quantities which can be interpreted physically and which can be measured with ALS techniques. For the calculation of the volume between the canopy surface and the terrain, which is called canopy volume V_{can}, the point-based canopy heights (4.1.2) are used. For the proposed model it is assumed that the stem volume can be expressed by a linear fraction of V_{can}. Therefore, model B uses only the V_{can} as input variable. To minimise the effects of short vegetation and stones, first-echo returns with heights less than 2 m above the ground are classified as ground hits and therefore, the heights are set to zero. For the calculation of the V_{can}, using Eq.(4.4), a circular sample plot area A is used.

$$V_{can} = A \cdot ch_{mean} \qquad (4.4)$$

where V_{can} is the canopy volume in m^3 and ch_{mean} is the mean height of all first-echo heights within A in m.

To consider the high variability in the vertical forest structure V_{can} is split into several canopy volumes $V_{can,i}$ depending on pre-defined canopy height ranges. In the current analyses canopy height ranges with two different canopy height intervals Δch are used. For method B1 Δch is set to 7.0 m, corresponding to five ($n = 5$) canopy height ranges from 2.0 to 9.0 m, 9.0 to 16.0 m, 16.0 to 23.0 m, 23.0 to 30.0 m and greater 30.0 m. For method B2 a Δch of 10.0 m is chosen corresponding to four ($n = 4$) canopy height ranges from 2.0 to 12.0 m, 12.0 to 22.0 m, 22.0 to 32.0 m and greater 32.0 m. These canopy height ranges are used to calculate n fractions of first-echo points $f_{fp,i}$ whose

heights are within the canopy height range *i* related to the total amount of first-echo points within the whole sample plot area (Figure 4.2).
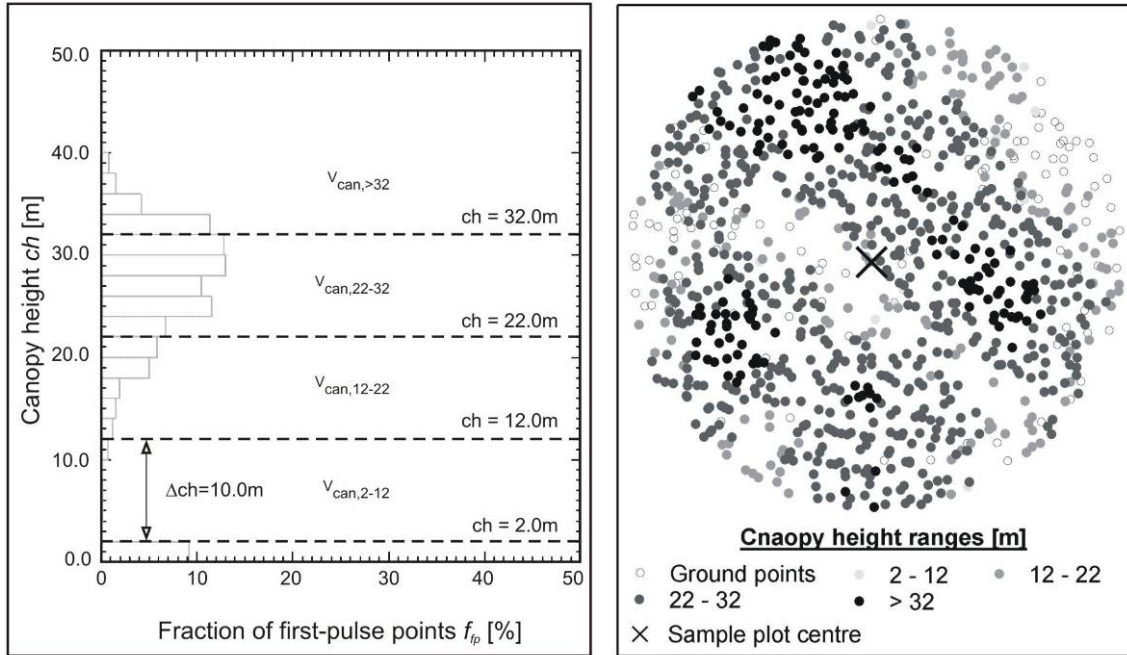
Figure 4.2: Distribution of first-echo ALS heights for a sample plot. The right figure shows the spatial distribution of first-echo points within a sample plot with a diameter of 20 m. The left figure shows the vertical distribution and the used canopy height ranges Δch, which is used to divide the sample plot in sub areas. For each sub area the canopy volume $v_{can,i}$, which is used as independent variables for the multiple regression analysis, is calculated.

The calculated $f_{fp,i}$ is used to divide the circular sample plot area into *n* sub areas. Finally, for each of these *n* sub areas the $V_{can,i}$ in m^3 is calculated by the following formula:

$$V_{can,i} = f_{fp,i} \cdot A \cdot ch_{mean,i} \tag{4.5}$$

where $ch_{mean,i}$ is the mean height of all first-echo heights within the sub area *i* and $f_{fp,i}$ is the fraction of first-echo points whose heights are within the canopy height range *i* and varies between 0 and 1. The sum of $f_{fp,i}$ is one, which guarantees that the sum of $V_{can,i}$ is equal to V_{can} as shown in Eq.(4.6) and Eq.(4.7).

$$\sum_{i=1}^{n} f_{fp,i} = 1 \tag{4.6}$$

$$\sum_{i=1}^{n} V_{can,i} = V_{can} \tag{4.7}$$

Each of these calculated $V_{can,i}$ represents the volume between the terrain and the surface canopy for the sub area i as shown in Figure 4.3.
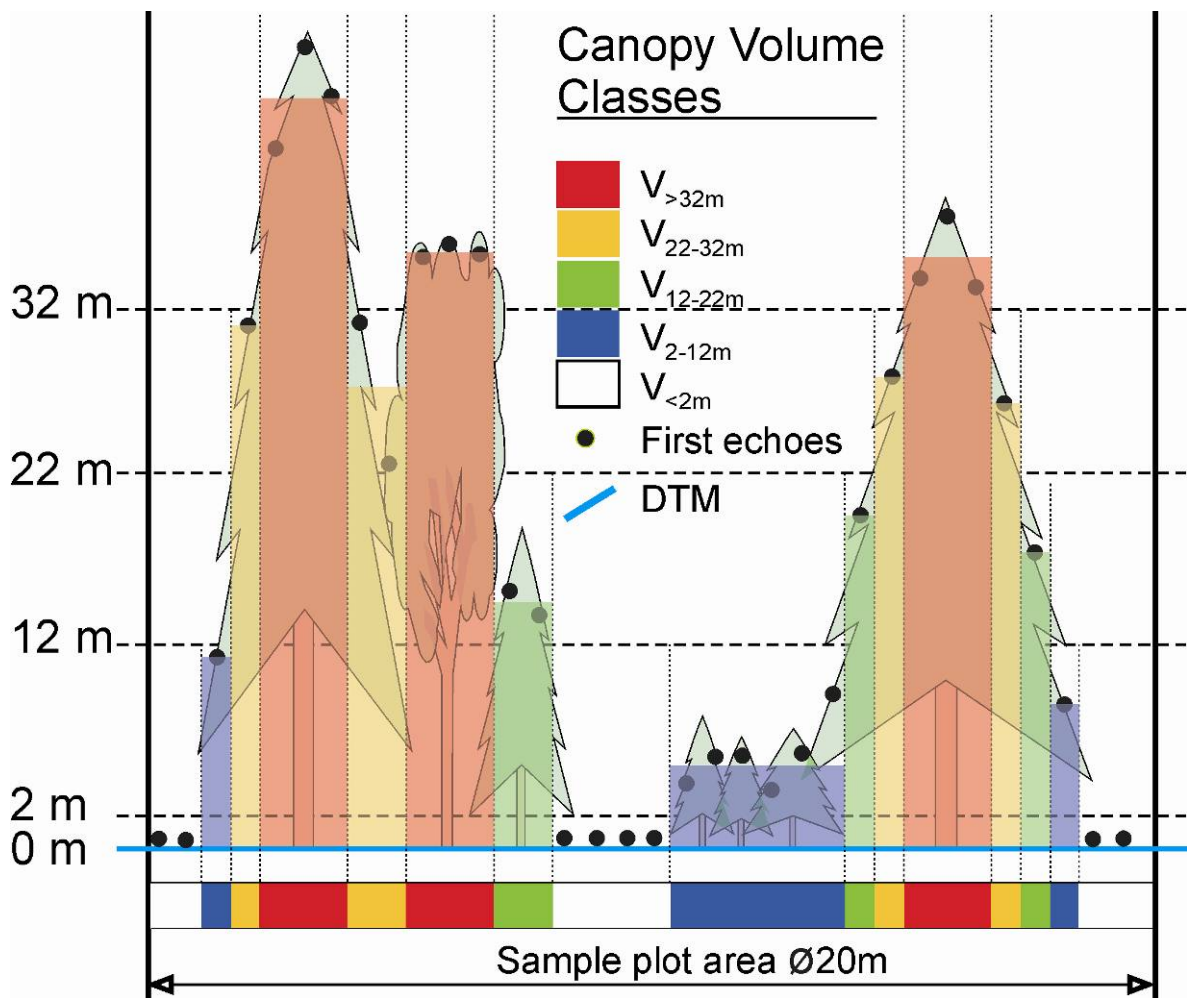
Figure 4.3: Canopy volume classes calculated from ALS data.

The specific canopy volumes $v_{can,i}$ in $m^3 m^{-2}$ is calculated by Eq.(4.8) and is used as independent variables for the regression analyses.

$$v_{can,i} = f_{fp,i} \cdot ch_{mean,i} \qquad\qquad\qquad (4.8)$$

where $v_{can,i}$ is the canopy volume for the canopy height interval i in $m^3 m^{-2}$, representative for the sample plot sub area i.

The calculated $v_{can,i}$ represents the canopy volume in $m^3 m^{-2}$ and can therefore be directly related to the stem volume $v_{stem,fi}$ ($m^3 ha^{-1}$) calculated from the forest inventory data. To take the different area units into considerations the factor 10^4 is used in Eq.(4.9) and Eq.(4.10). For the estimation of the stem volume the following two different linear formulas are tested:

$$v_{stem,fi} = \beta_0 + 10^4 \cdot \sum_{i=1}^{n} \beta_i \cdot v_{can,i} \qquad\qquad\qquad (4.9)$$

$$v_{stem,fi} = 10^4 \cdot \sum_{i=1}^{n} \beta_i \cdot v_{can,i} \qquad\qquad\qquad (4.10)$$

where $v_{stem,fi}$ is the stem volume calculated from the FI data in m^3 per ha; n is the number of canopy volumes; β_i are the unknown model parameters estimated with a least square approach.

As shown in Eq.(4.10) a calculated β_i-coefficient represents the ratio of canopy volume and stem volume. For example, a value of $\beta = 0.004$ means that 0.4 percent of the canopy volume is occupied by stem volume. Thus, the calculated β_i-coefficients have a physical meaning and can be more easily interpreted than the parameters of the multiplicative model A.

4.4.3. Sample plot size

As the forest inventory data were based on variable sample plot areas different diameters (18 m, 20 m, 22 m, 24 m and 26 m) are investigated for the calculation of the ALS parameters. The calculations are done for each diameter separately. The most appropriate sample plot size is used for the further analyses.

4.4.4. Effects of different acquisition times and point densities

As mentioned in section 2.3, the study region was covered by two ALS data sets with different point densities and acquisition times. Unfortunately, the overlapping area of the two data sets is small and therefore, only few sample plots are covered by both ALS flights. As the forest in the

study area is dominated by coniferous trees it is assumed that the vertical and horizontal forest structure of the sample plots is similar throughout the whole test site. To investigate the different acquisition times the summer ALS data set is thinned out that the point density is equally to those of the winter ALS data. Therefore, the 47 FI sample plots which are covered by the winter data and the 56 FI sample plots which are covered by the summer data are used for the analysis separately. Furthermore, for each of these FI subsets (winter, summer) different thinning out percentages (25%, 33%, 50%, 66% and 75%) are used to study the effects of different point densities under the same conditions of the ALS data acquisition.

4.4.5. Cross-validation

As the number of inventory sample plots is low it is not practical to split the data in training- and validation-data sets. Rather, a cross-validation procedure is used, where for each step one observation is excluded for the estimation of the β–coefficients. Since the model is fitted n times, where n is the number of observations, the prediction error for each excluded observation can be calculated. Finally, statistical parameters of the prediction errors can be calculated including the range of the errors, the mean and the standard deviation. For method A the bias corrected values are used.

4.4.6. Stem volume mapping

To map the stem volume for the whole study region the model with the smallest prediction errors derived from the cross-validation and the highest coefficient of determination R^2 is chosen. A moving window approach is used to calculate the stem volume with the estimated model parameters. The circular window size, which leads to the highest accuracies, is used for the stem volume mapping. Finally, the total stem volume is calculated from the derived stem volume map. To evaluate the amount of total stem volume a comparison with the total stem volume calculated from the FI data is done.

5. Results

5.1. Hydrologic relevant land cover classification

For the current study area the land cover classes buildings, sealed surfaces (roads, parking places), bare soils, gravel / riprap, pastures / meadows (short-, high-grass), scrubs (sparse, dense), forests (sparse, dense) and young forests (sparse, dense) were used. The differentiation of the land cover classes meadows with high-grass and dense scrubs was not possible in areas, which were covered by shadows in the CIR orthophotos, due to the missing spectral information and the inaccuracies in the object height model. Nevertheless, the quality of the land cover classification is high, as can be seen in Figure 5.1 (right). Unfortunately, the spectral information of the black areas in the CIR orthophoto (Figure 5.1, left), representing shaded areas (e.g. around buildings), could not be used for the land cover classification. With the help of ALS heights (Figure 5.1, middle), high thematic accuracies could be reached also for these areas. With minor manual post-processing of the land cover map, which is the common practice in commercial projects, a kappa coefficient higher than 0.95 is reached, which is a reasonable good result. Even considering the cost implications, this high thematic accuracy is only achievable with these datasets.
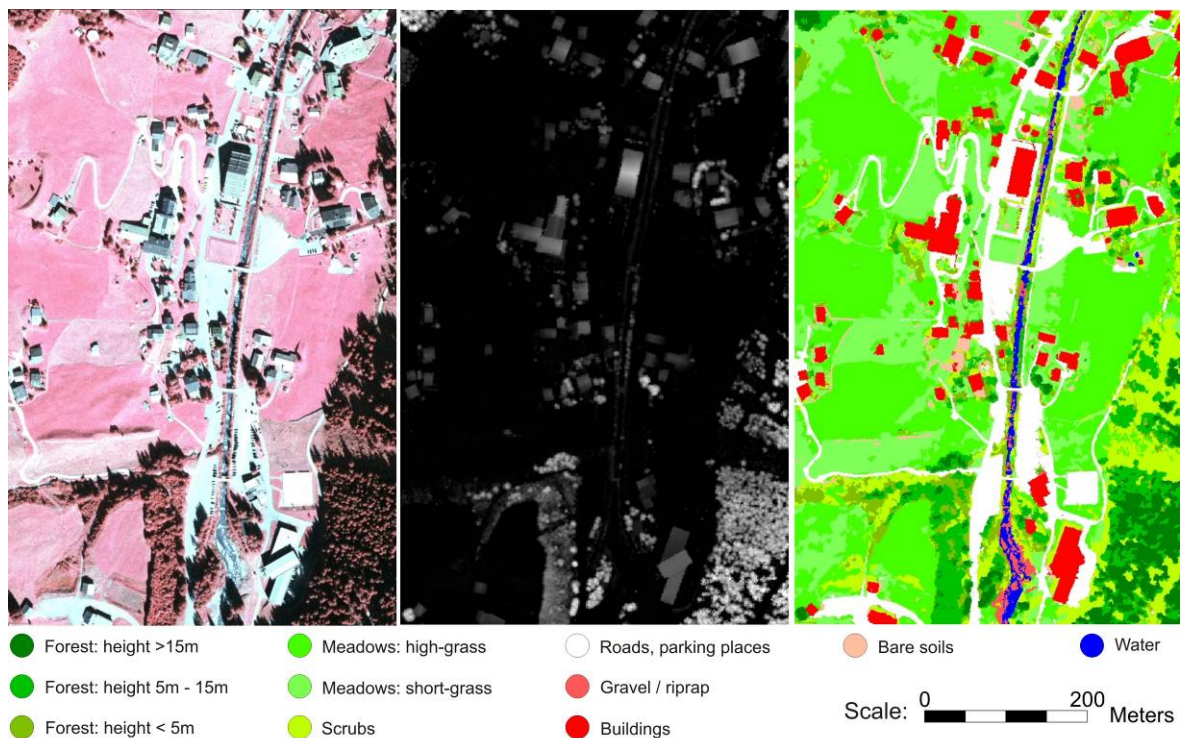
Figure 5.1: Land cover map with hydrologic / hydraulic relevant classes; shown is a subset of the study area; (left) CIR orthophotos; (middle) normalised digital surface model derived from ALS data; (right) land cover map with a spatial resolution of 0.25 m, derived from ALS data and CIR orthophotos.

5.2. *Accuracy of canopy height products*

The ALS derived canopy height model (CHM) is shown in Figure 5.2. A perspective view was chosen to better visualise the relationship between terrain and canopy height. One could observe that most of the forest can be found along relatively steep mountain slopes, while forest cover is relatively sparse in the valley bottoms, along mud- and debris flow channels and avalanche paths. With increasing altitude the forest cover decreases. However, particularly in the transition zone from forests to alpine meadows, patches of lower vegetation such as shrubs or dwarf pine are still evident in the CHM, as can be verified by orthophoto interpretations. While an initial visual inspection indicated a high quality, the CHM also contains some obvious errors. For example, some high canopy height values can be found in steep, barren terrain as visible along some of the mountain tops. Possibly, these artefacts were caused by multiple echoes over very steep, rough terrain due to the extended laser footprint size (~0.3 m) or because the filtering procedure classified rocks as non-terrain objects. Together with other artificial objects these artefacts should be removed in subsequent processing steps.
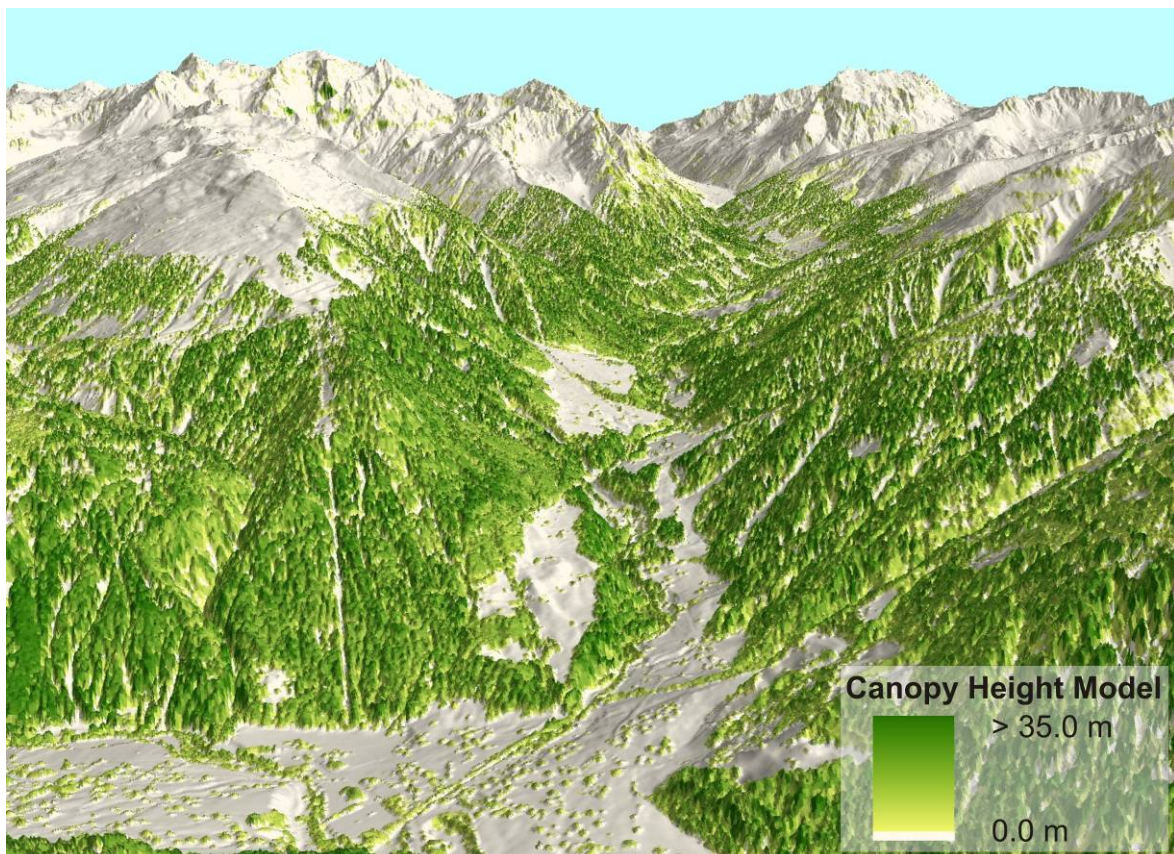
Figure 5.2: Canopy heights as measured by an airborne laser scanner over the study area. Buildings and artefacts visible along the mountain tops were not removed for the purpose of this figure.

5.2.1. Validation of the terrain model

In Figure 5.3 the results of the DTM validation using the 22 000 ground control points (GCPs) are shown. The figure shows that the root mean square (RMS) errors, defined by the standard deviations of the differences between the z-coordinates of the GCPs and the ALS derived DTM heights, are smaller than 20 cm for flat to gently sloping terrain (slope < 20%) and increase rapidly with the steepness of the terrain. In addition to the RMS errors the mean errors in dependence of the slope is also shown in Figure 5.3. The mean residuals were calculated by subtracting the DTM heights from the GCP heights. As shown in Figure 5.3 (right image) the mean errors are depending on the slope and are less than 5 cm for lower slopes (< 60%) and increase up to about 15 cm for steeper ones. This means that with increasing terrain slope the underestimation of the terrain height increase.
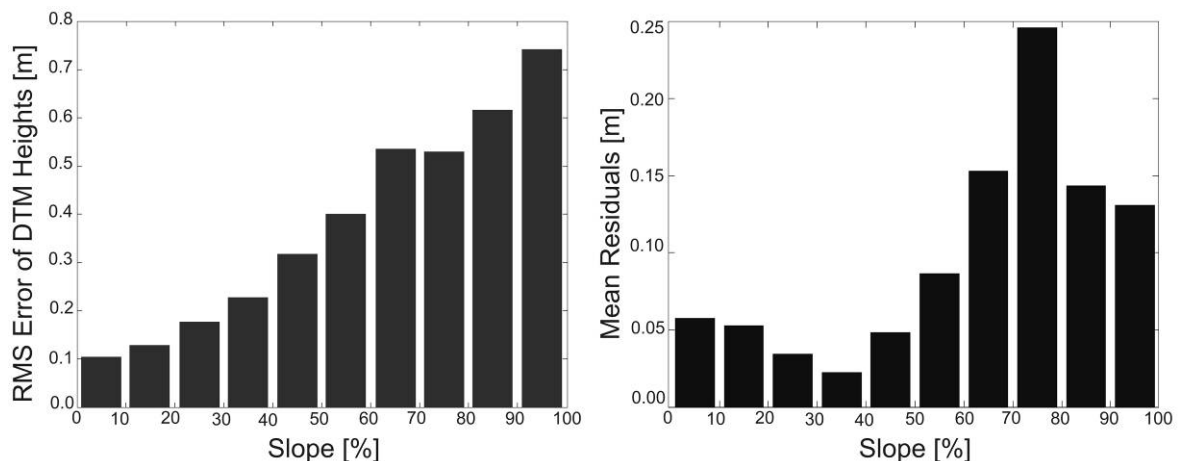
Figure 5.3: Root mean square error (left image) and mean residuals (right image) of laser scanner derived digital terrain model (DTM) for different slope classes derived from a validation with 22 000 ground control points. The residuals were calculated by subtracting the DTM heights from the control heights.

5.2.2. Validation of the canopy heights

A truly quantitative assessment of the ALS derived canopy heights with the data from the 103 inventory plots, each representing a roughly circular area with a varying diameter (Bitterlich plot), was done on a single-tree and an area-based approach.

Single-tree based validation

For the single-tree based approach three different search radii were used to extract the tree heights from the first-echo points as well as from the CHM. The coefficients of determination (R^2), the RMS errors and the mean residuals are shown in Table 5.1. As the ALS point densities are not equal for the entire study area they were calculated for the winter and the summer flight separately. The average point densities within the used search radii are 2.7 p/m^2 for the summer data and 0.9 p/m^2 for the winter data.

Table 5.1: Summary of tree heights extracted from first-echo points and from the CHM. For each radius the coefficients of determination (R²), the RMS errors and the mean residuals are shown for the winter, summer and merged data. The analyses were done using all (a) trees (196), the trees which are covered by the winter (w) ALS flight (80) and the trees which are covered by the summer (s) ALS flight (116).

Search radius [m]	R²			RMS error [m]			Mean residuals [m]		
	a	w	s	a	w	s	a	w	s
Point based (first-echo) tree heights									
1.0	0.89	0.90	0.86	2.40	2.47	2.27	0.80	0.37	1.03
1.5	0.88	0.89	0.85	2.55	2.80	2.37	1.12	0.80	1.33
2.0	0.88	0.89	0.82	2.63	2.70	2.56	1.40	1.03	1.65
Raster based (CHM) tree heights									
Window size ø 3 pixel	0.87	0.89	0.82	2.63	2.62	2.62	-0.05	-0.35	0.16

The highest R^2 for the correlations with the first-echo points are 0.89 (search radius 1.0 m) and 0.87 (search area 3x3 pixels) for the correlations with the grid-based CHM heights and are shown in Figure 5.4. The RMS errors are relatively large and are 2.40 m and 2.63 m respectively. The mean residuals, calculated by subtracting the reference tree height (forest inventory) from the extracted tree heights (first-echo points and CHM) range between 0.80 m and -0.05 m (Figure 5.4) and show for the first case an overestimation of the tree heights for the point-based tree height estimation.
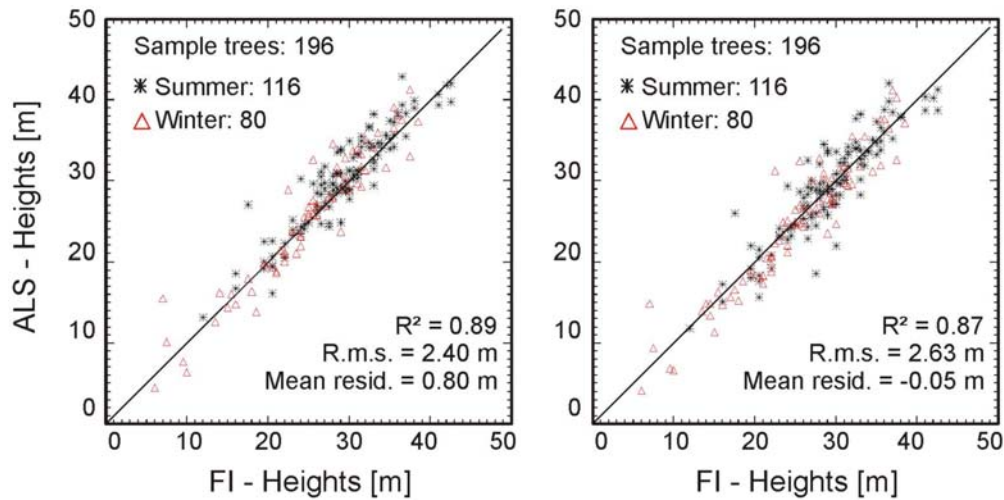
Figure 5.4: Comparison of single-tree heights derived from (ALS) data and 196 measured single-tree (spruce) heights. The ALS tree height estimations were based on the first-echo points (left) and on the grid-based CHM (right).

As described in the section 5.2.1 the DTM accuracy decreases with increasing terrain slope. To analyse if this fact is also influencing the accuracy of the derived single-tree heights the connection between the accuracy of the tree heights and the terrain slopes was analysed. As shown in Figure 5.5 there is no dependence between the RMS errors of the ALS derived single tree heights and the terrain slope. For Figure 5.5 (left) the tree heights were extracted from 3D first-echo points, whereas for Figure 5.5 (right) the tree heights were extracted from the grid-based canopy height model. In addition to the RMS error the mean residuals of the extracted single tree heights from the 3D first-echo points were plotted against the DTM slope.
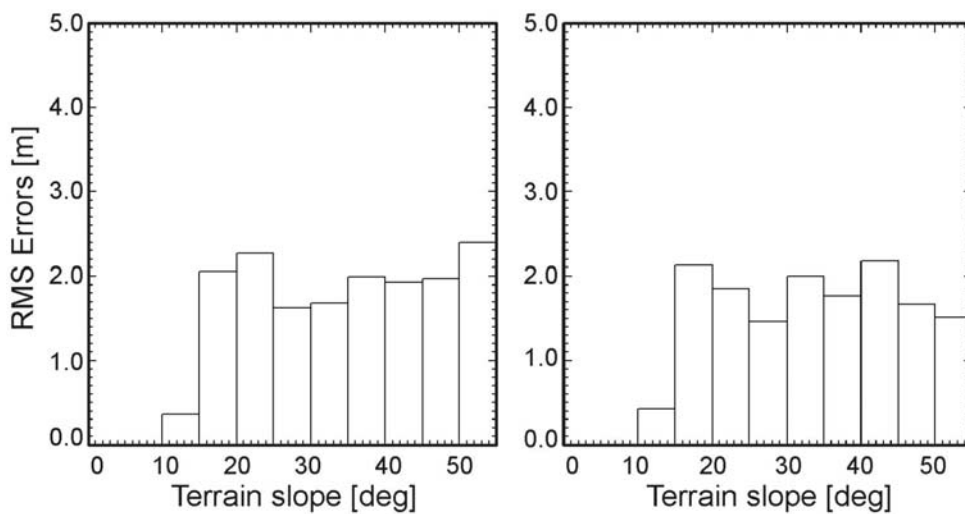
Figure 5.5: RMS errors of single tree heights versus terrain slope. For the left figure the tree heights were extracted from the 3D first-echo points, for the right figure from the grid-based canopy height model (CHM).

As shown in Figure 5.6 the mean residuals show an overestimation of the tree heights for slopes less than 45°. For slopes greater than 50° the mean residuals show a clear underestimation. Comparing the mean residuals of the DTM heights, as shown in Figure 5.3 (right image), with the mean residuals of the extracted single tree heights, it can be observed that the residuals of the terrain height increase considerable for slopes greater than 50° and that the residuals for slopes less then 45° are relatively constant. Assuming that the accuracy of the measured tree heights are uniformly distributed over the whole range of terrain slopes, these investigations show that with increasing terrain slopes the terrain underestimation increased. Therefore, an increase of the overestimation of the estimated tree heights could be expected. As can be seen in Figure 5.6 an underestimation of estimated tree heights for large slopes occur. This can either be explained by increasing planimetirc inaccuracies (e.g. spatial inaccuracies between ALS and forest inventory data) in steep slopes or by the fact that in steep slopes the tree height measurements with the Vertex III is more accurate than for lower slopes where the intersecting angle becomes low.
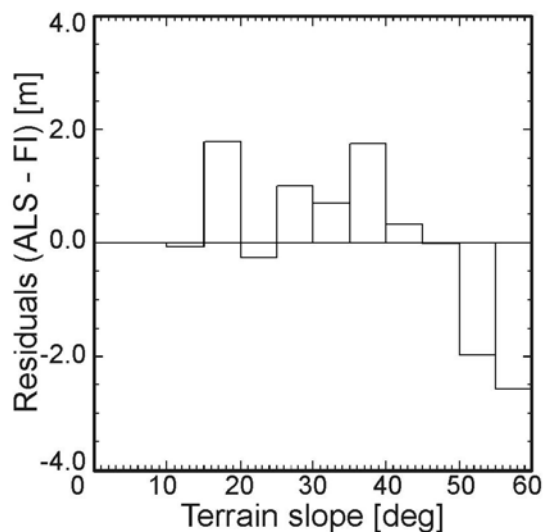
Figure 5.6: Mean residuals of single tree heights extracted from 3D first-echo points versus terrain slope.

Commonly, it is expected that tree heights estimated from ALS data show an underestimation due to penetration of the laser pulses into the canopy and due to the fact that laser beams hit some part of the canopy rather than tree tops. Therefore, additional investigations were done to study the observed overestimation of the tree height within this study area. As shown in Figure 5.7, a general overestimation of the estimated tree heights can be seen. Furthermore, a small increase of the overestimation with increasing tree heights can be observed. Due to these findings, it can be assumed that the underestimations of the field measured tree heights increase. From a practical

point of view this can be explained that it is more difficult to find the correct tree top position of high trees (e.g. h > 35 m) than of low trees especially within dense forests.
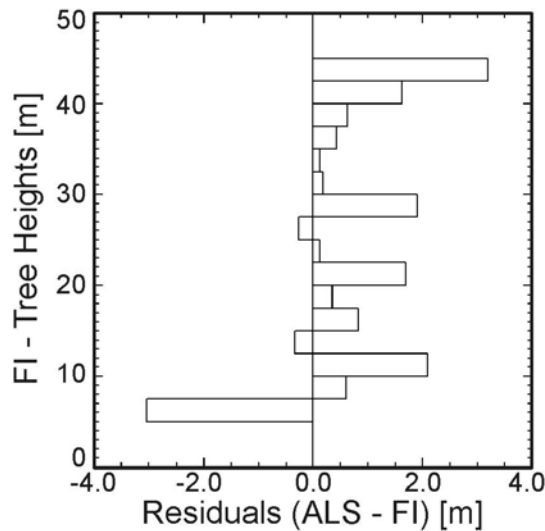
Figure 5.7: Mean residuals of single tree heights extracted from 3D first-echo points versus measured tree heights.

Table 5.2 shows the results of the extracted single-tree heights from first-echo ALS data with different point densities. Within the search radius of 1 m the average point density for the winter data is 0.9 p/m² and 2.7 p/m² for the summer data. Both data sets were thinned out with 25%, 33%, 50%, 66% and 75%. For the extraction of the tree heights the highest point within a search radius of 1 m was chosen, as this radius leads to the highest correlations as shown in Table 5.1. The coefficients of determinations decrease with decreasing point densities from R^2 = 0.90 to 0.84 for the winter data and from R^2 = 0.86 to 0.81 for the summer data. The RMS errors increase with decreasing point densities from 2.57 to 3.25 m and from 2.27 to 2.64 m for the winter and the summer data respectively. As expected, the mean residuals decrease for the winter data from 0.37 to -0.84 m and for the summer data from 1.03 to 0.02 m. The influence of different point densities was also investigated by Yu et al. (2004). They found that the bias of estimated tree heights (spruce) decreased from 0.0 m (10 p/m²) to -0.09 m (5 p/m²) and to -0.19 m (2.5 p/m²), whereas the standard deviation increased from 0.69 (10 p/m²) to 0.81 (5 p/m²) and to 0.95 m (2.5 p/m²). They also reported that the difference of the estimates between 10 and 5 p/m² was lower than the one between 5 and 2.5 p/m². Compared to the findings in this study it can be stated that the increase of the RMS errors corresponds to the same trend. Furthermore, the decrease of the bias for the summer data with a point density of ~2.7 p/m² to ~1.4 p/m² (50% of thinning out) is 0.39 m and is

high compared to the findings of Yu et al. (2004). However, if the non-linear function between point density and bias is considered the estimates of the current study seem to be realistic.

Table 5.2: Summary of tree heights extracted from first-echo points with different point densities. For each thinned out data set the coefficients of determination (R²), the RMS errors and the mean residuals are shown for the winter, summer and merged data. The analyses were done using all (a) trees (196), the trees which were covered by the winter (w) ALS flight (80) and the trees which were covered by the summer (s) ALS flight (116). The search radius was 1.0 m.

Percentage of thinning out [%]	R²			RMS error [m]			Mean residuals [m]		
	a	w	s	a	w	s	a	w	s
Single tree heights estimated from first-echo points with different point densities									
0	0.89	0.90	0.86	2.40	2.47	2.27	0.80	0.37	1.03
25	0.87	0.87	0.85	2.43	2.66	2.25	0.60	0.03	0.93
33	0.88	0.91	0.85	2.51	2.71	2.35	0.58	0.19	0.80
50	0.88	0.87	0.85	2.70	3.17	2.36	0.41	-0.07	0.64
66	0.86	0.87	0.86	2.75	3.07	2.29	0.07	-0.47	0.42
75	0.84	0.84	0.81	2.85	3.25	2.64	-0.20	-0.84	0.02

Area-based validation

For the area-based validation of the ALS canopy heights, both, the first-echo point cloud and the CHM were used for the investigations. As reference data Lorey's mean heights (h_L) of the 103 sample plots were used.

As shown in Table 5.3 the highest accuracies to estimate Lorey's mean heights from first-echo points can be achieved with a sample plot diameter of 25 m, a mean canopy height percentile of 84% (h_{84}) and a height threshold of 4 m. For these settings the R² is 0.79, the RMS error is 3.04 m and the average of the residuals is -0.53 m. The difference of the RMS errors between winter and summer data is 0.05 m as shown in Table 5.3. The analyses about the height thresholds show that thresholds greater equal 2 m lead to an eminent improvement of the accuracies, whereas the difference between 2 m and 4 m is small.

For the raster based estimation of Lorey's mean heights a sample plot diameter of 23 m, a mean canopy height percentile of 92% (h_{84}) and a height threshold of 2 m lead to the highest accuracies as shown in Table 5.3. The R² is 0.70 and is less than those of the point-based

estimation. Also the RMS error (RMSE = 3.90 m) is greater than those of the point-based estimation (RMSE = 3.04 m). The influences of the height thresholds on the achievable accuracies are similar to the point-based case. The difference of the RMS errors between winter and summer data is 0.17 m and is also similar to the point-based calculations.

In Figure 5.8 the scatter plots of the Lorey's mean heights derived from ALS data versus forest inventory data are shown.
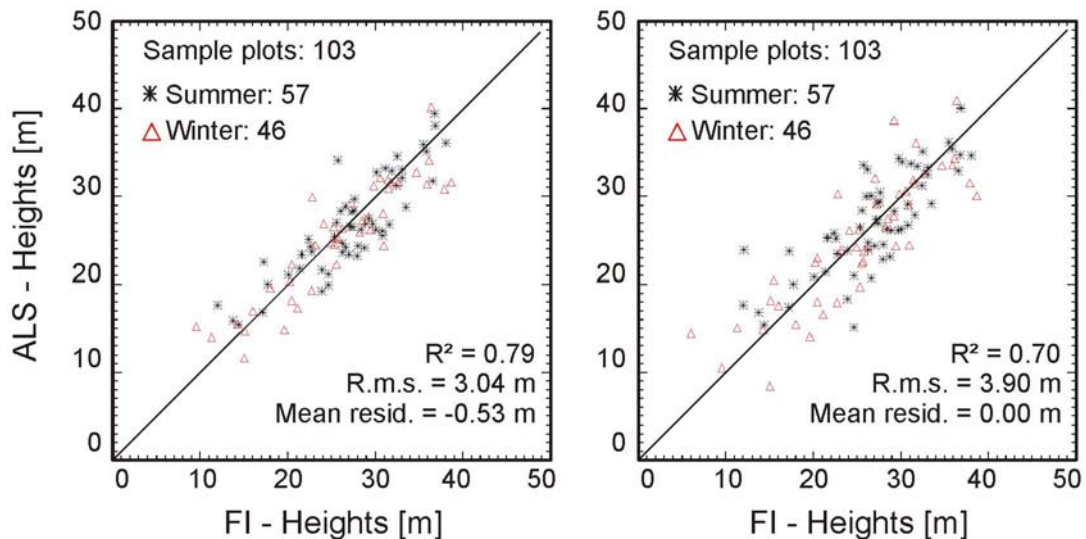
Figure 5.8: Comparison of Lorey's mean heights derived from ALS and 103 forest inventory plots. For the left scatter plot the Lorey's mean heights were derived from first-echo points. Settings: Diameter of the sample plots 25 m, height threshold 4 m, height percentile for the winter data was 83% and for the summer data 84%. For the right scatter plot Lorey's mean heights were extracted from the CHM. Settings: Diameter of the sample plots 23 m, height threshold 2 m, height percentile for the winter data was 92% and for the summer data 92%.

Table 5.3: Summary of Lorey's mean heights extracted from first-echo points and from the CHM. For each radius the fitted height percentile, the coefficients of determination (R²), the RMS errors and the mean residuals are shown for the winter, summer and merged data. The analyses were done using all (a) sample plots (103), the sample plots which were covered by the winter (w) ALS flight (46) and the plots which were covered by the summer (s) ALS flight (57).

Sample plot ø [m]; height thresh. [m]	Fitted height percentile [%]			R²			RMS error [m]			Mean residuals [m]		
	a	w	s	a	w	s	a	w	s	a	w	s
Lorey's mean heights estimated from first-echo points												
21; h_{th}=0m	88	88	89	0.57	0.70	0.46	5.21	4.76	5.33	-1.91	-1.72	-1.97
h_{th}=2m	85	84	85	0.77	0.82	0.70	3.41	3.34	3.43	-0.72	-0.80	-0.67
h_{th}=4m	84	85	84	0.77	0.82	0.71	3.24	3.12	3.34	-0.64	-0.69	-0.56
23; h_{th}=0m	88	88	89	0.60	0.71	0.47	4.84	4.51	5.09	-1.76	-1.55	-1.82
h_{th}=2m	84	84	85	0.79	0.84	0.72	3.19	3.32	3.22	-0.64	-0.76	-0.58
h_{th}=4m	84	84	84	0.79	0.83	0.74	3.07	3.04	3.13	-0.54	-0.64	-0.47
25; h_{th}=0m	88	87	89	0.61	0.73	0.49	4.60	4.28	4.73	-1.63	-1.44	-1.70
h_{th}=2m	84	83	85	0.79	0.82	0.74	3.19	3.36	3.09	-0.58	-0.63	-0.52
h_{th}=4m	84	83	84	0.79	0.82	0.75	3.04	3.08	3.03	-0.53	-0.65	-0.43
27; h_{th}=0m	88	87	89	0.58	0.72	0.48	4.73	4.28	4.75	-1.59	-1.30	-1.69
h_{th}=2m	84	82	85	0.78	0.80	0.75	3.22	3.51	3.01	-0.49	-0.49	-0.46
h_{th}=4m	83	82	84	0.75	0.77	0.79	3.13	3.32	3.03	-0.40	-0.42	-0.36
29; h_{th}=0m	88	87	89	0.56	0.69	0.45	4.82	4.46	4.85	-1.55	-1.26	-1.71
h_{th}=2m	84	82	85	0.76	0.77	0.76	3.37	3.76	2.92	-0.44	-0.43	-0.41
h_{th}=4m	83	82	84	0.76	0.75	0.76	3.20	3.61	2.90	-0.37	-0.38	-0.34
Lorey's mean heights estimated from canopy height model (CHM)												
21; h_{th}=0m	92	93	92	0.51	0.68	0.33	5.50	4.71	6.20	-2.29	-2.00	-2.62
h_{th}=2m	92	92	92	0.69	0.74	0.61	4.03	4.08	4.00	-0.17	-0.50	0.09
h_{th}=4m	92	92	92	0.68	0.73	0.61	4.05	4.15	4.01	0.24	-0.06	0.56
23; h_{th}=0m	92	92	92	0.52	0.68	0.35	5.32	4.59	5.90	-2.09	-1.77	-2.44
h_{th}=2m	92	92	92	0.70	0.74	0.62	3.90	4.06	3.89	-0.00	-0.28	0.23
h_{th}=4m	92	92	92	0.68	0.73	0.65	3.96	4.07	3.73	0.47	0.21	0.60
25; h_{th}=0m	92	92	92	0.54	0.69	0.37	5.06	4.49	5.53	-1.97	-1.56	-2.21
h_{th}=2m	92	92	92	0.68	0.72	0.62	3.96	4.10	3.87	0.19	-0.11	0.45
h_{th}=4m	92	92	92	0.69	0.72	0.65	3.87	4.11	3.71	0.62	0.39	0.82
27; h_{th}=0m	92	92	92	0.53	0.68	0.36	5.02	4.46	5.44	-1.82	-1.46	-2.11
h_{th}=2m	92	92	92	0.69	0.72	0.64	3.86	4.07	3.70	0.38	0.04	0.64
h_{th}=4m	92	92	92	0.68	0.71	0.64	3.89	4.13	3.71	0.79	0.47	1.05
29; h_{th}=0m	92	92	92	0.51	0.67	0.35	5.02	4.48	5.42	-1.73	-1.42	-1.99
h_{th}=2m	92	92	92	0.68	0.72	0.63	3.89	4.09	3.72	0.45	0.06	0.76
h_{th}=4m	92	92	92	0.67	0.70	0.64	3.93	4.21	3.70	0.89	0.55	1.14

In Table 5.4 the results of the analyses concerning the ALS point densities are shown. The original ALS data sets were thinned out with 25%, 33%, 50%, 66% and 75%. The original point density for the winter data is 0.9 p/m² and for the summer data 2.7 p/m². For all analyses the optimal settings, as have been founded in the above analyses (Table 5.3) are used. The analyses show that the influence of the point density on R^2 (winter data: R^2 = 0.79 – 0.82; summer data: R^2 = 0.73 – 0.75) is negligible. Also the influences on the RMS errors and on the mean residuals are

marginal as shown in Table 5.4. Furthermore, the differences between winter and summer data are not significant, as expected for forests dominated by spruce.

Table 5.4: Influence of the ALS point density on the achievable accuracy. For the analyses a sample plot diameter of 25 m and a height threshold of 4 m were used. The analyses were done for all (a) sample plots (103), for the sample plots covered by the winter (w) ALS data (46) and for the sample plots covered by the summer (s) ALS data (57).

Percentage of thinning out [%]	Fitted height percentile [%]			R²			RMS error [m]			Mean residuals [m]		
	a	w	s	a	w	s	a	w	s	a	w	s
Lorey's mean heights estimated from first-echo points with different point densities												
0	84	83	84	0.79	0.82	0.75	3.06	3.12	3.03	-0.53	-0.65	-0.43
25	84	84	83	0.79	0.82	0.75	3.05	3.06	3.09	-0.47	-0.55	-0.44
33	84	84	84	0.79	0.83	0.74	3.07	3.15	3.06	-0.54	-0.65	-0.44
50	83	83	84	0.77	0.78	0.73	3.06	3.05	3.09	-0.45	-0.58	-0.40
66	83	83	84	0.76	0.79	0.74	3.18	3.26	3.09	-0.40	-0.47	-0.38
75	83	83	84	0.77	0.81	0.73	3.17	3.26	3.12	-0.41	-0.42	-0.35

5.2.3. Summer versus winter airborne laser scanner data

The single-tree as well as the area-based validation of the canopy heights was done for both ALS data sets (winter/summer) separately. As the ALS point density for the winter data is less than those of the summer data, differences in the extracted single-tree heights as well as Lorey's mean heights are expected.

As shown Table 5.2 the average of the single-tree height residuals derived from the summer first-echo points (~2.7 p/m²) is 0.66 m higher than those derived from the winter ALS data (~0.9 p/m²). For the grid-based estimation a difference of 0.51 m is found as can be seen in Table 5.1. As the point densities and the acquisition times are different for both data sets these mentioned differences for the extracted tree heights were difficult to interpret. Therefore, the ALS data set with the higher point density (summer data) were thinned out to get an equal point density for both data sets. Using a thinning out percentage of 66%, the point density of the summer data is reduced to ~0.9 p/m² and is therefore comparable with the one from the winter data. For the summer data a decrease of the mean residuals of the extracted tree heights for the thinned out data ($\rightarrow$ thinning out

percentage 66% → ~0.9 p/m²) of 0.61 m is observed (Table 5.2). The decrease of the mean residuals of the winter data using a similar thinning out percentage of 66% is 0.84 m (Table 5.2) and is 0.23 m higher than those of the summer data, which can be explained by the non linearity between the point density and the accuracy as described in Yu et al. (2004). The average of the residuals of the extracted single tree heights based on the thinned out (66% → ~0.9 p/m²) summer ALS data is 0.42 m and is 0.05 m higher than the mean residuals of the winter data.

The residuals from the Lorey's mean heights, which were derived from first-echo points, are 0.22 m smaller for the summer data than for the winter data. For the CHM case the residuals of the summer data are 0.51 m below the one extracted from the winter data as shown in Table 5.3. To compare the Lorey's mean heights from the summer and the winter data the summer data were thinned out with a percentage of 66% as shown in Table 5.4. The average of the residuals from the winter data (~0.9 p/m²) is -0.65 m and is therefore 0.27 m higher than the one from the thinned out summer data (~0.9 p/m²). The difference of the residuals based on the original point densities is 0.22 m, whereas for the summer data the difference of the residuals between the point density of ~2.7 p/m² and ~0.9 p/m² (66% thinning out) is 0.05 m (Table 5.4). Due to the fact that the entire study area is dominated by coniferous trees this means that the differences of the extracted Lorey's main heights mainly depend on the different acquisition time of the ALS data.

For the small Winkel test site, where many deciduous trees are available, the results are summarized in Figure 5.9, which shows the summer DTM, the difference models of the DTMs and the DSMs and the densities of ground hits. The comparison shows that the summer and winter DTMs exhibit a high degree of agreement for the non-forested areas. There, the differences are generally below 30 cm and large parts are below 10 cm. However, over forested areas, which are often associated with steep slopes, large differences up to ±15 m were observed. Due to reduced penetration rates in summer, it is expected that the summer DTM is in general higher than the winter DTM. However, the results show that negative and positive differences are almost equally abundant. This can be explained by considering the number of classified ground hits, as shown in the top right image of Figure 5.9. One can observe that in winter there are many ground hits also in the forested area (blue dots), but there are very few hits during the summer (green dots). As a result, there are too few points for the computation of the summer DTM, which caused under- and overshooting of the interpolated DTM particularly in steep, forested terrain along breaklines. This is reflected by the smooth appearance of the summer DTM in these areas.
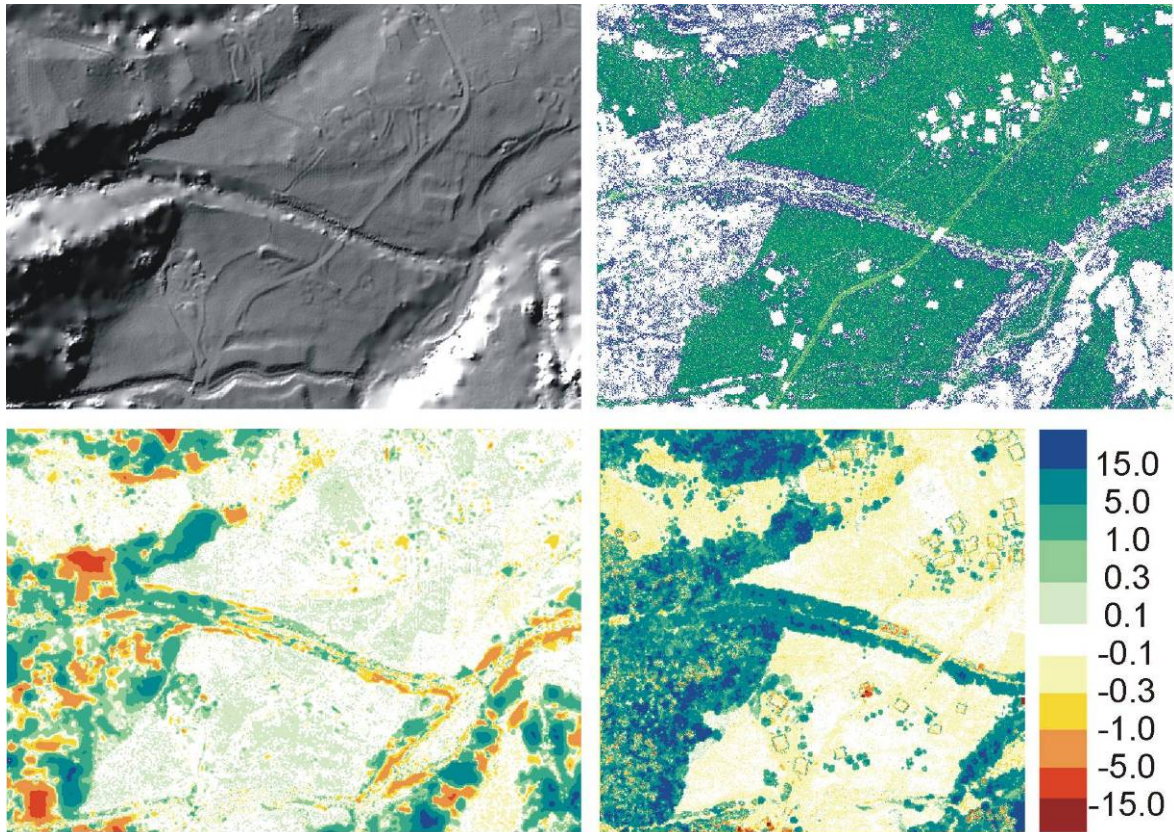
Figure 5.9: Top left image: Digital terrain model (DTM) derived from summer airborne laser scanner data for the Winkel test site. Top right: Number of ground hits during winter, indicated by the blue dots and summer, indicated by the green dots. Bottom left: Difference DTM (summer DTM minus winter DTM) given in meters. Bottom right: Difference DSM (summer DSM minus winter DSM) given in meters.

The large difference between the number of estimated ground hits in winter and summer was somewhat surprising, given that the forests are mixed deciduous-coniferous. The fact that the same filtering strategy was applied to both data sets excludes the possibility that a too rigid filtering strategy was selected for the summer data. This confirms that a large percentage of the trees in this study site is deciduous but also that coniferous tree crowns are more transparent for infrared laser pulses in winter than in summer. This finding coincides with the findings from Hadley and Smith (1986). They studied the seasonal influence on mortality of needles from timberline conifers in the Rocky Mountains, USA. The experiments showed that the needle mortality was higher in winter than in summer. They explained this effect mainly with the drying effects of winter wind.

Also for the digital surface models large differences can be observed over the forested areas, but this time the summer DSM is consistently higher or roughly of same height as the winter DSM (Figure 5.9). This is to be expected over patches of deciduous trees, where differences of 15 m or even higher can be observed. Interesting is the comparison between the summer- and winter DSM

and the density of ground hits during winter as shown in Figure 5.9 (top right). The comparison showed that in areas where there are no ground hits during winter, the difference between summer and winter DSM is minimal. Apparently, these areas are covered by coniferous species.

To investigate the penetration rate in areas dominated by coniferous trees the Valisera test site, which is mainly covered by a dense coniferous forest, was analysed. The Valisera test site is covered with 57% forest. The averaged penetration rate of last-echo points for the entire test site is 43% for the winter and 34% for the summer data. Within the forested areas of the Valisera test site the average penetration rate is 21% and 12% for the winter and summer data respectively. The summary of these analyses is given in Table 5.5.

Table 5.5: Penetration rates of first and last-echo ALS points under winter and summer conditions for the Valisera test site. The penetration rates were calculated for the entire test site as well as only for the forested areas.

Acquisition time	Entire test site		Forested area	
	Penetration rates [%]			
	Last-echo	First-echo	Last-echo	First-echo
Winter	43	42	21	20
Summer	34	34	12	12

Figure 5.10 shows the penetration rates of the last-echo points for both data sets. The calculations were based on a 3x3 m moving window. The shown penetration maps have a pixel size of 3 m. These analyses show that for dense coniferous forests the penetration rates are very low, but for snow free winter conditions the penetration rate is 9% higher than for summer conditions. Furthermore, Figure 5.10 shows that the high differences between winter and summer conditions can be observed along mud- and debris flow channels and avalanche paths, which are predominantly covered with low vegetation such as scrubs and bushes.
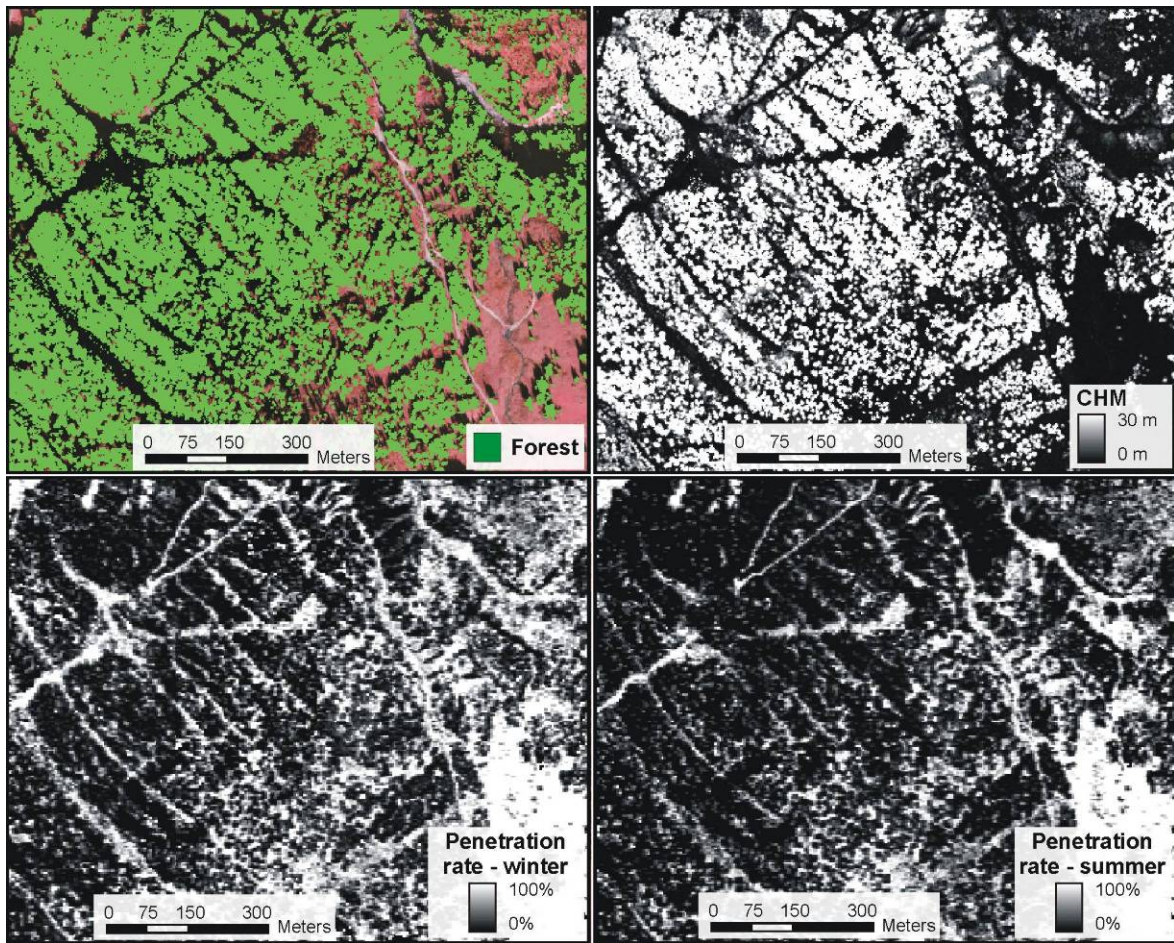
Figure 5.10: Penetration rates of last-echo points for the Valisera test site. The upper left image shows the forested area extracted from the CHM. As background image CIR orthophotos are shown. The upper right image shows the CHM. The two lower images show the penetration rates of last-echo points for winter (left) and summer (right) conditions.

5.3. Stem volume estimation

5.3.1. Method A

Sample plot size

For method A five different sample plot sizes (ø18 m, ø20 m, ø22 m, ø24 m and ø26 m) were tested separately. For these analyses all sample plots (103) were used for the multiple regression analyses. The final models and statistical parameters of the derived results are shown in Table 5.6.

Table 5.6: Evaluation of the appropriate sample plot size for method A. Shown are the final models, the condition numbers (κ), the bias correction factors (CF), the coefficients of determinations (R^2), the root mean square errors (RMSE [m^3ha^{-1}]) between estimated and ground reference values and the results of the cross-validation (minimum (min [m^3ha^{-1}]), maximum (max [m^3ha^{-1}]), mean (mean [m^3ha^{-1}]) and standard deviation (SD [m^3ha^{-1}])) for each sample plot size. The calculations were done using all (103) sample plots.

Sample plot size	Parameter							
	κ	CF	R^2	RMSE [m^3ha^{-1}]	Min [m^3ha^{-1}]	Max [m^3ha^{-1}]	Mean [m^3ha^{-1}]	SD [m^3ha^{-1}]
Ø18 m	$\ln v_{stem,fi} = 4.861837 - 0.419251 \ln h_{10l} + 0.857076 \ln d_{6f} - 0.123035 \ln d_{9l}$							
	19.9	1.025544	0.84* 0.83**	0.354* 101.4**	-1.151* -253.1**	1.442* 267.1**	0.000* 0.0**	0.376* 104.0**
Ø20 m	$\ln v_{stem,fi} = 3.178314 - 0.027323 \ln d_{2f} + 0.262734 \ln d_{7f} + 0.526734 \ln d_{6l}$							
	29.0	1.039258	0.81* 0.82**	0.379* 101.5**	-1.612* -264.9**	1.397* 291.0**	0.001* -0.1**	0.410* 105.0**
Ø22 m	$\ln v_{stem,fi} = 3.090095 - 0.031669 \ln d_{2f} + 0.609494 \ln d_{6f} + 0.204359 \ln d_{7l}$							
	29.0	1.033626	0.83* 0.83**	0.361* 99.1**	-1.794* -255.2**	1.088* 272.3**	0.001* 0.0**	0.385* 102.1**
Ø24 m	$\ln v_{stem,fi} = 4.662327 - 0.901615 \ln h_{0f} + 0.523643 \ln h_{30l} + 0.812855 \ln d_{6f}$							
	27.2	1.017166	0.85* 0.84**	0.343* 96.8**	-1.773* -254.7**	0.936* 204.1**	-0.002* -0.3**	0.365* 100.0**
Ø26 m	$\ln v_{stem,fi} = 4.662327 - 0.901615 \ln h_{0l} + 0.523643 \ln h_{40l} + 0.812855 \ln d_{6f}$							
	24.5	1.019927	0.84* 0.82**	0.355* 103.9**	-1.908* -338.4**	0.767* 282.1**	-0.001* -0.3**	0.375* 107.5**

* The values are calculated in the logarithmic scale. The quantities in the logarithmic scale are dimensionless.

** The values are calculated in the arithmetic scale. The bias was corrected using a ratio estimator (Snowdon, 1991).

As can be seen in Table 5.6 a sample plot size with a diameter of 24 m leads to the highest coefficient of determination (R^2 = 0.84) and to the lowest RMSE (RMSE = 96.8 m^3ha^{-1}) of the residuals derived from the cross-validation. The final model consists of three independent variables as shown in Table 5.6. The residuals derived from the cross-validation vary between -254.7 m^3ha^{-1} and 204.1 m^3ha^{-1} and have a standard deviation of 100.0 m^3ha^{-1}. The scatter plot of stem volumes derived from ALS data versus forest inventory data (103 sample plots) is shown in Figure 5.11.

Effects of different ALS point densities

The calculations were done for all (103), the winter (47) and the summer (56) sample plots separately. For the calculations a sample plot size of 24 m were used. The analyses were based on the original ALS points and on thinned out data sets. As thinning out percentage 66% were chosen, as this percentage decreases the point density of the summer data to about 0.9 p/m². Therefore, the results of the winter and the summer data are comparable. In Table 5.7 the final models with the estimated model coefficients, the coefficients of determinations (R^2), the root mean square errors (RMSE [m^3ha^{-1}]) between estimated and ground reference values, the condition numbers (κ) and the bias correction factors (CF) are shown. Furthermore, the results of the cross-validation (minimum (min [m^3ha^{-1}]), maximum (max [m^3ha^{-1}]), mean (mean [m^3ha^{-1}]) and standard deviation (SD [m^3ha^{-1}]) of the residuals) are shown. It can be observed that the final models include three to four different independent variables for different data sets and different point densities. The comparison between the results derived from the sample plots covered by the winter data (thinning out percentage was 0% → ~0.9 p/m²) and the sample plots covered by the summer data (thinning out percentage was 66% → ~0.9 p/m²) shows that the R² varies between 0.81 and 0.83 and the SD between 136.9 and 94.8 m^3ha^{-1}. That means that the difference in the SD can be explained by the different acquisition times. Furthermore, this statement can be confirmed by the small differences of the results derived from the original point densities and the thinned out ones as shown in Table 5.7.

Table 5.7: Summary of the stem volume analyses concerning the effects of different ALS point densities for method A. Shown are the derived coefficients of determinations (R^2), the root mean square errors (RMSE [m^3ha^{-1}]) between estimated and ground reference values and the condition numbers (κ). Furthermore, the results of the cross-validation (minimum (min [m^3ha^{-1}]), maximum (max [m^3ha^{-1}]), mean (mean [m^3ha^{-1}]) and standard deviation (SD [m^3ha^{-1}])) are shown. The calculations were done using all (A), the winter (W) and the summer (S) data corresponding to 103, 47 and 56 sample plots. The calculations were done based on the original ALS points and on thinned out (percentage of thinning out was 66%) data sets.

Perc. of thinning out [%]	Parameter								
	Time	κ	CF	R^2	RMSE [m^3ha^{-1}]	Min [m^3ha^{-1}]	Max [m^3ha^{-1}]	Mean [m^3ha^{-1}]	SD [m^3ha^{-1}]
0	A	$\ln v_{stem,fi} = 4.662327 - 0.901615 \ln h_{0,f} + 0.523643 \ln h_{30,l} + 0.812855 \ln d_{6,f}$							
		27.2	1.017166	0.91[*] 0.84[**]	0.343[*] 96.8[**]	-1.773[*] -254.7[**]	0.936[*] 204.1[**]	-0.002[*] -0.3[**]	0.365[*] 100.0[**]
	W	$\ln v_{stem,fi} = 5.402727 - 0.796747 \ln h_{0,f} - 0.101107 \ln d_{4,f} + 1.074957 \ln d_{6,f}$							
		19.7	1.012866	0.85[*] 0.81[**]	0.318[*] 125.2[**]	-1.044[*] -495.1[**]	0.953[*] 299.0[**]	0.000[*] -0.6[**]	0.355[*] 136.9[**]
	S	$\ln v_{stem,fi} = 2.069908 + 0.309163 \ln h_{90,l} - 0.065576 \ln d_{3,f} + 0.650659 \ln d_{6,f} + 0.524432 \ln h_{cv,l}$							
		19.1	1.023214	0.77[*] 0.86[**]	0.334[*] 79.5[**]	-1.754[*] -190.6[**]	1.068[*] 219.4[**]	0.000[*] -0.2[**]	0.384[*] 88.4[**]
66	A	$\ln v_{stem,fi} = 2.818110 - 0.074578 \ln d_{0,f} + 0.282504 \ln d_{7,f} + 0.606238 \ln d_{6,l}$							
		24.5	1.026639	0.84[*] 0.82[**]	0.356[*] 104.4[**]	-1.7996[*] -268.5[**]	0.968[*] 311.9[**]	0.000[*] -0.1[**]	0.375[*] 106.7[**]
	W	$\ln v_{stem,fi} = 2.505248 - 0.081361 \ln d_{2,l} + 0.684885 \ln d_{6,l} + 0.313229 \ln d_{8,l}$							
		18.6	1.022034	0.90[*] 0.85[**]	0.341[*] 109.7[**]	-1.303[*] -284.3[**]	0.944[*] 260.9[**]	-0.002[*] 0.3[**]	0.367[*] 117.4[**]
	S	$\ln v_{stem,fi} = 2.186756 + 0.342130 \ln h_{90,f} - 0.065298 \ln d_{3,l} + 0.629138 \ln d_{6,l} + 0.480778 \ln h_{cv,l}$							
		21.7	1.024893	0.76[*] 0.83[**]	0.340[*] 85.7[**]	-1.768[*] -245.0[**]	1.076[*] 242.7[**]	0.000[*] -0.8[**]	0.391[*] 94.8[**]

* The values are calculated in the logarithmic scale. The quantities in the logarithmic scale are dimensionless.

** The values are calculated in the arithmetic scale. The bias was corrected using a ratio estimator (Snowdon, 1991).

5.3.2. Method B

Sample plot size

As the most appropriate sample plot size was not known in advance the analyses were done for each sample plot size (ø18 m, ø20 m, ø22 m and ø24 m) separately. The results are summarised in Table 5.8. Shown are the condition numbers (κ), the coefficients of determinations (R^2), the RMSE [m^3ha^{-1}] and the standard deviation (SD [m^3ha^{-1}]) of the residuals derived from the cross-validation for methods B1 (canopy height intervals $\Delta ch = 7$ m) and B2 ($\Delta ch = 7$ m).

As shown in Table 5.8 a sample plot size with a diameter of 20 m leads to the highest R^2s, to the lowest RMSE and standard deviations of the residuals derived from the cross-validations. The differences between the parameters, which were calculated based on ø20 and ø22, are negligible. Even though the differences between method B1 and B2 are small, method B2 leads to higher

accuracies. Therefore, detailed model parameters of method B2 are summarised in Table 5.9. Shown are the results from method B2 with and without the interception term (β_0) for all, the winter and the summer sample plots. The R^2 is 0.87 using all sample plots and varies between 0.83 and 0.90 for the summer and winter sample plots respectively. The RMSE varies between 86.1 and 91.9 m^3ha^{-1} for all sample plots and varies between 88.4 and 92.3 m^3ha^{-1} for the winter and between 80.0 and 88.8 m^3ha^{-1} for the summer sample plots. The ranges of the residuals, which were estimated using a cross-validation, are quite large and are -243.3 to 265.6 m^3ha^{-1}, -205.1 to 351.0 m^3ha^{-1} and -222.3 to 258.1 m^3ha^{-1} corresponding to all, the winter and the summer sample plots. The standard deviations of these residuals vary between 90.0 and 91.9 m^3ha^{-1}, 89.8 and 107.3 m^3ha^{-1} and 86.9 to 90.1 m^3ha^{-1} representative for all, the winter and the summer sample plots. For methods B2 the scatter plots of stem volumes derived from ALS data versus forest inventory data (103 sample plots) is shown in Figure 5.11.

The differences of the results between the linear formulas with and without the interception term are small as shown in Table 5.9. Using the linear formula without the interception term a positive bias varying between 10.2 and 15.7 m^3ha^{-1} was introduced but has the advantage that the estimated model parameters (β_i) represent the fractions of the canopy volumes $v_{can, i}$, which are occupied by stem volumes.

Table 5.8: Summary of the analyses concerning the sample plot sizes used for methods B1 and B2. Shown are the coefficients of determinations (R^2), the root mean square errors (RMSE [m^3ha^{-1}]) between estimated and ground reference values, the condition numbers (κ) and the standard deviation of the residuals derived from the cross validation. For the calculations of the shown results the number of sample plots was 103. The calculations were done for four different sample plot sizes (Ø18, Ø20, Ø22, Ø24).

Parameters	Sample plot diameter			
	Ø18	Ø20	Ø22	Ø24
B1: $v_{stem,fi} = \beta_0 + 10^4 \cdot (\beta_1 v_{can,2-9} + \beta_2 v_{can,9-16} + \beta_3 v_{can,16-23} + \beta_4 v_{can,23-30} + \beta_5 v_{can,>30})$				
κ	14.6	17.6	20.0	23.3
R^2	0.86	0.87	0.87	0.86
RMSE [m^3ha^{-1}]	91.5	87.3	86.6	89.2
SD [m^3ha^{-1}]	97.0	92.6	91.9	94.6
B2: $v_{stem,fi} = \beta_0 + 10^4 \cdot (\beta_1 v_{can,2-12} + \beta_2 v_{can,12-22} + \beta_3 v_{can,22-32} + \beta_4 v_{can,>32})$				
κ	7.9	8.4	8.6	9.4
R^2	0.86	0.87	0.87	0.85
RMSE [m^3ha^{-1}]	89.8	86.1	86.6	88.6
SD [m^3ha^{-1}]	94.8	90.8	91.3	93.2
B1: $v_{stem,fi} = 10^4 \cdot (\beta_1 v_{can,2-9} + \beta_2 v_{can,9-16} + \beta_3 v_{can,16-23} + \beta_4 v_{can,23-30} + \beta_5 v_{can,>30})$				
κ	14.6	17.6	20.0	23.3
R^2	0.85	0.86	0.86	0.86
RMSE [m^3ha^{-1}]	96.1	91.4	90.8	92.7
SD [m^3ha^{-1}]	96.1	91.4	90.8	92.7
B2: $v_{stem,fi} = 10^4 \cdot (\beta_1 v_{can,2-12} + \beta_2 v_{can,12-22} + \beta_3 v_{can,22-32} + \beta_4 v_{can,>32})$				
κ	7.9	8.4	8.6	9.4
R^2	0.85	0.87	0.86	0.86
RMSE [m^3ha^{-1}]	94.7	90.4	90.3	91.4
SD [m^3ha^{-1}]	94.7	90.4	90.3	91.4
B1: $v_{stem,fi} = \beta_0 + 10^4 \cdot (\beta_1 v_{can,9-16} + \beta_2 v_{can,16-23} + \beta_3 v_{can,23-30} + \beta_4 v_{can,>30})$				
κ	9.1	11.0	12.1	13.4
R^2	0.86	0.87	0.87	0.86
RMSE [m^3ha^{-1}]	91.7	87.5	87.2	89.7
SD [m^3ha^{-1}]	96.2	91.9	91.5	94.2
B2: $v_{stem,fi} = \beta_0 + 10^4 \cdot (\beta_1 v_{can,12-22} + \beta_2 v_{can,22-32} + \beta_3 v_{can,>32})$				
κ	4.1	4.7	4.9	5.3
R^2	0.86	0.87	0.87	0.87
RMSE [m^3ha^{-1}]	89.8	86.1	86.6	88.6
SD [m^3ha^{-1}]	84.1	90.0	90.5	92.5
B1: $v_{stem,fi} = 10^4 \cdot (\beta_1 v_{can,9-16} + \beta_2 v_{can,16-23} + \beta_3 v_{can,23-30} + \beta_4 v_{can,>30})$				
κ	9.1	11.0	12.1	13.4
R^2	0.85	0.86	0.86	0.86
RMSE [m^3ha^{-1}]	96.9	92.0	91.0	92.9
SD [m^3ha^{-1}]	96.9	92.0	91.0	92.9
B2: $v_{stem,fi} = 10^4 \cdot (\beta_1 v_{can,12-22} + \beta_2 v_{can,22-32} + \beta_3 v_{can,>32})$				
κ	4.1	4.7	4.9	5.3
R^2	0.85	0.87	0.87	0.86
RMSE [m^3ha^{-1}]	96.5	91.9	92.1	93.3
SD [m^3ha^{-1}]	96.5	91.9	92.1	93.3

Table 5.9: Summary of model parameters for the method B2. Shown are the estimated model parameters β_i, the derived coefficients of determinations (R^2), the root mean square error (RMSE [m^3ha^{-1}]) between estimated and ground reference values and the statistic of the cross-validation results (minimum (min), maximum (max), mean (mean) and standard deviation (SD) of the residuals). The calculations were done for all (103), the winter (47) and the summer (56) sample plots separately. The size of the sample plots was 20 m.

Parameter	Winter and summer		winter		summer	
B2: $v_{stem,fi} = \beta_0 + 10^4 \cdot \left(\beta_1 v_{can,2-12} + \beta_2 v_{can,12-22} + \beta_3 v_{can,22-32} + \beta_4 v_{can,>32} \right)$						
β_0	85.2	-	49.1	-	118.0	-
β_1	-0.000314	0.002153	0.000787	0.002217	-0.001089	0.002419
β_2	0.002409	0.002908	0.002759	0.003076	0.0021477	0.002689
β_3	0.004458	0.004849	0.004789	0.004976	0.0039921	0.004692
β_4	0.001017	0.001438	0.001205	0.001513	0.0010967	0.001477
R^2	0.87	0.87	0.90	0.90	0.85	0.83
RMSE [m^3ha^{-1}]	86.1	90.4	88.4	89.9	80.0	88.8
Cross validation						
Min [m^3ha^{-1}]	-217.1	-217.0	-205.1	-200.8	-199.0	-188.3
Max [m^3ha^{-1}]	265.6	245.3	346.9	229.1	256.4	216.9
Mean [m^3ha^{-1}]	0.6	10.2	5.2	5.6	-0.2	14.1
SD [m^3ha^{-1}]	90.8	90.4	107.3	89.8	87.9	88.8
B2: $v_{stem,fi} = \beta_0 + 10^4 \cdot \left(\beta_1 v_{can,12-22} + \beta_2 v_{can,22-32} + \beta_3 v_{can,>32} \right)$						
β_0	81.0	-	61.8	-	106.5	-
β_1	0.002373	0.003585	0.002794	0.003698	0.001937	0.003541
β_2	0.004493	0.004672	0.004711	0.004823	0.004137	0.004445
β_3	0.001028	0.001539	0.001137	0.001578	0.001083	0.001643
R^2	0.87	0.87	0.90	0.90	0.85	0.84
RMSE [m^3ha^{-1}]	86.1	91.9	88.6	92.3	80.3	88.6
Cross validation						
Min [m^3ha^{-1}]	-214.0	-243.3	-199.2	-190.4	-182.6	-222.3
Max [m^3ha^{-1}]	253.2	243.3	351.0	230.3	258.1	207.7
Mean [m^3ha^{-1}]	0.6	15.7	5.0	13.3	-0.1	18.5
SD [m^3ha^{-1}]	90.0	91.9	105.8	92.3	86.9	90.1
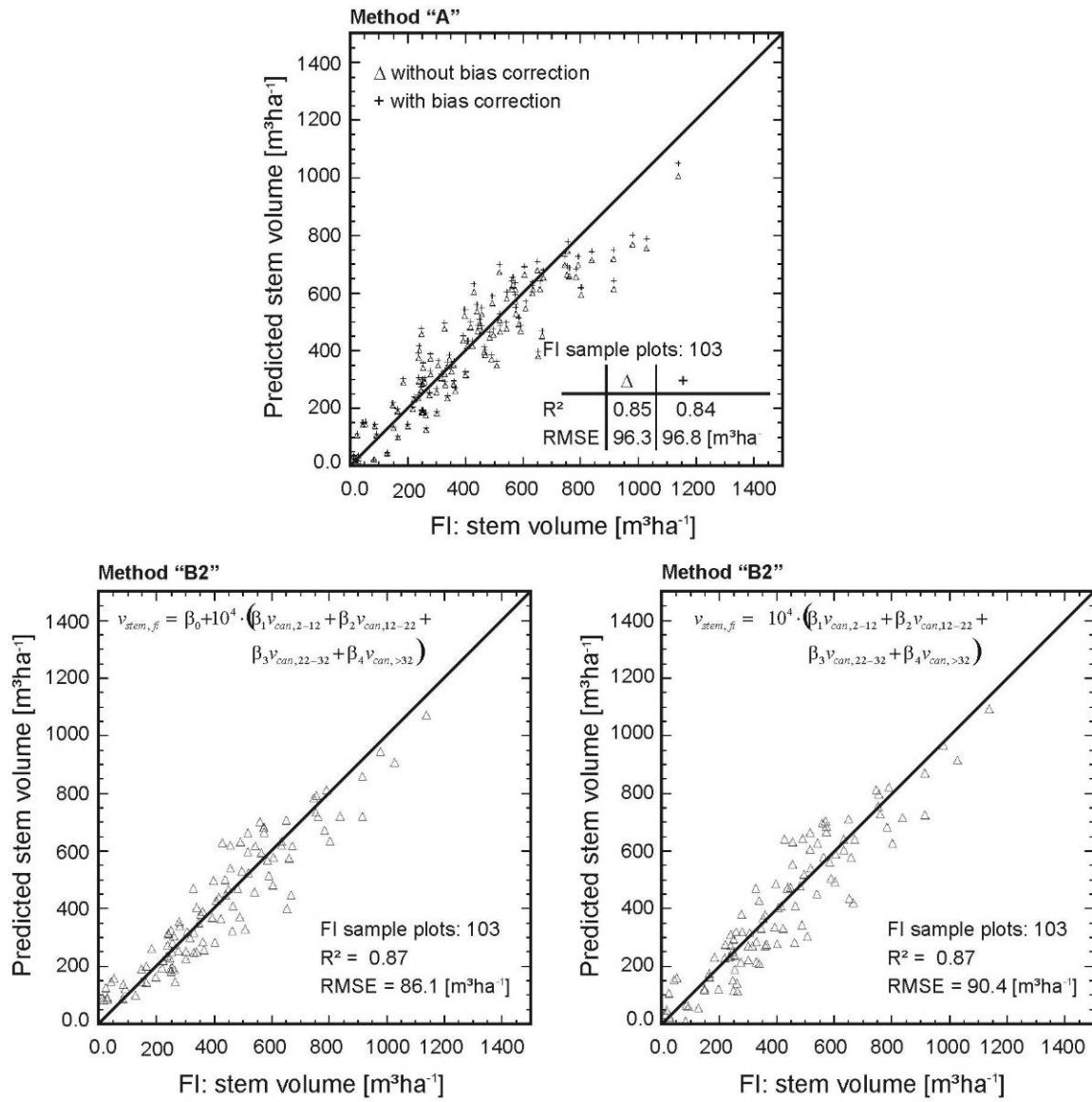
Figure 5.11: Scatter plots of stem volumes from ALS data versus forest inventory data. For the calculations of stem volumes method A and B (with and without the interception term) were used.

Effects of different ALS point densities

The investigations about the influences of the different ALS point densities on the derived stem volume accuracies are summarised in Table 5.10. A sample plot diameter of 20 m was used for the analyses, which were done using the linear function of method B2 with and without the interception term. The analyses were done for all, the winter and the summer sample plots separately using the original ALS data and thinned out (25%, 33%, 50%, 66% and 75%) data sets. The analyses show the low influence of the ALS point density on the achievable accuracies.

Concerning the effects of different point densities it can be stated that the differences in the R²s, the RMSEs and the SDs can be neglected. The comparison between winter and summer acquisition times shows that the R²s and the RMSEs are marginal smaller for summer than for winter data. Other than for the R²s, the SDs are higher for winter than for summer data as shown in Table 5.10.

Table 5.10: Influence of the ALS point density on the achievable accuracy. For the analyses method B2 with a sample plot diameter of 20 m was used. The analyses were done for all (a) sample plots (103), for the sample plots covered by the winter (w - 47) and by the summer (s – 56) ALS data. The analyses are based on the original data and on thinned out (25%, 33%, 50%, 66% and 75%) data. Shown are the R^2, the RMSE [m^3ha^{-1}], the statistics of the cross-validation (min [m^3ha^{-1}], max [m^3ha^{-1}], mean [m^3ha^{-1}], standard deviation [m^3ha^{-1}] of the residuals) and the model parameter β_i for the linear model with and without the interception term.

	R^2	RMSE [m^3ha^{-1}]	Min [m^3ha^{-1}]	Max [m^3ha^{-1}]	Mean [m^3ha^{-1}]	SD [m^3ha^{-1}]	β_0	β_1	β_2	β_3	β_4
Percentage of thinning out: 0%											
a	0.87	86.1	-217.1	265.6	0.6	90.8	85.2	-0.000314	0.002409	0.004458	0.001017
	0.87	90.4	-217.0	245.3	10.2	90.4	-	0.002153	0.002908	0.004849	0.001438
w	0.90	88.4	-205.1	346.9	5.2	107.3	49.1	0.000787	0.002758	0.004789	0.001205
	0.90	89.8	-200.8	229.1	5.6	89.8	-	0.002217	0.003076	0.004976	0.001513
s	0.85	80.0	-199.0	256.4	-0.2	87.9	118.0	-0.001089	0.002148	0.003992	0.001097
	0.83	88.8	-188.3	216.9	14.1	88.8	-	0.002419	0.002689	0.004692	0.001477
Percentage of thinning out: 25%											
a	0.87	86.6	-216.8	268.7	0.6	91.2	85.0	-0.000296	0.002421	0.004442	0.001037
	0.86	90.9	-216.9	246.2	10.2	90.9	-	0.002147	0.002925	0.004829	0.001459
w	0.90	89.3	-204.7	328.6	4.9	107.1	49.0	0.000906	0.002778	0.004767	0.001230
	0.90	90.7	-200.3	229.4	5.7	90.7	-	0.002217	0.003097	0.004953	0.001539
s	0.85	80.2	-198.6	256.9	-0.2	88.0	117.9	-0.001077	0.002151	0.003986	0.001105
	0.83	89.0	-188.3	220.2	14.1	89.0	-	0.002487	0.002673	0.004696	0.001462
Percentage of thinning out: 33%											
a	0.87	86.8	-216.8	264.8	0.6	91.4	85.4	-0.000313	0.002425	0.004433	0.001044
	0.86	91.2	-217.0	245.1	10.3	91.2	-	0.002137	0.002933	0.004823	0.001468
w	0.90	90.3	-205.7	315.3	4.6	106.9	49.8	0.000778	0.002776	0.004756	0.001243
	0.90	91.2	-201.1	229.2	5.8	91.2	-	0.002213	0.003101	0.004946	0.001555
s	0.85	80.2	-198.5	256.8	-0.1	88.0	118.0	-0.001080	0.002151	0.003986	0.001104
	0.83	89.0	-188.4	219.5	14.1	89.0	-	0.002403	0.002703	0.004681	0.001488
Percentage of thinning out:50%											
a	0.87	86.3	-213.6	265.4	0.6	91.0	85.2	-0.000329	0.002429	0.004424	0.001047
	0.86	90.7	-213.6	246.2	10.2	90.7	-	0.002124	0.002931	0.004814	0.001471
w	0.90	89.3	-199.0	321.2	4.7	106.7	49.4	0.000742	0.002785	0.004734	0.001257
	0.90	90.7	-194.6	231.0	5.7	90.7	-	0.002172	0.003104	0.004924	0.001567
s	0.85	80.0	-196.5	257.1	-0.2	87.8	117.5	-0.001067	0.002154	0.003991	0.001097
	0.83	88.8	-185.9	219.1	14.0	88.8	-	0.002410	0.002698	0.004685	0.001478
Percentage of thinning out: 66%											
a	0.86	88.9	-215.6	261.5	0.5	93.5	86.1	-0.000286	0.002481	0.004352	0.001127
	0.86	93.3	-217.4	246.2	10.5	93.3	-	0.002128	0.003013	0.004741	0.001558
w	0.89	93.8	-209.4	270.0	3.3	107.5	51.3	0.000821	0.002851	0.004647	0.001361
	0.89	95.3	-204.1	230.8	6.2	95.3	-	0.002264	0.003196	0.004843	0.001681
s	0.85	80.6	-197.2	258.1	-0.2	88.5	117.8	-0.001045	0.002162	0.003967	0.001127
	0.83	89.4	-188.8	225.2	14.2	89.4	-	0.002362	0.002743	0.00465	0.001520
Percentage of thinning out: 75%											
a	0.87	88.3	-215.6	261.5	0.5	93.5	85.7	-0.000389	0.002535	0.004330	0.001124
	0.86	82.7	-215.0	238.0	10.5	92.7	-	0.002041	0.003054	0.004720	0.001547
w	0.89	91.9	-207.4	261.6	3.1	105.1	51.1	0.000675	0.002913	0.004623	0.001363
	0.89	93.5	-202.2	221.6	6.1	93.5	-	0.002151	0.003243	0.004824	0.001675
s	0.85	81.0	-192.4	260.6	-0.3	88.8	116.7	-0.001019	0.002182	0.003955	0.001117
	0.83	89.7	-186.0	225.4	14.1	89.7	-	0.002321	0.002773	0.004626	0.001505

5.3.3. Stem volume mapping

As shown in Table 5.9 method B2 with a sample plot size of ø20 m achieved the highest accuracy. Therefore, the estimated model parameters of method B2 were used to map the stem volume for the whole study area. A 3D-view of the stem volume map is shown in Figure 5.12. The spatial sampling of the derived stem volume map is 1 m. Finally, the total stem volume was calculated from the forest inventory data as well as from the ALS derived stem volume map and is 1 569 650 m^3 and 1 581 750 m^3 respectively. The values show a very good agreement and differ less than 1%, which indicates the goodness of the fitted model.
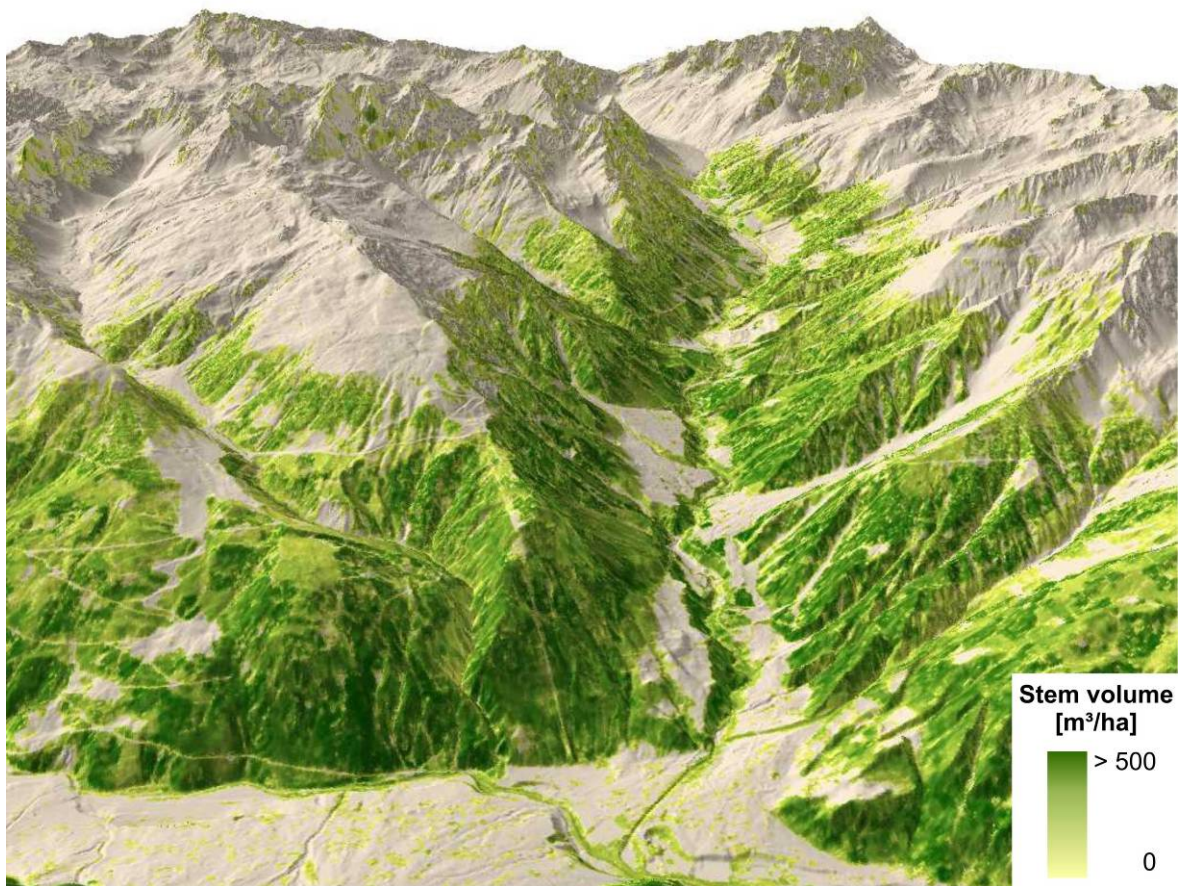
Figure 5.12: 3D-view of stem volume calculated from airborne laser scanner (ALS) and forest inventory data. It can clearly be seen that the protection forests covering steep slopes are characterised through high stem volume quantities. Furthermore, the decrease of stem volume near the timberline can be noted. The line of sight is from north to south.

6. Discussion

6.1. Experiences from a hydrologic relevant large-area land cover classification

The applicability of airborne laser scanning data for a hydrologic relevant land cover classification was tested by applying them over a large-area catchment within the study area. It was demonstrated and discussed what is already feasible now in an operational fashion for hydrologic applications. This was not only done to highlight what can be done now, but also show required technological improvements and research needs for using ALS in such difficult topographic condition.

So far, studies on the potential of ALS for providing input data for hydrologic / hydraulic applications were confirmed to small test sites. Kondoh and Higuchi (2001), Wealands et al. (2004), Schmugge et al. (2002), De Roo et al. (2001) and others outlined the usefulness of remotely sensed data for distributed hydrological models. Those studies suggest the combined use of ALS data in combination with high spatial resolution multi-spectral imagery for estimating aerodynamic landscape roughness, vegetation cover and leaf area indices. Furthermore, the ALS data can be used for the determination of roughness coefficients for river flood models in two ways: The roughness coefficients can either be derived from the vegetation heights, type and density as reported by Cobby et al. (2003) and Mason et al. (2003) or be connected to hydraulic relevant land cover classes (Brügelmann and Bollweg, 2004). However, it is not clear how close these suggested applications are to becoming operational.

As a large-area example, the derived land cover classes shown in Figure 5.1 (right) can be used for the determination of roughness coefficients of hydraulic river flood models. The empirical roughness coefficients for each land cover class can be found in the literature. As described before, a more physically based approach is the calculation of the roughness coefficient from the ALS data directly, which requires the correct measurement of vegetation heights also for short vegetation types such as grasses or scrubs. As the laser pulse duration of current ALS systems is in the order of 10 ns it is only possible to distinguish vegetation classes, which are taller than 1.5 meters (Wagner et al., 2003). Furthermore, it is not always clear which vegetation height is represented by the measured laser echo due to different penetration depths (Wagner et al., 2004a). These facts make it impossible to measure short vegetation heights directly with current systems. For the near future an improvement of this situation is expected mainly due to the rapid development of ALS technology. Especially the shortening of the pulse duration, which leads to an improved range resolution, and the use of full-wave laser scanner systems, seems to be very promising.

6.2. *Large-area canopy height mapping*

The results show that state-of-the-art ALS data, acquired for the main purpose of generating a DTM, are also an attractive data source for mapping canopy heights of alpine forests. However, it should not be expected that all ALS data are equally suited for this task. In this particular case, the derived canopy heights appeared to be very consistent for the entire 128 km^2 study area owing to the favourable circumstance that the region was dominated by coniferous tree species (spruce and fir). Therefore, surface models derived from both, winter and summer ALS acquisitions, could be merged into one data set as shown in Figure 3.3. It was also advantageous that a significant fraction of the forested area was covered by both the winter and the summer flight. In such a case it is ensured that a sufficient number of ground hits are available from the winter flight to produce a high-quality DTM and that the top of the canopy is well represented by the summer data.

6.2.1. *Validation of the terrain model*

The results of the DTM validation showed that the RMS errors for terrain slopes greater than 60% rise up to more than 0.5 m. Nevertheless, for relatively flat terrain similar values were reported by many other authors, e.g. Hodgson and Bresnahan (2004) who found RMS errors in the range of 17 to 26 cm for different land cover in Richland Country, South Carolina (pavement, low and high grass, bush/low tree, evergreen and deciduous forest). These authors also pointed out that observed errors on 25° slopes were about twice those on relatively low slopes due to relative horizontal displacements of the DTM and the ground control points. Furthermore, they hypothesized that an interactive effect of terrain slope with other factors (e.g. laser footprint, scanning angle, etc.) could further enhanced errors for steeper terrain. For open areas, Hyyppä et al. (2005) reported standard deviations of up to 0.25 m for slopes less than 30° and up to 0.45 m for slopes greater than 30°. For forested areas they found that elevation errors for "under-tree-areas" increased more dramatically for slopes greater than 15° than for open areas. Finally, Takahashi et al. (2005a) found RMS errors of 0.27 m for gentle yet rough terrain with slopes ranging between 3 and 30° and 0.58 m for steep slopes (25–48°). Therefore, the calculated RMS errors of the current study, which arise more than 0.50 m for slopes greater than 60° are comparable to those reported in the literature and seem to be realistic.

In contrast to the expected overestimation of terrain heights the analyses showed an underestimation of the terrain heights. This phenomenon can be explained by the fact that the used ground control points were mainly located along roadsides and therefore along breaklines, which were not explicit modelled during the DTM generation. Thus, the use of a three dimensional

modelling algorithm as for example described by Briese (2004b) would increase the DTM accuracy in those areas considerably.

As the used ground reference data were predominantly located on open areas the derived validation results are not representative for the DTM accuracy in forests. To check the DTM accuracy representative for forests, the ALS point cloud could be thinned out depending on the penetration rates of laser pulses in forest as summarised in 5.2.3. Based on the thinned out ALS points a DTM could be generated and the available ground control points could be used for an accuracy assessment. Due to temporal reasons, this proposed procedure could not be done within this thesis.

6.2.2. *Validation of the canopy heights*

The results of the quantitative assessments of the ALS derived single-tree heights were surprising. From a physical point of view an underestimation would be expect mainly due to the low ALS point density, the small footprint size of approximately 0.3 m in diameter and the conical tree crowns of spruces. Reasons for the overestimation of the tree heights are manifold and not yet fully understood. However, the following reasons are assumed to be responsible. First of all, within the study area the ALS last-echo penetration rate in coniferous forests is about 12% for summer conditions and 22% for winter conditions (Table 5.5), which is relatively low. Thus, for the interpolation of the terrain model under tree crowns a low number of ground points is available. According to Kraus et al. (2004) the terrain point density fundamentally influences the DTM accuracy and therefore, especially for rough forest terrain, surface smoothing effects and underestimation of the terrain heights appear as shown in Figure 5.3. Secondly, an overestimation of the ALS derived tree heights can occur if trees lean toward the lower side of slopes as described in Hirata (2004). Thirdly, the timberline is situated at about 1,950 m. Especially for higher altitudes the probability that trees are interlocked to each other increases. Therefore, it is more difficult to extract single-tree heights. Additionally to these facts possible inaccuracies of the field measurements have to be considered. Rössler (May, 2000) reported standard deviations of 0.34 m for tree height measurements using a Vertex hypsometer and a tripod. Furthermore, he mentioned that inaccuracies of ±0.4 m occur due to different operators. Finally, the observed overestimation can be related to the used reference tree heights. As described in section 3.2.3, within a sample plot only the height of the tree with the median basal area were measured in the field. For the analyses of the tree height accuracies only these measured tree heights were used. Considering that tree collectives can be found in the study area, it can occur that the height of a neighbouring higher tree

was extracted from the ALS data. Considering all these uncertainties the derived correlations between the field-measured and the ALS derived tree heights are satisfactory.

The area-based validation of the ALS canopy heights is more complex as the forest inventory data do not reflect the canopy heights in a comparable manner to the ALS data. As already mentioned in the section 3.2.3, only the median tree heights were measured and the remaining heights were calculated based on *dbh*-height curves. Due to the expected inaccuracies of this approach, which range between 1.3 and 1.9 m (Prodan, 1965) and the variable sample plot areas the calculated reference quantities (Lorey's mean heights) are difficult to use. Nevertheless, the observed correlations between canopy height percentiles and Lorey's mean heights are good and confirm the consistency of the calculated canopy heights within the entire study area for different terrain conditions and ALS system configurations.

Finally, the investigation regarding the use of first-echo point clouds versus grid-based CHMs clearly showed that the derived results are comparable to each other. Especially for large area applications the use of grid-based CHMs leads to shorter executing times and therefore to lower costs.

6.2.3. Effects of different ALS point densities to canopy heights

The original point density of the winter ALS data is 0.9 and 2.7 p/m^2 for the summer data. Using different thinning out percentages (25%, 33%, 50%, 66% and 75%) the effects of point densities to the achievable accuracies of the extracted canopy heights (single-tree heights, Lorey's mean heights) were investigated. The analyses were only done for the extraction of the canopy heights from the 3D point clouds.

The accuracies of the extracted single-tree heights show a strong dependency on the point density. As can be seen in Table 5.2 the RMS errors and the mean residuals increase and the R^2s decrease with decreasing point densities. It can be recognised that the increase of the RMS errors and the mean residuals are less for the summer than for the winter data, which can be explained by the higher transparency for infrared laser pulses in winter than in summer (Hadley and Smith, 1986) and by the non-linear connection between the point density and the accuracy (Yu et al., 2004). Even though R^2 decreases with decreasing point densities the achievable accuracies for winter (R^2 = 0.84, point density ~0.2 p/m^2) as well as for summer data (R^2 = 0.81, point density ~0.7 p/m^2) are high.

The influence of different point densities on the achievable accuracies of the extracted Lorey's mean heights is low. Especially, for R^2 no influence can be observed. The RMS errors increase from 3.12 to 3.26 m for the winter and from 3.03 to 3.12 m for the summer data whereas the mean residuals decrease from 0.65 to 0.42 m for winter and from 0.43 to 0.35 m for summer data.

Finally, it can be stated that the influence of different point densities on the achievable accuracies is lower for Lorey's mean heights than for single tree heights. This can be explained by the averaging effects of the area based approach for extracting Lorey's mean heights. It could be shown that for the description of canopy heights for large areas, which are covered with ALS data with varying point densities, the Lorey's mean height is an appropriate forest parameter for operational canopy height mapping.

6.2.4. Summer versus winter ALS data

For the comparison between winter and summer ALS data the different point densities of both data sets have to be considered. Therefore, a thinning out percentage of 66% was used to reduce the point density of the summer data to ~0.9 p/m^2 which is similar to the point density of the winter data. The investigations about the derived accuracies show slight differences for the estimation of single-tree heights as well as area-based Lorey's mean heights. Even though the R^2s are lower for the summer (single tree heights: $R^2 = 0.86$; Lorey's mean heights: $R^2 = 0.74$) than for the winter (single tree heights: $R^2 = 0.90$; Lorey's mean heights: $R^2 = 0.82$) data the RMS errors show no significant differences as shown in Table 5.2 and Table 5.4. The mean residuals of the extracted single tree heights are 0.05 m higher for summer than for winter data. Similar to the single tree heights the Lorey's mean heights are 0.27 m lower for winter than for summer data. These low differences can be related to the fact that the study area is dominated by coniferous trees.

The small experiments within the Winkel and Valisera test sites show that the most critical part of canopy height assessment from ALS data is the correct estimation of the terrain height. As the flying altitudes and the local incidence angles for both ALS data sets are similar, these different system parameters can be neglected. Especially for deciduous forests, summer data have some disadvantages for DTM mapping of rough terrain. As can be seen in Figure 5.9 differences up to several meters are observed along breaklines where no ground points are available. The results of the Valisera test site indicate that for coniferous forests the penetration rate for both winter and summer conditions is very low and therefore, the correct classification of terrain points is of high importance to derive a DTM with a high accuracy. As mentioned in Wagner et al. (2006b), small-footprint full-waveform systems provide in addition to multiple echoes, information about the echo

width, the amplitude and the cross-section of each target. This could improve the separation of ALS points into terrain and off-terrain points and therefore, the DTM quality.

6.3. Stem volume estimation

The results of this study show for the first time that airborne laser scanning data can successfully be used for stem volume mapping in a large alpine region in Austria. In contrast to boreal regions, the forests in Austria are characterised by a high heterogeneity of forest structure. As shown in Table 3.1 the standard deviations of tree heights, diameters at breast height, numbers of trees per plot and trees per hectare are high and are typical for a highly structured forest. In the study region a major part of the forest serves as protection forest. Due to former management practices this protection forest is characterised by very high stem volumes, which achieve more than 1 100 m^3ha^{-1}. As reference data already available forest inventory data, which were acquired within variable sample plot sizes, were used. The results show that such reference data can successfully be used to calibrate area-based stem volume estimation algorithms.

6.3.1. Method A

An objective of this study was to test the practicability of the multiplicative model, described by Næsset (2004b) for this alpine study area. The derived coefficient of determination ($R^2 = 0.84$) is comparable with those derived from boreal forests ($R^2 = 0.83 – 0.97$) reported in Næsset (2004b). Furthermore, Næsset (2004b) summarised that the standard deviations of the differences between predicted and ground reference values ranged from 32.9 to 67.8 $m^3 ha^{-1}$ (17.5 to 22.5%), which is comparable to 96.8 $m^3 ha^{-1}$ (22.9%) derived in this study. In general, the results are good especially for sample plots with lower stem volumes (Figure 5.11). Nevertheless, for higher stem volumes this model shows some underestimations mainly due to the high heterogeneity of the vertical forest structure in this study region. Even though the bias correction improve the accuracy for higher stem volumes additional improvements are advisable. A possible way to minimise this shortcoming is to divide the reference FI plots into several predefined classes according to age classes and site quality, as for example done by Næsset (2004b). The problem with such an approach is that a high number of FI plots must be available for each defined class, which enhance the costs for field work.

For regional mapping of mountainous areas, the practical usage of this model appears to be limited because the independent variables are known to change depending on different ALS system

parameters as for example the flying altitudes. A further critical point of this multiplicative model is the fact that for the primary regression model a high number of different independent variables are calculated from both, first- and last-echo ALS data. Also the final regression models include parameter calculated from both echoes as can be seen in Næsset (2004b). Thus, for using this model over mountainous areas with ALS data characterised through varying system parameters, one has to consider the findings of Næsset (2004a), that the effects of different flying altitudes on estimated canopy heights and densities are more pronounced for the last-echo reflections than for the first-echo reflections.

6.3.2. Method B

Method B uses a linear model, which considers only the canopy volumes calculated for sub areas within sample plots. The division of a sample plot area depends on predefined canopy heights. Within this thesis linear equations with and without the interception term were investigated as summarised in Table 5.8. For both equation types only canopy volumes are used as independent variables, which simplify the calculations and the physical interpretability of the derived results. The equations without the interception term have the advantage that the independent variables (canopy volumes) have a physically explicit connection between the stem– and the canopy volume, which is represented by the β_i-coefficients. Therefore, the estimated β_i-coefficients, shown in Table 5.8, represent the canopy- / stem volume ratios. Thus a plausibility check of the estimated β_i-coefficients can easily be done. The β_i-coefficients indicate that the major part of stem volume can be found in areas with canopy heights of 22 to 32 m as can be seen in Table 5.9. Also, the contributions of canopy volumes calculated for areas with canopy heights less than 9 m for method B1 and 12 m for method B2 are statistically not significant and can therefore be neglected as shown in Table 5.8 and Table 5.9. This confirms the practical experiences that only dominant and predominant trees are the main contributors of stem volume. A further reason is that for the calculation of the reference stem volume trees with a *dbh* less than 10 cm, corresponding to tree heights less than approx. 5.6 m, are not included as mentioned in 3.2.3. The findings about the canopy height thresholds are similar to those of Maclean and Krabill (1986). They regressed the stem volume against the cross-sectional area of an Airborne Oceanographic Lidar (AOL) - generated profile of forest. They found that canopy height thresholds of about 10.0 to 12.5 m led to the best correlations.

In general, the results of the linear models using the two predefined canopy height ranges show good accuracies, summarised in Table 5.8 ($R^2 = 0.86 – 0.87$; RMSE = 86.1 – 92.0 m^3 ha^{-1} and SD = 90.0 – 92.0 m^3 ha^{-1}). As shown in Figure 5.11 the accuracies at low stem volumes

($v_{stem} < \sim 80$ m^3 ha^{-1}) is not very satisfactory using the linear equation including the interception term. This overestimation for low stem volume quantities is minimised by the linear equation without the interception term as can be seen in Figure 5.11.

The use of a full cross-validation procedure guarantees unique and reproducible results. As can be seen in Table 5.9 the range of the residuals of the estimated stem volumes are relatively large. Reason for that could be that the used reference data are based on sample plots with variable sizes and that not all trees within the plots were measured and therefore not included into the stem volume estimation.

6.3.3. Sample plot size

As the reference data are based on variable sample plot sizes different diameter of the sample plots were analysed for the calculation of the independent variables.

For the multiplicative model (method A), the highest coefficient of determination ($R^2 = 0.84$) and the smallest standard deviation (SD = 100.0 m^{3}ha^{-1}), derived from the cross-validation, identify the most appropriate sample plot size, which has a diameter of 24.0 m. Furthermore, the analyses about the sample plot size show that for all different diameters a different set of independent variables leads to the highest accuracies as can be seen in Table 5.6.

The analyses for investigating the appropriate sample plot sizes for the methods B1 and B2 show that a diameter of 20.0 m leads to the highest accuracies as summarised in Table 5.8. Depending on the used linear formula (with and without the interception term) the standard deviation of the residuals derived from the cross-validation vary between 90.0 and 91.9 m^{3}ha^{-1}, whereas the coefficients of determinations are constant ($R^2 = 0.87$).

As the reference forest inventory data were based on variable sample plot sizes, about 74% and 85% of the measured trees are within the sample plot sizes with a diameter of 20.0 and 24.0 m respectively (Figure 3.7). Due to the statistically based calculations of the forest inventory data (e.g. Lorey's mean height, stem volume per hectare) these discrepancies can be explained.

6.3.4. Effects of different ALS point densities

The effects of different ALS point densities on the achievable stem volume accuracies were investigated for methods A and B2. The analyses were done on the original and on the thinned out ALS data clouds.

For the multiplicative model (method A) a thinning out percentage of 66% was applied for the winter and the summer data. The results do not repeat a dependency between achievable accuracies and point densities as shown in Table 5.7. As the multiple regression analyses lead to different sets of independent variables of the final models, a comparison of the results is difficult. The results from the merged data set show a decrease of R^2 from 0.84 to 0.82 and an increase of the RMS error from 96.8 to 104.4 m^3ha^{-1}. For the winter data an increase of R^2 from 0.81 to 0.85 is observed, whereas the RMS errors decrease from 125.2 to 109.7 m^3ha^{-1} with decreasing point densities. For the summer data a decrease of R^2 from 0.86 to 0.83 and an increase of the RMS errors from 79.5 to 85.7 m^3ha^{-1} occur.

Method B2 is divided in two variants, namely the linear equation with and without the interception term. The analyses showed that both variants are not affected by the investigated point densities as shown in Table 5.10. Using the linear equation without the interception term the coefficients of determinations vary (R^2) between 0.89 and 0.90 and the RMS error between 89.8 and 95.3 m^3ha^{-1} for the winter data. For the summer data R^2 is 0.83 and the RMS error vary between 88.8 and 89.7 m^3ha^{-1}. Therefore, the proposed model B2 can successfully be used for stem volume estimation based on ALS data sets with varying point densities.

6.3.5. Summer versus winter ALS data

As already mentioned in 6.3.4 an objective comparison between winter and summer data is difficult for method A, as the final models include different sets of independent variables. However, the R^2s of the winter and the summer data are similar and are 0.81 for the winter data (original point density ~0.9 p/m^2) and 0.83 for the summer data (thinned out percentage ~0.9 p/m^2). The RMS errors are relatively large and are 125.2 and 85.7 m^3ha^{-1} for the winter and the thinned out summer data respectively (Table 5.7).

The different point densities of the winter and summer data have no significant influence on the derived stem volume accuracies using method B2. Even though the R^2 vary between 0.90 and 0.83, the differences of the RMS errors (89.4 – 89.8 m^3ha^{-1}) can be neglected (Table 5.10). Therefore, it can be stated that the proposed method B2 can not only be used for ALS data with

different point densities but also for ALS data with different acquisition times, which is commonly the case for large area ALS projects in alpine regions.

6.3.6. Stem volume mapping

The perspective view of the derived stem volume map, shown in Figure 5.12, shows clearly the protection forests, which cover the steep slopes. These areas are characterised by high stem volume quantities which can be explained by the former forest management. Furthermore, the decrease of stem volume near the timberline can be noted which corresponds to the real condition. The good agreement of the total stem volumes derived from the FI data and the ALS stem volume map demonstrates that ALS data in combination with available field measured FI data are a practicable data source for stem volume mapping with high spatial resolution.

7. Conclusion

7.1. Hydrologic relevant land cover classification

Since the disastrous floods in Austria in the years 2002 and 2005, large airborne laser scanning (ALS) campaigns have been carried out along several river courses (e.g. the rivers "Kamp", "Drau", "Alm" and parts of the "Danube", etc.). The Austrian federal state of Vorarlberg has mapped the whole areas of their provinces with ALS during the last 4 years. Furthermore, the federal state of Tirol is mapping the whole district area with ALS within the next years. Several other federal states of Austria have similar intentions. Therefore, ALS data are already available or will become available for many complete catchment areas in the near future. The same trend can be observed in many other countries. Additionally, orthophotos are often available countrywide and will be updated at regular intervals of 5-10 years. This high spatial resolution data source is in use for updating topographic maps, for agricultural purposes and for several other environmental applications. Until now ALS flight campaigns are expensive but in consideration of the fact, that the level of automation for the data processing is very high and that the data can be used for multiple purposes, ALS data provide an attractive information source. For small study areas, the potential of ALS data to derive hydrologic / hydraulic relevant information has already been shown in several studies. In this thesis the experiences of processing ALS data were discussed, which were acquired in the framework of a commercial mapping project, for a large mountainous region. It could be shown that the simultaneously hybrid block adjustment for georeferencing the laser scanner strips and the hierarchic robust filtering technique are adequate methods to derive DTMs, DSMs and other subsequent products e.g. canopy height models or building layers. However, some inaccuracies of the canopy height model arose in areas covered by homogeneous meadows with high-grass or scrubs due to the technical limitations of the current laser scanner systems. New ALS systems, which provide calibrated intensities of the laser echoes or which record the full echo-waveform, may provide crucial information to overcome these problems (Wagner et al., 2004a) and a more physically approach for deriving e.g. roughness coefficients can be applied.

Finally, this study showed that the complementary informational content of ALS data and CIR orthophotos is an excellent data source for object-oriented land cover classifications needed for hydrologic / hydraulic applications. For example, these data can be used as input data for two dimensional hydraulic river flood models. The high quality of topographic and thematic input information for hydrologic / hydraulic models leads to a reduction of uncertainties of the model outputs. Furthermore, they can be used to support the preparation of the necessary information needed for integrated river basins to comply with the EU Water Framework Directive.

7.2. Canopy height mapping for complex mountainous terrain

The large-area application of ALS for mapping tree or stand heights in complex alpine environments is challenging because forests often have a very heterogeneous vertical and horizontal structure. Furthermore, alpine forests are mostly situated in steep terrain, data acquisition and post-processing methods are more demanding and hence, more costly than over flat terrain. Therefore, the introduction of ALS for alpine forestry applications is lacking behind, comparable to applications over other environments, as for example for boreal forest mapping in Scandinavia.

In this thesis it was shown that now ALS has also reached maturity for large area mapping of canopy heights of alpine forests. For operational applications some manual post-editing may still be necessary but overall, the performed analyses of the canopy heights indicated a high quality throughout the 128 km^2 mountainous study area.

For ALS flight planning it is necessary to know what forest types can be found in the study area. If the area is predominantly covered by coniferous forests, as was the case for this study area, both winter and summer acquisitions can be used effectively. For mapping deciduous or mixed forests, summer data are preferred because the top of deciduous trees can only be well reconstructed from green canopies. This outweighs the disadvantage that in summer the limited number of ground hits can cause large errors in the DTM, and subsequently the CHM, particularly over rugged terrain. Clearly, the best results are achieved if ALS data from both leaves-off and leaves-on conditions are available. The ideal scenario would therefore be to create a base-line DTM from ALS data acquired during leaves-off, snow-free conditions and then to use summer acquisitions for reconstructing the top of the forest canopy and for monitoring changes in subsequent years. An alternative to summer ALS data could be stereoscopic analyses of aerial images or of high resolution satellite images such as those provided by IKONOS. Due to the high structural diversity of mountainous forests and the fact that they are normally located in steep terrain, which increases shadowing, fully-automatic stereoscopic analyses seem to be unrealistic in alpine environments.

Although canopy height is the most important quantitative parameter, which can directly be derived from ALS data, most forestry applications do not need canopy height maps as such. The potential interest in CHMs lies in the fact that value-added products related to individual trees (position, height, crown diameter, canopy shape, diameter at breast height, basal area, etc.) or tree stands (crown cover fraction, stand height, stem volume, biomass, etc.) can be derived (Popescu et al., 2003). Thus, an extensive quality control of the ALS derived canopy heights is essential, because ALS sensor characteristics, flight parameters, filtering methods, modelling strategies for

the terrain and surface model and finally the surface properties themselves, can all impair the quality of the CHM and therefore, any derived parameter. For the quantitative quality check of a CHM, reference data are necessary and unfortunately, the measurement of single-tree heights is much easier than the measurement of canopy heights over a pre-defined grid. Consequently, ALS derived canopy heights cannot be readily compared and validated with existing forest inventory data. Nevertheless, it was shown in this study that a single-tree and an area-based validation of the canopy heights can be done with already existing forest inventory data.

In this study good correlations were found between field-measured single-tree heights and ALS canopy heights ($R^2 = 0.87$–0.89) derived from the 3D first-echo points and the CHM respectively. The achieved accuracy of the Lorey's mean heights derived from the 3D first-echo points is $R^2 = 0.79$ and from the CHM $R^2 = 0.70$. The calculations of the Lorey's mean heights were based on canopy height percentiles from first-echo points within a diameter of 25 m and from CHM heights within a diameter of 23 m. The analyses showed that only slight differences between the first-echo points and the grid-based CHM occur. However, these results also showed that the tree heights extracted from the CHM were about 0.85 m below the tree heights derived from the first-echo points. The Lorey's mean heights derived from the 3D points differed 0.53 m from those derived from the CHM. Thus, for large area applications a grid-based CHM can be employed successfully including the advantage of shorter processing times.

7.3. Stem volume estimation

This thesis showed that the multiplicative method from Næsset (2004b) can also be used for alpine forests. However, the model is based on a pure statistical approach and its parameters can therefore not be interpreted physically. This can easily be demonstrated by looking at the physical units of the significant variables in the final regression models as shown in Table 5.6. Due to the high number of independent variables the primary multiplicative regression model is rather complex. The logarithmic transformation of this regression model allows to use a simple linear model, but introduces additional calculations steps and thus potential additional error sources.

Therefore, a less complex model was proposed using only few parameters related to canopy volumes calculated from first-echo ALS data. All parameters of the developed linear model have clearly defined physical units, which allow a physical interpretation of the results. This is not the case for models that use logarithmic transformation of variables as for example used by Holmgren (2004), Maclean and Krabill (1986), or Næsset (2004b). The analyses in this study showed that for a mountainous study region this linear model works well and that reliable and robust results can be

derived. Furthermore, it was shown that this simple linear approach can successfully be used for highly structured forests as well as for ALS data with varying properties (point densities and acquisition times). The low number of independent variables and the physical interpretability of the estimated β-coefficients simplify the plausibility check and a possible transfer of this model to other regions.

Finally, these analyses indicated that forest inventory data whose measurements are based on the angle gauge method can successfully be used as reference data. The analyses showed that for the derivation of the independent variables for the empirical models, different sample plot sizes led to the best correlations.

7.4. *Final remarks and outlook*

Today, ALS is the most commonly used remote sensing technique to capture topographic data for the generation of high accurate DTMs and has widely replaced aerial photography for that purpose in many countries. Currently, extensive ALS campaigns are accomplished for DTM mapping activities in Austria. Thus, ALS data are available for large regions and provide an attractive data source for applied sciences and for several operational users. Especially, for forestry applications ALS is one of the most promising remote sensing techniques to estimate relevant parameters as reported in several studies (Hyyppä et al., 2004; Lim et al., 2003; Næsset et al., 2004). These studies summarise the use of ALS for operational forest inventories in Finland, Norway and Sweden. However, until now the use of ALS for forestry applications in complex alpine environments was confirmed to small study areas. Therefore, a focus of this thesis was the investigation of the applicability of ALS data for large area applications over complex alpine environments. On the basis of two application areas (hydrologic / hydraulic land cover classification activities and forestry applications) it was analysed and discussed what can be reached with current ALS data and already available algorithms. Additionally to these investigations, a new approach to estimate stem volume from ALS data was developed and the results were analysed and compared with results from a widely used algorithm.

The analyses within this thesis showed that the complementary informational content of ALS data and aerial photographs is an excellent data source for object-oriented land cover classifications. Particularly for areas with complex topographic conditions ALS as an active remote sensing technique has several advantages compared to aerial photographs, which are commonly in use for that purpose. Overall, the high potential of ALS data for land cover classifications could be

shown but there are still a number of limitations that require further research and development work.

Due to technical limitations of current ALS systems the laser pulse duration is in the range of 5 ns to 10 ns, which leads to a range resolution of 0.75 m to 1.5 m as described in 2.3.4. Therefore, for land cover classes (e.g. sealed surfaces, bare soil, grassland, grain, shrubs, etc.) with object heights below the achievable range resolution a differentiation of these classes is not possible. As these land cover classes have different surface roughness the use of this information for hydrologic / hydraulic relevant applications is limited. To minimise this shortcoming either more direct approaches to estimate the surface roughness from ALS data are needed or additional information (e.g. spectral information from multi-spectral imagery, amplitude and echo width from full waveform ALS data) are required to classify each three dimensional laser point directly (Ducic et al., 2006; Wagner et al., 2006a). Furthermore, continuous technical improvements of ALS systems lead to shorter pulse durations (e.g. the Riegl LMS-Q560 has a pulse duration of 4 ns) and therefore, to higher range resolutions.

The fusion of ALS data and high spatial resolution imagery (e.g. air photos, satellite images) is still a challenging task. As these images show spatial displacements of off-terrain points dependent on their distances from the photo's nadir point, a combined analysis has to consider these facts. To improve the geometric quality of image data a suitable digital surface model (e.g. DSM generated from ALS data) is necessary to calculate true orthophotos. Currently, the true orthophoto production is a very time consuming and therefore, a very costly process, which limits the operational use until now. Consequently, automated algorithms are needed to use the full information content of both data sources in a cost-effective way.

In addition to the land cover classification activities this thesis concentrated on the application of ALS in forestry. As an active remote sensing technique ALS is independent of the sun as illumination source and is therefore not influenced by topographic shadows. Airborne laser scanning provides detailed information not only about the horizontal distribution of forests but also about the vertical structure, the canopy surface and the terrain surface. Therefore, the most important measurable quantity of ALS systems is the vegetation height (e.g. canopy height, tree height), which provides the input for the estimation of further forest parameters such as stem volume. In this thesis two area-based models to estimate stem volume from ALS data were investigated. It was shown that the widely used multiplicative regression model developed by Næsset (2002) could successfully be transferred from Scandinavian forests to a complex and multilayered forest in the western part of Austria. Furthermore, a less complex linear model to estimate stem volume was developed and tested. The analyses showed that the results of both models are comparable. Due to the physical interpretability of the used input parameter and the

estimated β–coefficients of the linear model the plausibility check of the results and a possible transfer of this model to other regions seem to be less complex. In addition to the outlined analyses future research activities can be formulated as follows:

- As ALS data are available for the entire province of Vorarlberg it is planed to use the linear model for the whole area of about 2 600 km². As reference data the national forest inventory data should be used. The challenge of such a large area application is that a low number of reference sample plots is available and that these sample plots are distributed to different forest types.

- Until now, the models were tested for coniferous dominated forests and therefore, the estimation of stem volume also for deciduous and mixed forest should be investigated. It is expected that for different forest types (e.g. coniferous -, mixed - and deciduous forests) either individual regression models are needed or an additional parameter concerning the forest type must be added to the model. Such stratum-specific analyses require a forest classification. Popescu et al. (2004) report that the combined analyses of ALS data and multi-spectral imagery have a great potential to differentiate between tree species, which requires e.g. the generation of true orthophotos as described above. Finally, it is of interest if the calibrated β-coefficients of the developed linear model could be used to characterise different forests types in different regions.

- Currently, ALS is a rapidly developing technology. Therefore, the availability of additional information for each measured point such as those from full-waveform ALS (e.g. amplitude, echo width, cross section) is expected. To use these new information for forestry applications further research is needed. In the future higher point densities are expected, which will enable the successful estimation of single-tree based parameters.

- For operational applications of ALS data, quality control is of vital importance. Particularly over such difficult terrain, as can be found in the Austrian Alps, quality control has to be done very carefully. Within this thesis the quality of the derived surface models (e.g. DTM, DSM, CHM) were validated with forest inventory data and ground control points. To keep efforts and costs as low as possible, existent external reference data (e.g. ground control points and forest inventory data) should be used in any case. But, as the results of this thesis showed, the comparison between forest inventory and ALS data is not straight forward. Therefore, additional studies are required for a better understanding of the linkage between ALS derived forest parameters (e.g. canopy height values, stem volume) and existing forest inventory data. In addition to the derived surface models the quality of the ALS data itself has to be checked. Therefore, it is planed to develop new methods and standards for quality control of ALS data.

- One of the main advantages of ALS techniques is the possible high degree of automatisation, covering the whole processing chain, from the acquisition to the analyses. In general, a high degree of automatisation for all processing steps leads to an increasing objectivity and therefore, to a repeatability of the results and to a reduction of the subjective influence of an individual operator. Furthermore, for the repeatability it is important to document all performed acquisition and processing steps, which can easily be reached with automated methods. Today, ALS data cover large areas and the amount of data is huge. Thus, the analyses can only be managed within an acceptable time frame with a highly automated processing chain. Finally, short processing times decrease the costs, which is essential for the operational usage of ALS data in a various field of applications.

8. References

Ackermann, F., 1999. Airborne laser scanning - present status and future expectations. ISPRS Journal of Photogrammetry & Remote Sensing 54, 64-67.

Ackermann, F. and Kraus, K., 2004. Reader commentary: Grid based digital terrain models. Geoinformatics 7, 28-31.

Axelsson, P., 1999. Processing of laser scanner data - algorithms and applications. Photogrammetry & Remote Sensing 54, 138-147.

Baatz, M. and Schäpe, A., 2000. Multiresolution Segmentation: An optimization approach for high quality multi-scale image segmentation. Angewandte Geographische Informationsverarbeitung XII. Beiträge zum AGIT-Symposium Salzburg 2000, Vol., Salzburg, 12.

Baltsavias, E.P., 1999a. Airborne laser scanning: basic relations and formulas. ISPRS Journal of Photogrammetry & Remote Sensing 54, 199-214.

Baltsavias, E.P., 1999b. Airborne laser scanning: existing systems and firms and other resources. ISPRS Journal of Photogrammetry & Remote Sensing 54 (2-3), 165-198.

Baltsavias, E.P., 1999c. A comparison between photogrammetry and laser scanning. ISPRS Journal of Photogrammetry & Remote Sensing 54, 83-94.

Baskerville, G.L., 1972. Use of logarithmic regression in the estimation of plant biomass. Canadian Journal of Forest Research 2, 49-53.

Beauchamp, J.J. and Olson, J.S., 1973. Corrections for bias in regression estimates after logarithmic transformation. Ecology 54 (6), 1403-1407.

Benz, U.C., Hofmann, P., Willhauck, G., Lingenfelder, I. and Heynen, M., 2004. Multi-resolution, object-oriented fuzzy analysis of remote sensing data for GIS-ready information. Photogrammetry & Remote Sensing 58, 239-258.

BFW, May, 2006. http://web.bfw.ac.at/i7/oewi.oewi0002.

Blair, J.B., Rabine, D.L. and Hofton, M.A., 1999. The Laser Vegetation Imaging Sensor: a medium-altitude, digitisation-only, airborne laser altimeter for mapping vegetation and topography. ISPRS Journal of Photogrammetry & Remote Sensing 54 (2-3), 115-122.

Blaschke, T. and Strobl, J., 2001. What's wrong with pixels? Some recent developments interfacing remote sensing and GIS. GIS - Zeitschrift für Geoinformationssysteme 6/2001, 12-17.

Briese, C., 2004a. Breakline Modelling from Airborne Laser Scanner Data. Doctoral Thesis, Institut of Photogrammetry and Remote Sensing (I.P.F.), Vienna University of Technology, Vienna, 67 pp.

Briese, C., 2004b. Three-dimensional Modelling of Breaklines from Airborne Laser Scanner Data. International Archives of Photogrammetry, Remote Sensing and Spatial Information Sciences XXXV (Part B/3), 1097 - 1102.

Briese, C., Pfeifer, N. and Dorninger, P., 2002. Applications of the Robust Interpolation for DTM Determination. International Archives of Photogrammetry and Remote Sensing XXXIV (Part 3A), 55-61.

Brügelmann, R. and Bollweg, A.E., 2004. Laser Altimetry for River Management. International Archives of Photogrammetry and Remote Sensing, XXth ISPRS Congress, Istanbul, Turkey, 12-23 July 2004, CDROM.

Burman, H., 2002. Laser strip adjustment for data calibration and verification. International Archives of Photogrammetry and Remote Sensing XXXIV, 3, 67-72.

Charlton, M.E., Large, A.R.G. and Fuller, I.C., 2003. Application of Airborne LIDAR in River Environments: The River Coquet, Northumberland, UK. Earth Surface Processes and Landforms 28, 299-306.

Cobby, D.M., Mason, D.C. and Davenport, I.J., 2001. Image processing of airborne scanning laser altimetry data for improved river flood modelling. ISPRS Journal of Photogrammetry & Remote Sensing 67, 121-138.

Cobby, D.M., Mason, D.C., Horritt, M.S. and Bates, P.D., 2003. Two-dimensional hydraulic flood modelling using a finite-element mesh decomposed according to vegetation and topographic features derived from airborne scanning laser altimetry. Hydrological Processes 17, 1979-2000.

Crombaghs, M., Brügelmann, R. and De Min, E., 2000. On the adjustment of overlapping strips of laseraltimeter height data. International Archives of Photogrammetry and Remote Sensing XXXIII, 3A, 230-237.

Darwish, A., Leukert, K. and Reinhardt, W., 2003. Urban Land-Cover Classification: An Object Based Perspective. Proceedings 2nd GRSS/ISPRS Joint Workshop on Data Fusion and Remote sensing over Urban Areas, 278-282.

De Roo, A.P.J., Odijk, M., Schmuck, G., Koster, E. and Lucieer, A., 2001. Assessing the Effects of Land Use Changes on Floods in the Meuse and Oder Cathment. Physics and Chemistry of the Earth 26 (7-8), 593-599.

Dickerson, M., Drysdale, R., McElfresh, S. and Welzl, E., 1997. Fast greedy triangulation algorithms. Computational Geometry: Theory and Applications 8, 67-86.

Drake, J.B., Dubayah, R.O., Clark, D.B., Knox, R.G., Blair, J.B., Hofton, M.A., Chazdon, R.L., Weishampel, J.F. and Prince, S.D., 2002. Estimation of tropical forest structural characteristics using large-footprint lidar. Remote Sensing of Environment 79, 305-319.

Dubayah, R. and Drake, J., 2000. Lidar Remote Sensing for Forestry. Journal of Forestry 98, 44-46.

Ducic, V., Hollaus, M., Ullrich, A., Wagner, W. and Melzer, T., 2006. 3D Vegetation Mapping and Classification using Full-Waveform Laser Scanning. Workshop on 3D Remote Sensing in Forestry, 14-15 Feb. 2006, Vol., Vienna.

eCognition, May, 2006. http://www.definiens-imaging.com.

Flewelling, J.W. and Pienaar, L.V., 1981. Multiplicative Regression with Lognormal Errors. Forest Science 27 (2), 281-289.

Flood, M., 2001. Laser Altimetry: From Science to Commercial Lidar Mapping. Photogrammetric Engineering & Remote Sensing 11, 1209-1217.

Gaveau, D.L.A. and Hill, R.A., 2003. Quantifying canopy height underestimation by laser pulse penetration in small-footprint airborne laser scanning data. Canadian Journal of Remote Sensing 29 (5), 650-657.

Govers, G., Takken, I. and Helming, K., 2000. Soil roughness and overland flow. Agronomie 20, 131-146.

Haala, N. and Brenner, C., 1999. Extraction of buildings and trees in urban environments. ISPRS Journal of Photogrammetry & Remote Sensing 54 (2-3), 130-137.

Haala, N. and Walter, V., 1999. Automatic Classification of Urban Environments for Database Revision using LIDAR and Color Aerial Imagery. International Archives of Photogrammetry and Remote Sensing, 3-4 June, 1999, Vol. Vol. 32, Part 7-4-3 W6, Valladolid, Spain, 7.

Hadley, J.L. and Smith, W.K., 1986. Wind Effects on Needles of Timberline Conifers: Seasonal Influence on Mortality. Ecology 67 (1), 12-19.

Harding, D.J., Lefsky, M.A., Parker, G.G. and Blair, J.B., 2001. Laser altimeter canopy height profiles; Methods and validation for closed-canopy, broadleaf forests. Remote Sensing of Environment 76, 283-297.

Heurich, M. and Weinacker, H., 2004. Automated tree detection and measurement in temperate forests of central Europe using laserscanning data. International Archives of Photogrammetry, Remote Sensing and Spatial Information Sciences XXXVI (Part 8/W2), 198-203.

Hirata, Y., 2004. The Effects of Footprint Size and Sampling Density in Airborne Laser Scanning to Extract Individual Trees in Mountainous Terrain. International Archives of Photogrammetry, Remote Sensing and Spatial Information Sciences XXXVI (Part 8/W2), 283-287.

Hodgson, M.E. and Bresnahan, P., 2004. Accuracy of Airborne Lidar-Derived Elevation: Empirical Assessment and Error Budget. Photogrammetric Engineering & Remote Sensing 70 (3), 331-339.

Hodgson, M.E., Jensen, J.R., Tullis, J.A., Riordan, K.D. and Archer, C.M., 2003. Synergistic Use of Lidar and Color Aerial Photography for Mapping Urban Parcel Imperviousness. Photogrammetric Engineering & Remote Sensing 69 (9), 973-980.

Hoffmann, A. and Van der Vegt, J.W., 2001. New Sensor systems and new Classification Methods: Laser- and Digital Camera-data meet object-oriented strategies. GIS - Zeitschrift für Geoinformationssysteme 1, 18-23.

Hollaus, M., Wagner, W., Eberhöfer, C. and Karel, W., 2006. Accuracy of large-scale canopy heights derived from LiDAR data under operational constraints in a complex alpine environment. ISPRS Journal of Photogrammetry & Remote Sensing 60 (5), 323-338.

Hollaus, M., Wagner, W. and Kraus, K., 2005. Airborne laser scanning and usefulness for hydrological models. Advances in Geosciences 5, 57-63.

Holmgren, J., 2003. Estimation of Forest Variables using Airborne Laser Scanning. Thesis, Department of Forest Resource Management and Geomatics, Swedish University of Agricultural Sciences, Umeå, 43 pp.

Holmgren, J., 2004. Prediction of Tree Height, Basal Area and Stem Volume in Forest Stands Using Airborne Laser Scanning. Scandinavian Journal of Forest Research 19 (6), 543-553.

Holmgren, J. and Jonsson, T., 2004. Large Scale Airborne Laser Scanning of Forest Resources in Sweden. International Archives of Photogrammetry, Remote Sensing and Spatial Information Sciences XXXVI (Part 8/W2), 157-160.

Holmgren, J., Nilsson, M. and Olsson, H., 2003. Estimation of tree height and stem volume on plots using airborne laser scanning. Forest Science 49 (3), 419-428.

Hoschek, J. and Lasser, D., 1993. Fundamentals of Computer Aided Geometric Design. A K Peters Ltd.

Houghton, R.A., 2005. Aboveground Forest Biomass and the Global Carbon Balance. Global Change Biology 11 (6), 945-958.

Huber, M., Schickler, W., Hinz, S. and Baumgartner, A., 2003. Fusion of LIDAR Data and Aerial Imagery for Automatic Reconstruction of Building Surfaces. 2nd GRSS\ISPRS Joint Workshop on Remote Sensing and Data Fusion over Urban Areas, URBAN_2003, May 22-23, Vol., Berlin, Germany, May, 5.

Hyyppä, H., Yu, X., Hyyppä, J., Kaartinen, H., Kaasalainen, S., Honkavaara, E. and Rönnholm, P., 2005. Factors affecting the quality of DTM generation in forested areas. International Archives of Photogrammetry, Remote Sensing and Spatial Information Sciences XXXVI (Part 3/W19), 97-102.

Hyyppä, J., Hyyppä, H., Litkey, P., Yu, X., Haggrén, H., Rönnholm, P., Pyysalo, U., Pitkänen, J. and Maltamo, M., 2004. Algorithms and Methods of Airborne Laser Scanning for Forest Measurements. International Archives of Photogrammetry, Remote Sensing and Spatial Information Sciences XXXVI (Part 8/W2), 82-89.

Hyyppä, J. and Inkinen, M., 1999. Detecting and estimating attributes for single trees using laser scanner. The Photogrammetric Journal of Finland 16 (2), 27-42.

Journel, A.G. and Huijbregts, C.J., 1978. Mining Geostatistics. Academic Press, New York.

Kaasalainen, S., Ahokas, E., Hyyppä, J. and Suomalainen, J., 2005. Study of Surface Brightness From Backscattered Laser Intensity: Calibration of Laser Data. IEEE GEOSCIENCE AND REMOTE SENSING LETTERS 2 (3), 255-259.

Kager, H., 2004. Discrepancies between overlapping laser scanner strips - simultaneous fitting of aerial laser scanner strips. International Archives of Photogrammetry, Remote Sensing and Spatial Information Sciences XXXV (Part B/1), 555-560.

Katzenbeisser, R., 2002. Technical Note on: Intensity. http://toposys.de/pdf-ext/Engl/TN-Intensity.pdf, 5.

Katzenbeisser, R., 2003. Technical Note on: Echo Detection. http://toposys.de/pdf-ext/Engl/echo-detec3.pdf, 12.

Keylwerth, R., 1954. Ein Beitrag zur qualitativen Zuwachsanalyse. Holz als Roh- und Werkstoff 12, 41-44.

Kilian, J., Haala, N. and Englich, M., 1996. Capture and evaluation of airborne laser scanner data. International Archives of Photogrammetry and Remote Sensing XXXI, B3, 383-388.

Kondoh, A. and Higuchi, A., 2001. Relationship between satellite-derived spectral brightness and evapotranspiration from a grassland. Hydrological Processes 15, 1761-1770.

Koukal, T., 2004. Nonparametric Assessment of Forest Attributes by Combination of Field Data of the Austrian Forest Inventory and Remote Sensing Data. Dissertation Thesis, Institut für Vermessung, Fernerkundung und Landinformation; Department für Raum, Landschaft und Infrastruktur, Universität für Bodenkultur Wien, Vienna, 115 pp.

Kraus, K., 1998. Interpolation nach kleinsten Quadraten versus Krige-Schätzer. Österreichische Zeitschrift für Vermessung & Geoinformation (VGI) 86. Jahrg. (Heft 1), 45 - 48.

Kraus, K., 2000. Photogrammetrie, Band 3, Topographische Informationssysteme. Dümmler, 419 pp.

Kraus, K., 2003a. Airborne Laser Scanning. Newsletter EuroSDR 2, 11-12.

Kraus, K., 2003b. Laser-Scanning - ein Paradigmawechsel in der Photogrammetrie. Bulletin SEV/VSE (invited) 9, 19-22.

Kraus, K., 2003c. LaserScanDTMs for Modeling Flood Risk Areas. GIS (Geo-Informations-Systeme) 12, 26-31.

Kraus, K., Briese, C., Attwenger, M. and Pfeifer, N., 2004. Quality Measures for Digital Terrain Models. International Archives of Photogrammetry, Remote Sensing and Spatial Information Sciences XXXV (Part B/2), 113 - 118.

Kraus, K. and Mikhail, E.M., 1972. Linear least-squares interpolation. Photogrammetric Engineering 38, 1016-1029.

Kraus, K. and Pfeifer, N., 1998. Determination of terrain models in wooded areas with airborne laser scanner data. ISPRS Journal of Photogrammetry & Remote Sensing 53 (4), 193-203.

Kraus, K. and Pfeifer, N., 2001. Advanced DTM generation from LIDAR data. International Archives of Photogrammetry and Remote Sensing, Volume XXXIV-3/W4, Annapolis, MD, 22-24 Oct., Vol., 22-24 Oct., 23-30.

Lanchaster, P. and Salkauskas, K., 1986. Curve and surface fitting. An Introduction. Academic Press.

Lefsky, M.A., Cohen, W.B., Acker, S.A., Parker, G.G., Spies, T.A. and Harding, D., 1999a. Lidar Remote Sensing of the Canopy Structure and Biophysical Properties of Douglas-Fir Western Hemlock Forests. Remote Sensing of Environment 70 (3), 339-361.

Lefsky, M.A., Cohen, W.B., Parker, G.G. and Harding, D.J., 2002. Lidar Remote Sensing for Ecosystem Studies. BioScience 52 (1), 19-30.

Lefsky, M.A., Harding, D., Cohen, W.B., Parker, G. and Shugart, H.H., 1999b. Surface Lidar Remote Sensing of Basal Area and Biomass in Deciduous Forests of Eastern Maryland, USA. Remote Sensing of Environment 67 (1), 83-98.

Leica, 2006. http://www.leica-geosystems.com/corporate/en/ndef/lgs_57629.htm. Last accessed October, 2006.

Lillesand, T.L., Kiefer, R.W. and Chipman, J.W., 2004. Remote Sensing and Image Interpretation, Fifth Edition. John Wiley & Sons, Inc., 763 pp.

Lim, K., Treitz, P., Wulder, M., St-Onge, B. and Flood, M., 2003. LIDAR remote sensing of forest structure. Progress in Physical Geography 27 (1), 88-106.

Maas, H.-G. and Vosselman, G., 2004. Flugzeug-Laserscanning. Photogrammetrie, Fernerkundung, Geoinformation (PFG) 4/2004, 257-258.

Maclean, G.A. and Krabill, W.B., 1986. Gross-Merchantable Timber Volume Estimation Using an Airborne LIDAR System. Canadian Journal of Remote Sensing 12 (1), 7-18.

Marks, K. and Bates, P., 2000. Integration of high-resolution topographic data with floodplain flow models. Hydrological Processes 14, 2109-2122.

Mason, D.C., Cobby, D.M., Horritt, M.S. and Bates, P.D., 2003. Floodplain friction parameterization in two-dimensional river flood models using vegetation heights derived from airborne scanning laser altimetry. Hydrological Processes 17, 1711-1732.

Matikainen, L., Hyyppä, J. and Hyyppä, H., 2003. Automatic Detection of Buildings from Laser Scanner Data for Map Updating. International Archives of Photogrammetry, Remote Sensing and Spatial Information Sciences XXXIV (Part 3/W13), 7 pp.

Means, J.E., Acker, S.A., Harding, D.J., Blair, J.B., Lefsky, M.A., Cohen, W.B., Harmon, M.E. and McKee, W.A., 1999. Use of Large-Footprint Scanning Airborne Lidar to Estimate Forest Stand Characteristics in the Western Cascades of Oregon. Remote Sensing of Environment 67 (3), 298-308.

Melzer, T. and Briese, C., 2004. Extraction and Modeling of Power Lines from ALS Point Clouds. Austrian Association for Pattern Recognition (ÖAGM), Vol., Hagenberg, 06-17-2004 - 06-18-2004, 47 - 54.

Morsdorf, F., Meier, E., Kötz, B., Itten, K.I., Dobbertin, M. and Allgöwer, B., 2004. LIDAR-based geometric reconstruction of boreal type forest stands at single tree level for forest and wildland fire management. Remote Sensing of Environment 92 (2), 353-362.

Næsset, E., 1997a. Determination of mean tree height of forest stands using airborne laser scanner data. ISPRS Journal of Photogrammetry & Remote Sensing 52 (2), 49-56.

Næsset, E., 1997b. Estimating Timber Volume of Forest Stands Using Airborne Laser Scanner Data. Remote Sensing of Environment 61 (2), 246-253.

Næsset, E., 2002. Predicting forest stand characteristics with airborne scanning laser using a practical two-stage procedure and field data. Remote Sensing of Environment 80 (1), 88-99.

Næsset, E., 2004a. Effects of different flying altitudes on biophysical stand properties estimated from canopy height and density measured with a small-footprint airborne scanning laser. Remote Sensing of Environment 91 (2), 243-255.

Næsset, E., 2004b. Practical Large-scale Forest Stand Inventory Using a Smallfootprint Airborne Scanning Laser. Scandinavian Journal of Forest Research 19 (2), 164-179.

Næsset, E., 2005. Assessing sensor effects and effects of leaf-off and leaf-on canopy conditions on biophysical stand properties derived from small-footprint airborne laser data. Remote Sensing of Environment 98 (2-3), 356-370.

Næsset, E., Bollandsås, O.M. and Gobakken, T., 2005. Comparing regression methods in estimation of biophysical properties of forest stands from two different inventories using laser scanner data. Remote Sensing of Environment 94 (4), 541-553.

Næsset, E., Gobakken, T., Holmgren, J., Hyyppä, H., Hyyppä, J., Maltamo, M., Nilsson, M., Olsson, H., Persson, Å. and Söderman, U., 2004. Laser scanning of forest resources: the Nordic experience. Scandinavian Journal of Forest Research 19 (6), 482-499.

Nelson, R., Parker, G. and Hom, M., 2003. A Portable Airborne Laser System for Forest Inventory. Photogrammetric Engineering & Remote Sensing 69 (3), 267-273.

Nilsson, M., 1996. Estimation of Tree Heights and Stand Volume Using an Airborne Lidar System. Remote Sensing of Environment 56 (1), 1-7.

Parker, G.G., Lefsky, M.A. and Harding, D.J., 2001. Light transmittance in forest canopies detemined using airborne laser altimetry and in-canopy quantum measurements. Remote Sensing of Environment 76, 298-309.

Pereira, L.M.G. and Wicherson, R.J., 1999. Suitability of laser data for deriving geographical information A case study in the context of management of fluvial zones. Photogrammetry & Remote Sensing 54, 105-114.

Pfeifer, N., 2003. Oberflächenmodelle aus Laserdaten. Österreichische Zeitschrift für Vermessung & Geoinformation (VGI) Heft 4/2003, 243-252.

Pfeifer, N., Elberink, S.O. and Filin, S., 2005. Automatic Tie elements Detection for Laser Scanner Strip Adjustment. V/3 Workshop "Laser scanning 2005", Vol. ISPRS WG III/3, III/4, Enschede, the Netherlands, September 12-14, 2005, 174-179.

Pfeifer, N., Köstli, A. and Kraus, K., 1998a. Interpolation and Filtering of Laser Scanner Data - Implementation and First Results. International Archives of Photogrammetry, Remote Sensing and Spatial Information Sciences XXXII (Part 3\1), 153-159.

Pfeifer, N., Köstli, A. and Kraus, K., 1998b. Interpolation and Filtering of Laser Scanner Data - Implementation and First Results. International Archives of Photogrammetry and Remote Sensing, Vol. Vol. XXXII, Part 3\1, Columbus, Ohio, USA, 153-159.

Pollanschütz, J., 1974. Formzahlfunktionen der Hauptbaumarten Österreichs. Allgemeine Forstzeitung 85 (12), 341-343.

Popescu, S.C., Wynne, R.H. and Nelson, R.F., 2002. Estimating plot-level tree heights with lidar: local filtering with a canopy-height based variable window size. Computers and electronics in agriculture 37 (1-3), 71-95.

Popescu, S.C., Wynne, R.H. and Nelson, R.F., 2003. Measuring individual tree crown diameter with lidar and assessing its influence on estimating forest volume and biomass. Canadian Journal of Remote Sensing 29 (5), 564-577.

Popescu, S.C., Wynne, R.H. and Scrivani, J.A., 2004. Fusion of small-footprint lidar and multispectral data to estimate plot-level volume and biomass in deciduous and pine forests in Virginia, U.S.A. Forest Science 50 (4), 551-565.

Prodan, M., 1965. Holzmeßlehre. Sauerländer, Frankfurt am Main, 644 pp.

R Development Core Team, 2005. R: A language and environment for statistical computing. In: R.F.f.S. Computing (Editor), Vienna, Austria. http://www.R-project.org.

Rees, W.G., 2001. Physical principles of remote sensing. Cambridge University Press, Cambridge, 343 pp.

Rössler, G., May, 2000. Höhenmeßverfahren auf Dauerversuchsflächen. http://bfw.ac.at/100/1232.html.

Rottensteiner, F. and Briese, C., 2003. Automatic Generation of Building Models from LiDAR Data and the Integration of Aerial Images. International Society of Photogrammetry and Remote Sensing, Proceedings of the ISPRS working group III\3 workshop "3-D reconstruction from airborne laserscanner and InSAR data", 8-10 October, Vol. Volume XXX IV, PART 3 \ W13, Dresden, Germany.

Rottensteiner, F., Trinder, J., Clode, S. and Kubik, K., 2005a. Automated delineation of roof planes from LIDAR data. ISPRS WG III/3, III/4, V/3 Workshop "Laser scanning 2005", Vol., Enschede, the Netherlands, September 12-14, 2005, 221-226.

Rottensteiner, F., Trinder, J., Clode, S. and Kubik, K., 2005b. Using the Dempster-Shafer Method for the Fusion of LIDAR Data and Multi-spectral Images for Building Detection. Information Fusion 6 (4), 283-300.

Russ, W., 2004. Mehr Wald - ein positiver Trend? BFW-Praxisinformation, Nr. 3-2004, Wien, 4-7.

Schadauer, K., Niese, G. and König, U., 1997. Wie gefährdet ist Österreichs Schutzwald? Österreichische Forstzeitung 108 (2), 11-13.

Schardt, M., Ziegler, M., Wimmer, A., Wack, R. and Hyyppä, J., 2002. Assessment of Forest Parameters by Means of Laser Scanning. International Archives of Photogrammetry, Remote Sensing and Spatial Information Sciences XXXIV (Part 3/A), 302-309.

Schmugge, T.J., Kustas, W.P., Ritchie, J.C., Jackson, T.J. and Rango, A., 2002. Remote sensing in hydrology. Advances in Water Resources 25, 1367-1385.

Scop++, May, 2006. http://ipf.tuwien.ac.at/products; http://www.inpho.de.

Shiver, B.D. and Borders, B.E., 1996. Sampling techniques for forest resource inventory. John Wiley & Sons Inc., New York.

Sithole, G. and Vosselman, G., 2004. Experimental comparison of filter algorithms for bare-Earth extraction from airborne laser scanning point clouds. ISPRS Journal of Photogrammetry & Remote Sensing 59 (1-2), 85-101.

Smith, R.J., 1993. Logarithmic Transformation Bias in Allometry. American Journal of Physical Anthropology 90, 215-228.

Smith, S.L., Holland, D.A. and Longley, P.A., 2004. The Importance of Understanding Error in LIDAR Digital Elevation Models. International Archives of Photogrammetry, Remote Sensing and Spatial Information Sciences XXXV (Part B4), 996-1001.

Snowdon, P., 1991. A ratio estimator for bias correction in logarithmic regressions. Canadian Journal of Forest Research 21, 720-724.

Sohn, G. and Dowman, I., 2003. Building Extraction using LiDAR DEMs and IKONOS Images. International Society of Photogrammetry and Remote Sensing, Proceedings of the ISPRS working group III\3 workshop "3-D reconstruction from airborne laserscanner and InSAR data", Vol. Volume XXX IV, PART 3\W13, Dresden, Germany, 7.

Sprugel, D.G., 1983. Correcting for bias in log-transformed allometric equations. Ecology 64 (1), 209-210.

Stand Montafon Forstfonds, May, 2006. http://www.stand-montafon.at/forstfonds.

Sterba, H., 1991. Holzmesslehre [Forest measurements]. Vorlesungsunterlagen. Heft 3 der Berichte aus der Abteilung Holzmesskunde und Inventurfragen. Institut für forstliche Ertragslehre, Universität für Bodenkultur, Wien 169 pp.

Süß, H., 1984. Programm zur Auswertung von betrieblichen Forstinventuren mittels Winkelzählproben, Institute of Forest growth and Yield research. University of Natural Resources and Applied Life Sciences, Vienna.

Takahashi, T., Yamamoto, K., Senda, Y. and Tsuzuku, M., 2005a. Estimating individual tree heights of sugi (Cryptomeria japonica D. Don) plantations in mountainous areas using small-footprint airborne LiDAR. Journal of Forest Research 10 (2), 135-142.

Takahashi, T., Yamamoto, K., Senda, Y. and Tsuzuku, M., 2005b. Predicting individual stem volumes of sugi (Cryptomeria japonica D. Don) plantations in mountainous areas using small-footprint airborne LiDAR. Journal of Forest Research 10 (4), 305-312.

Terrasolid, 2006. http://www.terrasolid.fi. Last accessed October 2006.

Van der Sande, C.J., De Jong, S.M. and De Roo, A.P.J., 2003. A segmentation and classification approach of IKONOS-2 imagery for land cover mapping to assist flood risk and flood damage assessment. International journal of Applied Earth Observation and Geoinformation 4, 217-229.

Vosselman, G. and Maas, H.-G., 2001. Adjustment and Filtering of Raw Laser Altimetry Data. OEEPE Workshop on Airborne Laserscanning and Interferometric SAR for Detailed Digital Elevation Models, 1.-3. March 2001, Vol., Stockholm, 11.

Wagner, W., Eberhöfer, C., Hollaus, M. and Summer, G., 2004a. Robust Filtering of Airborne Laser Scanner Data for Vegetation Analysis. International Archives of Photogrammetry, Remote Sensing and Spatial Information Sciences XXXVI (Part 8/W2), 56-61.

Wagner, W., Hollaus, M., Briese, C. and Ducic, V., 2006a. 3D vegetation mapping using full-waveform airborne laser scanners. International Journal of Remote Sensing. Submitted.

Wagner, W., Ullrich, A. and Briese, C., 2003. Der Laserstrahl und seine Interaktion mit der Erdoberfläche. Österreichische Zeitschrift für Vermessung und Geoinformation (VGI) 91. Jahrgang (2003), 4, 223-235.

Wagner, W., Ullrich, A., Ducic, V., Melzer, T. and Studnicka, N., 2006b. Gaussian decomposition and calibration of a novel small-footprint full-waveform digitising airborne laser scanner. ISPRS Journal of Photogrammetry & Remote Sensing 60 (2), 100-112.

Wagner, W., Ullrich, A., Melzer, T., Briese, C. and Kraus, K., 2004b. From single-pulse to full-waveform airborne laser scanners: Potential and practical challenges. International Society for

Photogrammetry and Remote Sensing XXth Congress, Vol XXXV, Part B/3, 12-23 July 2004, Commission 3, Vol. Vol. XXXV, part B3, Istanbul, Turkey, 6.

Wealands, S.R., Grayson, R.B. and Walker, J.P., 2004. Quantitative comparison of spatial.elds for hydrological model assessment - some promising approaches. Advances in Water Resources 28, 15-32.

Wehr, A. and Lohr, U., 1999. Airborne laser scanning - an introduction and overview. ISPRS Journal of Photogrammetry & Remote Sensing 54, 68-82.

Weitkamp, C., 2005. Lidar: Introduction. In: T. Fujii and T. Fukuchi (Editors), Laser Remote Sensing. Taylor & Francis Group, LLC, Boca Raton London New York Singapore, pp. 1-36.

Yu, X., Hyyppä, H., Kaartinen, H., Hyyppä, J., Ahokas, E. and Kaasalainen, S., 2005. Applicability of First Pulse Derived Digital Terrain Models for Boreal Forest Studies. International Archives of Photogrammetry, Remote Sensing and Spatial Information Sciences XXXVI (Part 3/W19), 97-102.

Yu, X., Hyyppä, J., Hyyppä, H. and Maltamo, M., 2004. Effects of flight altitude on tree height estimation using airborne laser scanning. International Archives of Photogrammetry, Remote Sensing and Spatial Information Sciences XXXVI (Part 8/W2), 96-101.

Zhang, K., Chen, S.-C., Whitman, D., Shyu, M.-L., Yan, J. and Zhang, C., 2003. A Progressive Morphological Filter for Removing Nonground Measurements From Airborne LIDAR Data. IEEE Transaction on Geoscience and Remote Sensing 41 (4), 872-882.

Zwally, H.J., Schutz, B., Abdalati, W., Abshire, J., Bentley, C., Brenner, A., Bufton, J., Dezio, J., Hancock, D., Harding, D., Herring, T., Minster, B., Quinn, K., Palm, S., Spinhirne, J. and Thomas, R., 2002. ICESat's laser measurements of polar ice, atmosphere, ocean, and land. Journal of Geodynamics 34, 405-445.

Curriculum Vitae

Name: Dipl.-Ing. Markus Hollaus

Date and place of birth: November 27, 1973 in Schwaz/Tirol, Austria

1980 – 1984   Elementary school in Aschau/Zillertal

1984 – 1988   Secondary school in Zell/Zillertal

1988 – 1993   Grammar school for civil engineering in Innsbruck

06 / 1993   School leaving exam (Matura)

1993 – 2000   Studies of Land & Water Management and Engineering at the University of Natural Resources and Applied Life Sciences (BOKU), Vienna

1998   Exchange semester at the Norwegian University of Science and Technology (NTNU), Norway

03 / 2000   Diploma examination. Title of the diploma thesis: *Hydrologic services for agricultural purposes with respect to remote sensing.*

2000   Military service

2001 – 2003   Research assistant at the Institute of Surveying, Remote Sensing and Land Information (IVFL) at the BOKU, Vienna

Since 2004   Research assistant at the Christian Doppler Laboratory on "Spatial Data from Laser Scanning and Remote Sensing" at the Institute of Photogrammetry and Remote Sensing (I.P.F.), Vienna University of Technology

Vienna, 25. October 2006